

Brave New World: Jet Production (and Disappearance) at the LHC Using the ATLAS Detector

Eric Feng
(University of Chicago / ATLAS)



RPM Seminar
Lawrence Berkeley National Laboratory
2011 January 4



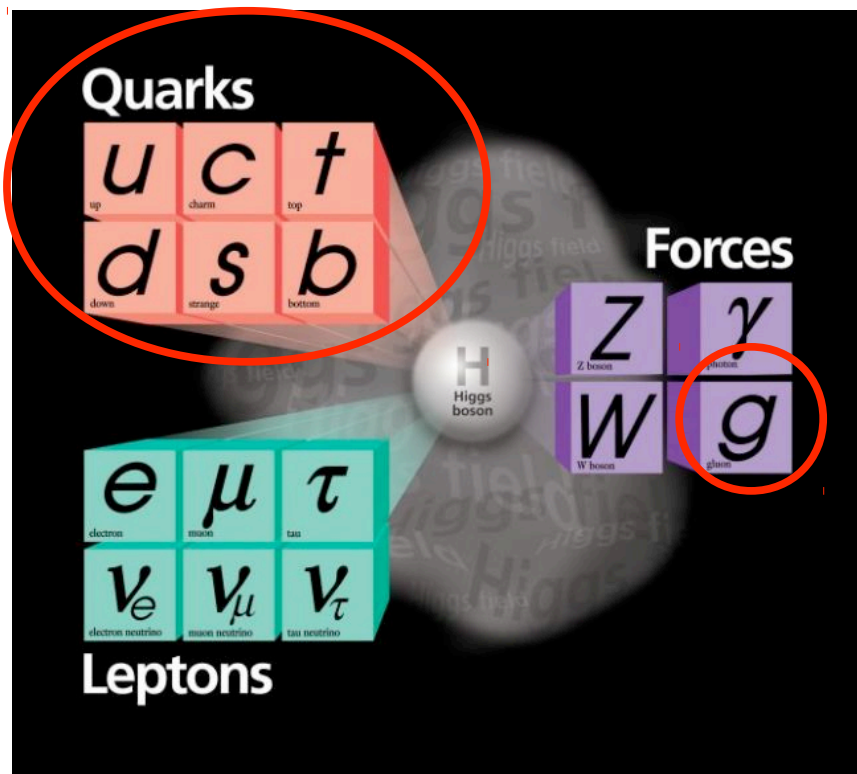
Outline

- Introduction to QCD and jet physics
- **ATLAS Experiment at the LHC**
 - Event displays of interesting jets & dijet events
 - Jet performance and calibration
- **Inclusive jet and dijet cross-sections**
 - Laboratory for perturbative QCD
- **Searches for exotica using dijets**
 - Resonances and contact interactions
- **Jet quenching in lead ion collisions**
- Conclusions and outlook

QCD and jet physics

Introduction

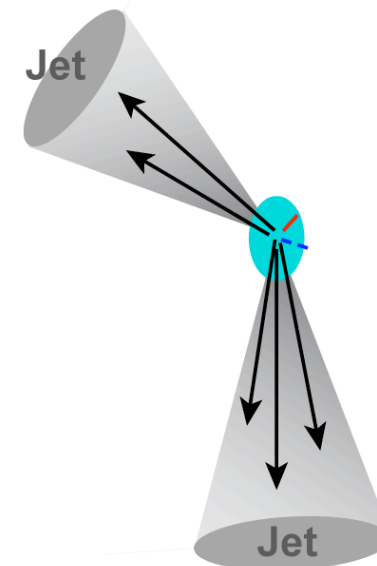
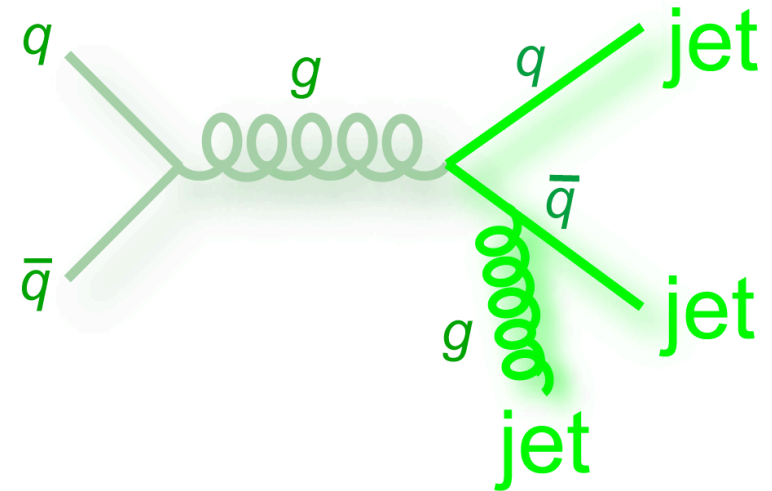
- Quantum chromodynamics (QCD) is the theory of the strong interaction, one of the three fundamental forces in the Standard Model



$$\begin{aligned}
 & -\frac{1}{2}\partial_\nu g_\mu^a \partial_\nu g_\mu^a - g_s f^{abc} \partial_\mu g_\nu^a g_\mu^b g_\nu^c - \frac{1}{4}g_s^2 f^{abc} f^{ade} g_\mu^b g_\nu^c g_\mu^d g_\nu^e + \\
 & \frac{1}{2}ig_s^2 (\bar{q}_i^\mu \gamma^\mu q_j^\mu) g_\mu^a + \bar{G}^a \partial^2 G^a + g_s f^{abc} \partial_\mu \bar{G}^a G^b g_\mu^c - \partial_\nu W_\mu^+ \partial_\nu W_\mu^- - \\
 & M^2 W_\mu^+ W_\mu^- - \frac{1}{2}\partial_\nu Z_\mu^0 \partial_\nu Z_\mu^0 - \frac{1}{2\epsilon_0} M^2 Z_\mu^0 Z_\mu^0 - \frac{1}{2}\partial_\mu A_\nu \partial_\mu A_\nu - \frac{1}{2}\partial_\mu H \partial_\mu H - \\
 & \frac{1}{2}g^2 H^2 - \partial_\mu \phi^+ \partial_\mu \phi^- - M^2 \phi^+ \phi^- - \frac{1}{2}\partial_\mu \phi^0 \partial_\mu \phi^0 - \frac{1}{2\epsilon_0} M \phi^0 \phi^0 - \beta_h (2M^2 H + \\
 & \frac{2M}{g} H + \frac{1}{g^2} (H^2 + \phi^0 \phi^0 + 2\phi^+ \phi^-)) + \frac{2M^4}{g^2} \alpha_h - ig_{cw} [\partial_\mu Z_\nu^0 (W_\mu^+ W_\nu^- - \\
 & W_\nu^+ W_\mu^-) - Z_\nu^0 (W_\mu^+ \partial_\nu W_\mu^- - W_\mu^+ \partial_\nu W_\nu^-) + Z_\mu^0 (W_\nu^+ \partial_\mu W_\nu^- - \\
 & W_\nu^- \partial_\mu W_\mu^+) - ig_{sw} [\partial_\nu A_\mu (W_\mu^+ W_\nu^- - W_\nu^+ W_\mu^-) - A_\nu (W_\mu^+ \partial_\nu W_\mu^- - \\
 & W_\mu^- \partial_\nu W_\mu^+) + A_\mu (W_\nu^+ \partial_\mu W_\nu^- - W_\nu^- \partial_\mu W_\mu^+)] - \frac{1}{2}g^2 W_\mu^+ W_\mu^- W_\nu^+ W_\nu^- + \\
 & \frac{1}{2}g^2 W_\mu^+ W_\nu^- W_\mu^+ W_\nu^- + g^2 c_w^2 (Z_\mu^0 W_\nu^+ Z_\nu^0 W_\mu^- - Z_\mu^0 Z_\nu^0 W_\mu^+ W_\nu^-) + \\
 & g^2 s_w^2 (A_\mu W_\nu^+ A_\nu W_\mu^- - A_\mu A_\nu W_\mu^+ W_\nu^-) + g^2 s_w c_w [A_\mu Z_\nu^0 (W_\mu^+ W_\nu^- - \\
 & W_\nu^+ W_\mu^-) - 2A_\mu Z_\mu^0 W_\nu^+ W_\nu^-] - g\alpha [H^3 + H\phi^0 \phi^0 + 2H\phi^+ \phi^-] - \\
 & \frac{1}{8}g^2 \alpha_h [H^4 + (\phi^0)^4 + 4(\phi^+ \phi^-)^2 + 4(\phi^0)^2 \phi^+ \phi^- + 4H^2 \phi^+ \phi^- + 2(\phi^0)^2 H^2] - \\
 & gM W_\mu^+ W_\mu^- H - \frac{1}{2}g \frac{M}{c_w^2} Z_\mu^0 Z_\mu^0 H - \frac{1}{2}ig [W_\mu^+ (H\partial_\mu \phi^- - \phi^- \partial_\mu H) - W_\mu^- (\phi^+ \partial_\mu H - \\
 & H\partial_\mu \phi^+) + \frac{1}{2}g \frac{1}{c_w} (Z_\mu^0 (H\partial_\mu \phi^0 - \phi^0 \partial_\mu H) - ig \frac{s_w^2}{c_w} Z_\mu^0 (W_\mu^+ \phi^- - W_\mu^- \phi^+) + \\
 & ig s_w M A_\mu (W_\mu^+ \phi^- - W_\mu^- \phi^+) - ig \frac{1-2c_w^2}{2c_w} Z_\mu^0 (\phi^+ \partial_\mu \phi^- - \phi^- \partial_\mu \phi^+) + \\
 & ig s_w A_\mu (\phi^+ \partial_\mu \phi^- - \phi^- \partial_\mu \phi^+) - \frac{1}{4}g^2 W_\mu^+ W_\mu^- [H^2 + (\phi^0)^2 + 2\phi^+ \phi^-] - \\
 & \frac{1}{4}g^2 \frac{1}{c_w^2} Z_\mu^0 Z_\mu^0 [H^2 + (\phi^0)^2 + 2(2s_w^2 - 1)^2 \phi^+ \phi^-] - \frac{1}{2}g^2 \frac{s_w^2}{c_w} Z_\mu^0 \phi^0 (W_\mu^+ \phi^- + \\
 & W_\mu^- \phi^+) - \frac{1}{2}ig^2 \frac{s_w^2}{c_w} Z_\mu^0 H (W_\mu^+ \phi^- - W_\mu^- \phi^+) + \frac{1}{2}g^2 s_w A_\mu \phi^0 (W_\mu^+ \phi^- + \\
 & W_\mu^- \phi^+) + \frac{1}{2}ig^2 s_w A_\mu H (W_\mu^+ \phi^- - W_\mu^- \phi^+) - g^2 \frac{2s_w}{c_w} (2c_w^2 - 1) Z_\mu^0 A_\mu \phi^+ \phi^- - \\
 & g^1 s_w^2 A_\mu A_\mu \phi^+ \phi^- - \bar{e}^\lambda (\gamma \partial + m_e^\lambda) e^\lambda - \bar{\nu}^\lambda \gamma \partial \nu^\lambda - \bar{u}_j^\lambda (\gamma \partial + m_u^\lambda) u_j^\lambda - \\
 & \bar{d}_j^\lambda (\gamma \partial + m_d^\lambda) d_j^\lambda + ig s_w A_\mu [-(\bar{e}^\lambda \gamma^\mu e^\lambda) + \frac{2}{3}(\bar{u}_j^\lambda \gamma^\mu u_j^\lambda) - \frac{1}{3}(\bar{d}_j^\lambda \gamma^\mu d_j^\lambda)] + \\
 & \frac{ig}{4c_w} Z_\mu^0 [(\bar{\nu}^\lambda \gamma^\mu (1 + \gamma^5) \nu^\lambda) + (\bar{e}^\lambda \gamma^\mu (4s_w^2 - 1 - \gamma^5) e^\lambda) + (\bar{u}_j^\lambda \gamma^\mu (\frac{2}{3}s_w^2 - \\
 & 1 - \gamma^5) u_j^\lambda) + (\bar{d}_j^\lambda \gamma^\mu (1 - \frac{2}{3}s_w^2 - \gamma^5) d_j^\lambda)] + \frac{ig}{2\sqrt{2}} W_\mu^+ [(\bar{\nu}^\lambda \gamma^\mu (1 + \gamma^5) e^\lambda) + \\
 & (\bar{u}_j^\lambda \gamma^\mu (1 + \gamma^5) C_{\lambda k} d_j^k)] + \frac{ig}{2\sqrt{2}} W_\mu^- [(\bar{e}^\lambda \gamma^\mu (1 + \gamma^5) \nu^\lambda) + (\bar{d}_j^\lambda C_{\lambda k}^\dagger \gamma^\mu (1 + \\
 & \gamma^5) u_j^k)] + \frac{ig}{2\sqrt{2}} \frac{m_h^2}{M} [-\phi^+ (\bar{\nu}^\lambda (1 - \gamma^5) e^\lambda) + \phi^- (\bar{e}^\lambda (1 + \gamma^5) \nu^\lambda)] - \\
 & \frac{g}{2} \frac{m_h^2}{M} [H (\bar{e}^\lambda e^\lambda) + i\phi^0 (\bar{e}^\lambda \gamma^5 e^\lambda)] + \frac{ig}{2M\sqrt{2}} \phi^+ [-m_h^2 (\bar{u}_j^\lambda C_{\lambda k} (1 - \gamma^5) d_j^k) + \\
 & m_h^2 (\bar{u}_j^\lambda C_{\lambda k} (1 + \gamma^5) d_j^k) + \frac{ig}{2M\sqrt{2}} \phi^- [m_h^2 (\bar{d}_j^\lambda C_{\lambda k}^\dagger (1 + \gamma^5) u_j^k) - m_h^2 (\bar{d}_j^\lambda C_{\lambda k}^\dagger (1 - \\
 & \gamma^5) u_j^k) - \frac{g}{2} \frac{m_h^2}{M} H (\bar{u}_j^\lambda u_j^k) - \frac{g}{2} \frac{m_h^2}{M} H (\bar{d}_j^\lambda d_j^k) + \frac{ig}{2} \frac{m_h^2}{M} \phi^0 (\bar{u}_j^\lambda \gamma^5 u_j^k) - \\
 & \frac{ig}{2} \frac{m_h^2}{M} \phi^0 (\bar{d}_j^\lambda \gamma^5 d_j^k) + \bar{X} + (\partial^2 - M^2) X + \bar{X} - (\partial^2 - M^2) X - \bar{X}^0 (\partial^2 - \\
 & \frac{M^2}{c_w^2}) X^0 + \bar{Y} \partial^2 Y + ig_{cw} W_\mu^+ (\partial_\mu \bar{X}^0 X^- - \partial_\mu \bar{X}^+ X^0) + ig_{sw} W_\mu^+ (\partial_\mu \bar{Y} X^- - \\
 & \partial_\mu \bar{X}^+ Y) + ig_{cw} W_\mu^- (\partial_\mu \bar{X}^- X^0 - \partial_\mu \bar{X}^0 X^+) + ig_{sw} W_\mu^- (\partial_\mu \bar{X}^- Y - \\
 & \partial_\mu \bar{Y} X^+) + ig_{cw} Z_\mu^0 (\partial_\mu \bar{X}^+ X^- - \partial_\mu \bar{X}^- X^+) + ig_{sw} A_\mu (\partial_\mu \bar{X}^+ X^- - \\
 & \partial_\mu \bar{X}^- X^+) - \frac{1}{2}gM [\bar{X}^+ X^+ H + \bar{X}^- X^- H + \frac{1}{c_w^2} \bar{X}^0 X^0 H] + \\
 & \frac{1-2c_w^2}{2c_w} igM [\bar{X}^+ X^0 \phi^+ - \bar{X}^- X^0 \phi^-] + \frac{1}{2c_w} igM [\bar{X}^0 X^- \phi^+ - \bar{X}^0 X^+ \phi^-] + \\
 & igM s_w [\bar{X}^0 X^- \phi^+ - \bar{X}^0 X^+ \phi^-] + \frac{1}{2}igM [\bar{X}^+ X^+ \phi^0 - \bar{X}^- X^- \phi^0]
 \end{aligned}$$

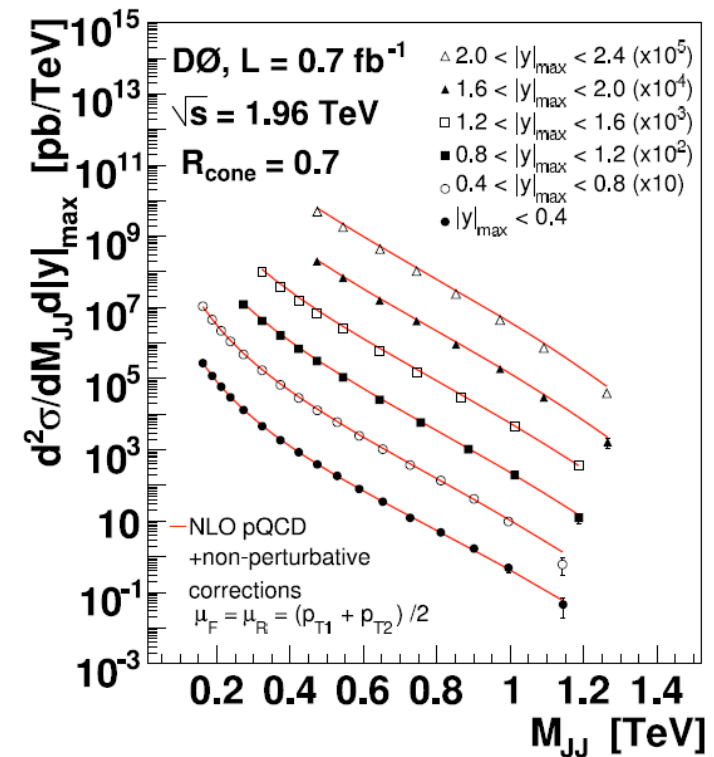
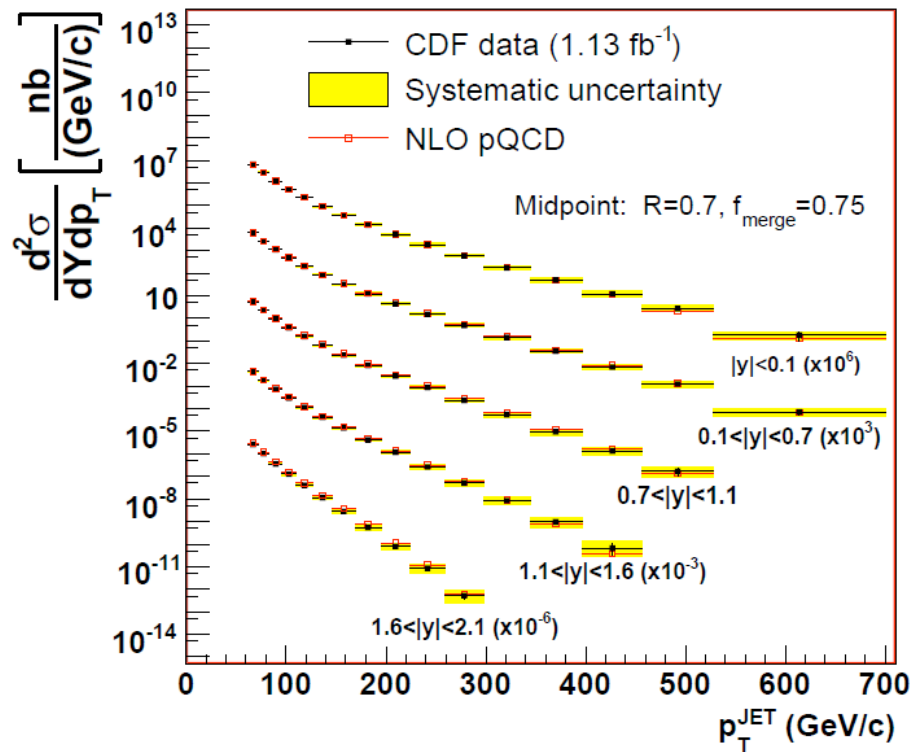
QCD & Jets at the LHC

- QCD is ideal candidate for early LHC physics
- Strongly coupled theory \rightarrow large production cross-sections for jets (collimated flows of hadrons)
- Relatively “simple” final state topologies with close connection to detector performance, e.g. jet calibration
- Tests of Standard Model
 - Probes of NLO perturbative QCD
 - Also sensitive to non-perturbative effects
- Jets are perfect to discover new physics
 - Large production cross-sections and small backgrounds
 - Highest sensitivity to new physics with early data
- Background to many new physics channels



Existing jet measurements

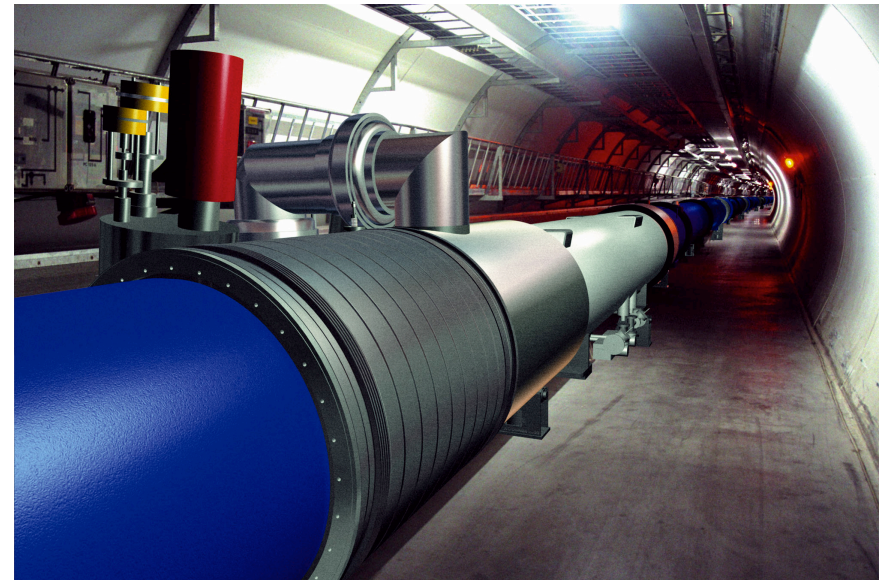
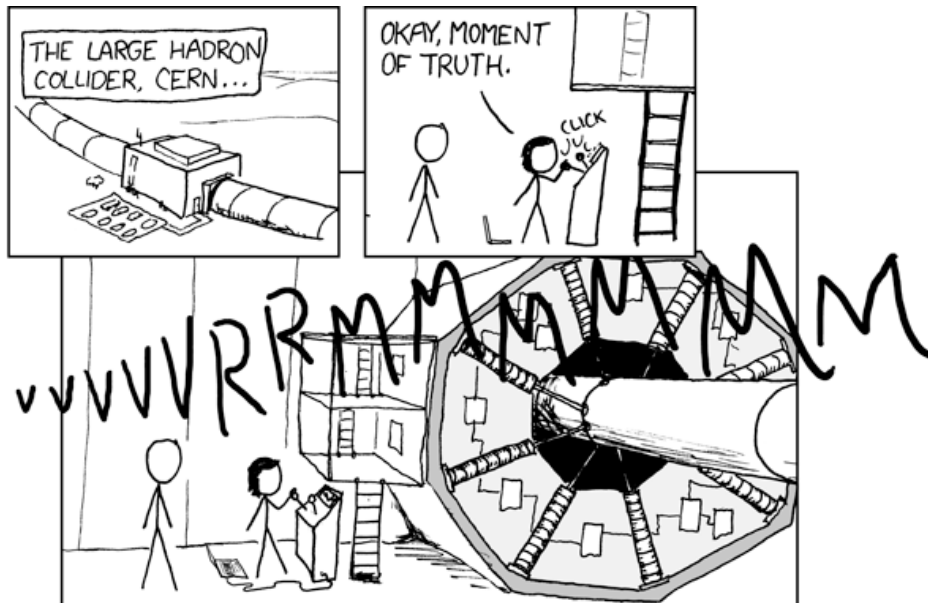
- Many jet measurements using Tevatron ppbar collider at Fermilab
- Inclusive jet pT spectrum extends to p_T of 700 GeV (left: CDF)
- Dijet mass spectrum up to 1.4 TeV (right: D0)



Enter the LHC...

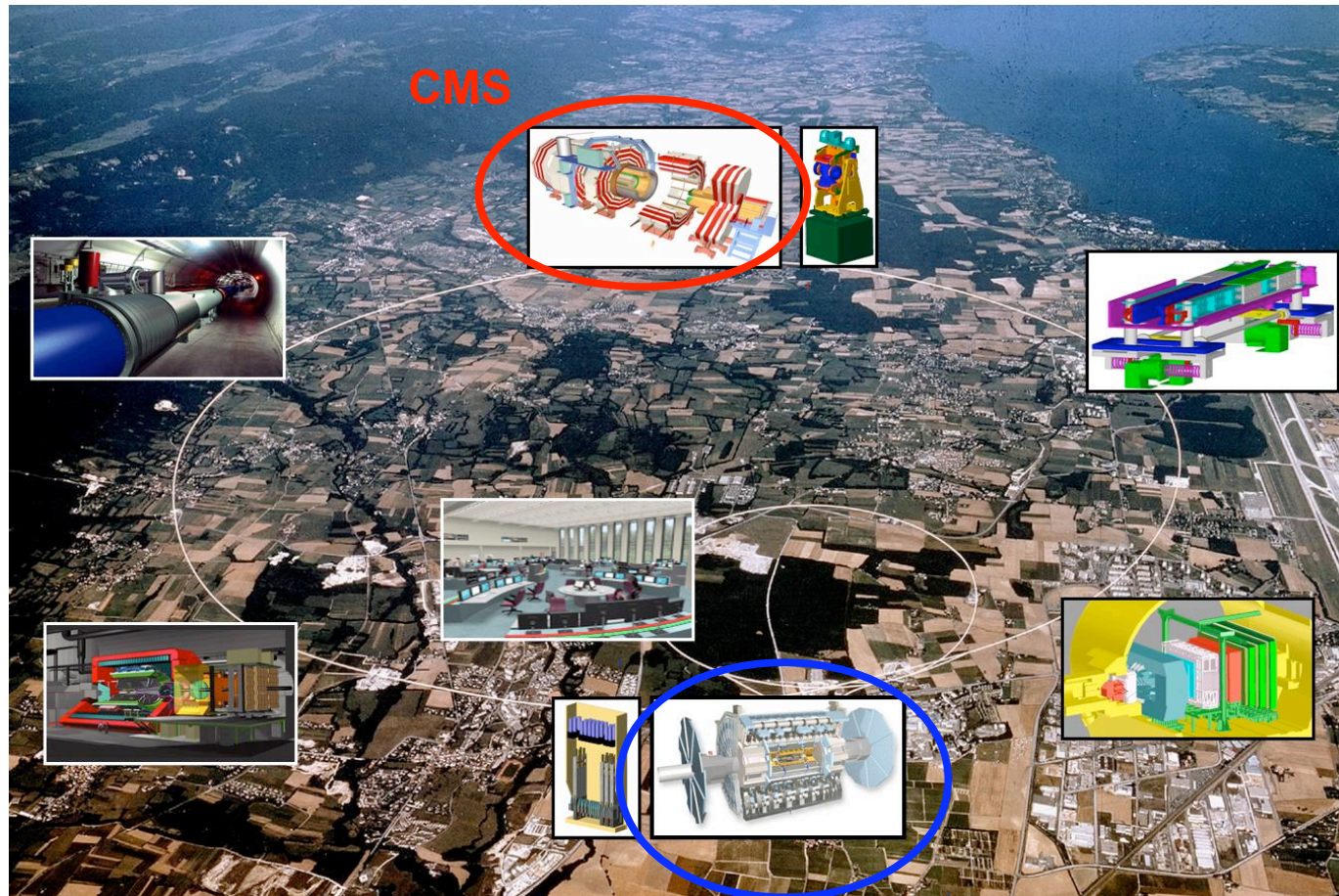
High- p_T jet factory

- CERN Large Hadron Collider (LHC) in Geneva, Switzerland has a monopoly on high- p_T jet production
- Highest p_T jets and largest dijet masses ever produced
 - pp collisions at $\sqrt{s} = 7$ TeV (design of 14 TeV)
 - 3.5 times larger center-of-mass energy than Tevatron



CERN Large Hadron Collider

- ATLAS and CMS are two general-purpose detectors at the LHC
- Relatively small statistics, but *accelerating* quickly



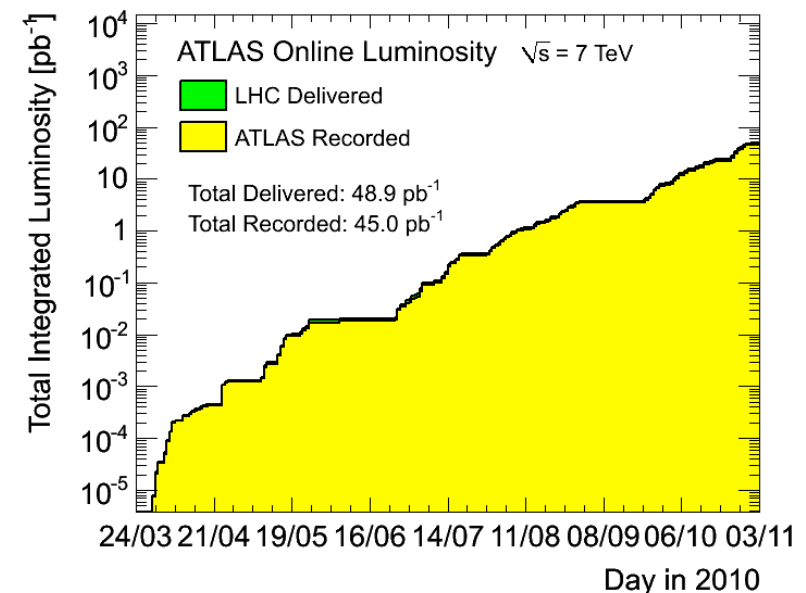
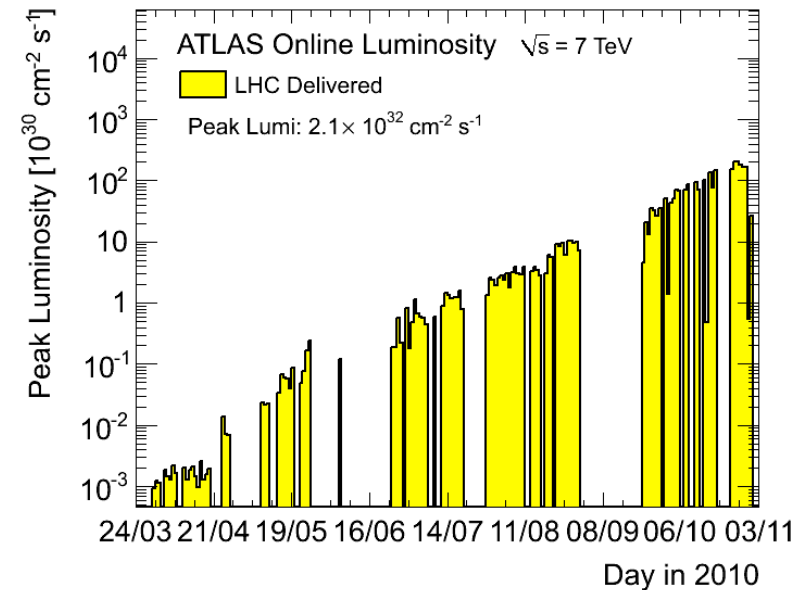
LHC proton beams at 3.5 TeV

- After initial hiccup during first beam in November 2008, performance of the LHC has been outstanding
 - First collisions at 900 GeV in late 2009
 - Collisions at 7 TeV in early 2010
 - Intense media coverage led to unintended comedy at times



Luminosity of the machine

- Instantaneous luminosity increased by 5 orders of magnitude since March
 - Peak instantaneous luminosity in 2010 = $2.1 \times 10^{32} \text{ cm}^{-2} \text{ s}^{-1}$
- Dataset
 - ICHEP (July): 17 nb^{-1}
 - These results: 3 pb^{-1}
 - Full 2010 dataset (Winter): 45 pb^{-1}

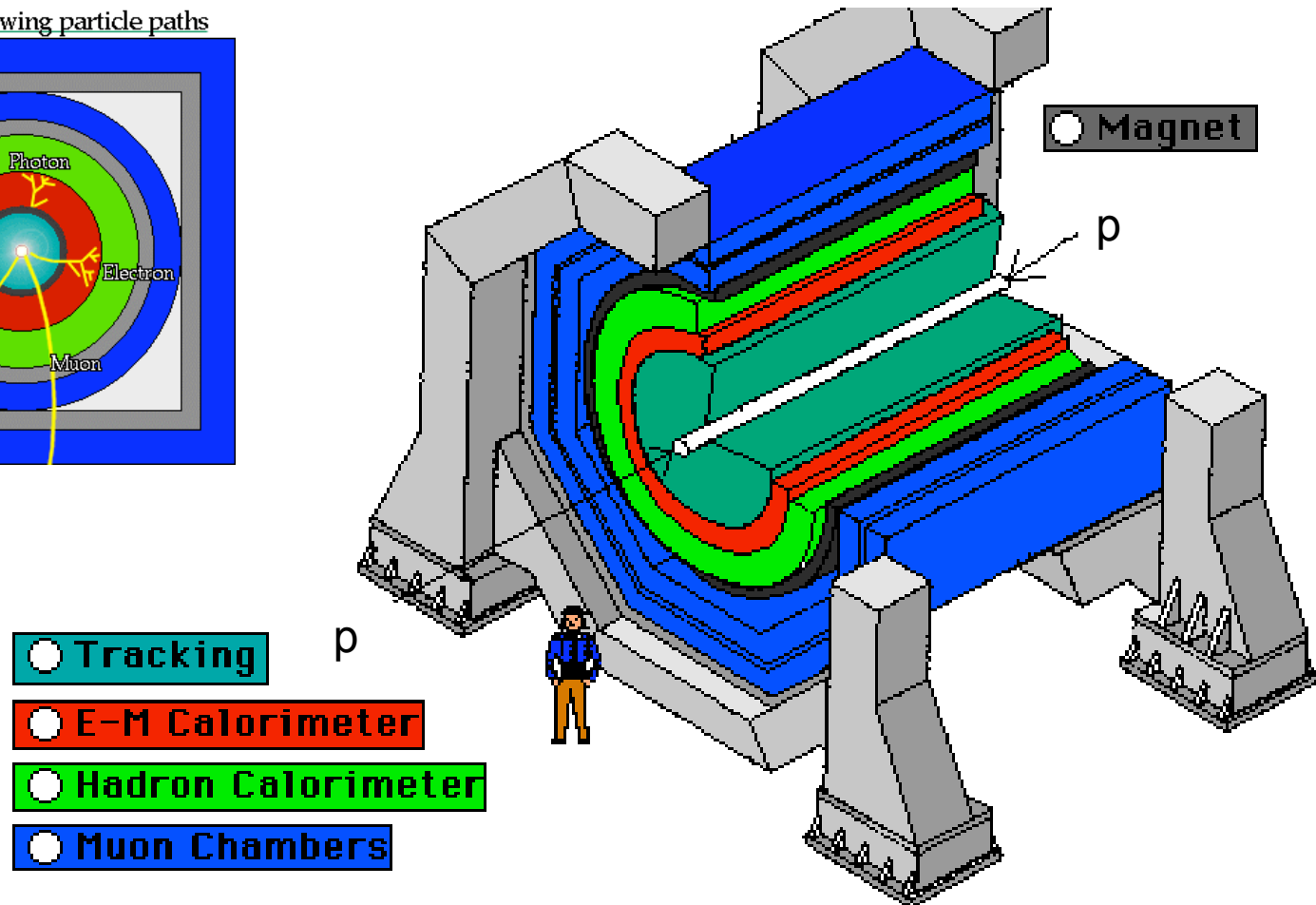
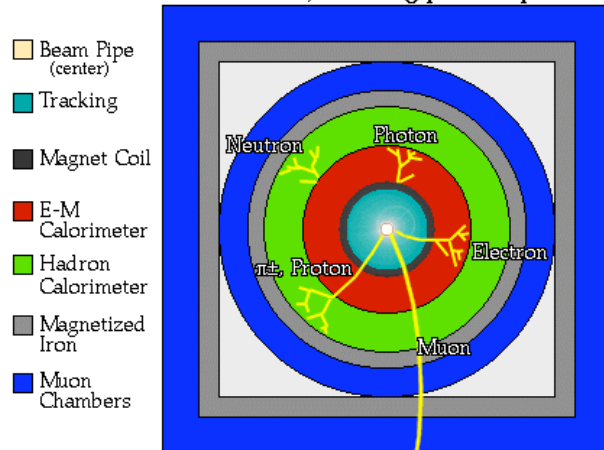


The ATLAS experiment

ATLAS Detector (schematic)

- Schematic of a general-purpose detector

A detector cross-section, showing particle paths



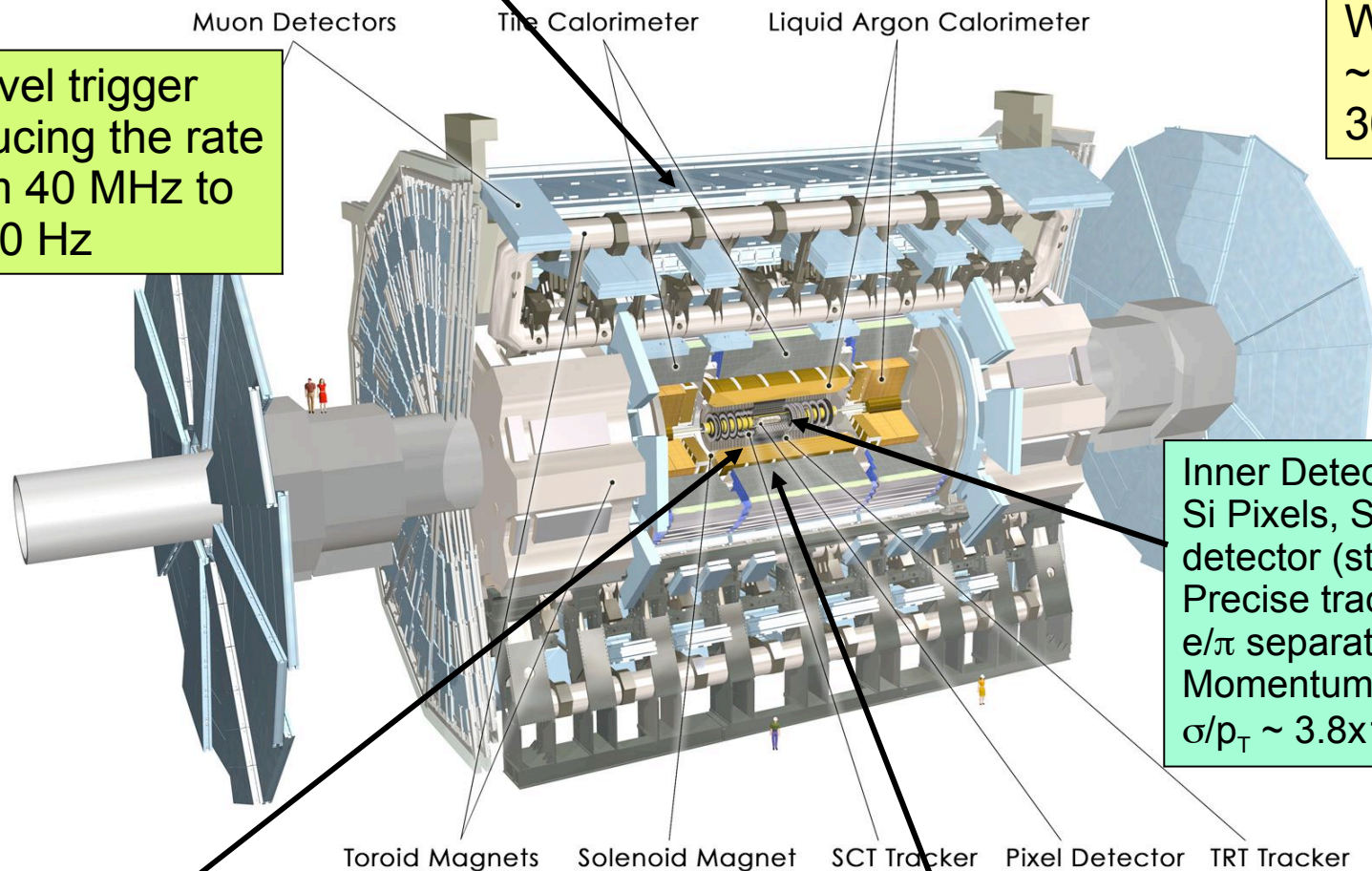
Muon Spectrometer ($|\eta| < 2.7$) : air-core toroids with gas-based muon chambers
Muon trigger and measurement with momentum resolution $< 10\%$ up to $E_\mu \sim 1$ TeV

ATLAS Detector

Length : ~ 46 m
Radius : ~ 12 m
Weight : ~ 7000 tons
 $\sim 10^8$ electronic channels
3000 km of cables

3-level trigger
reducing the rate
from 40 MHz to
 ~ 200 Hz

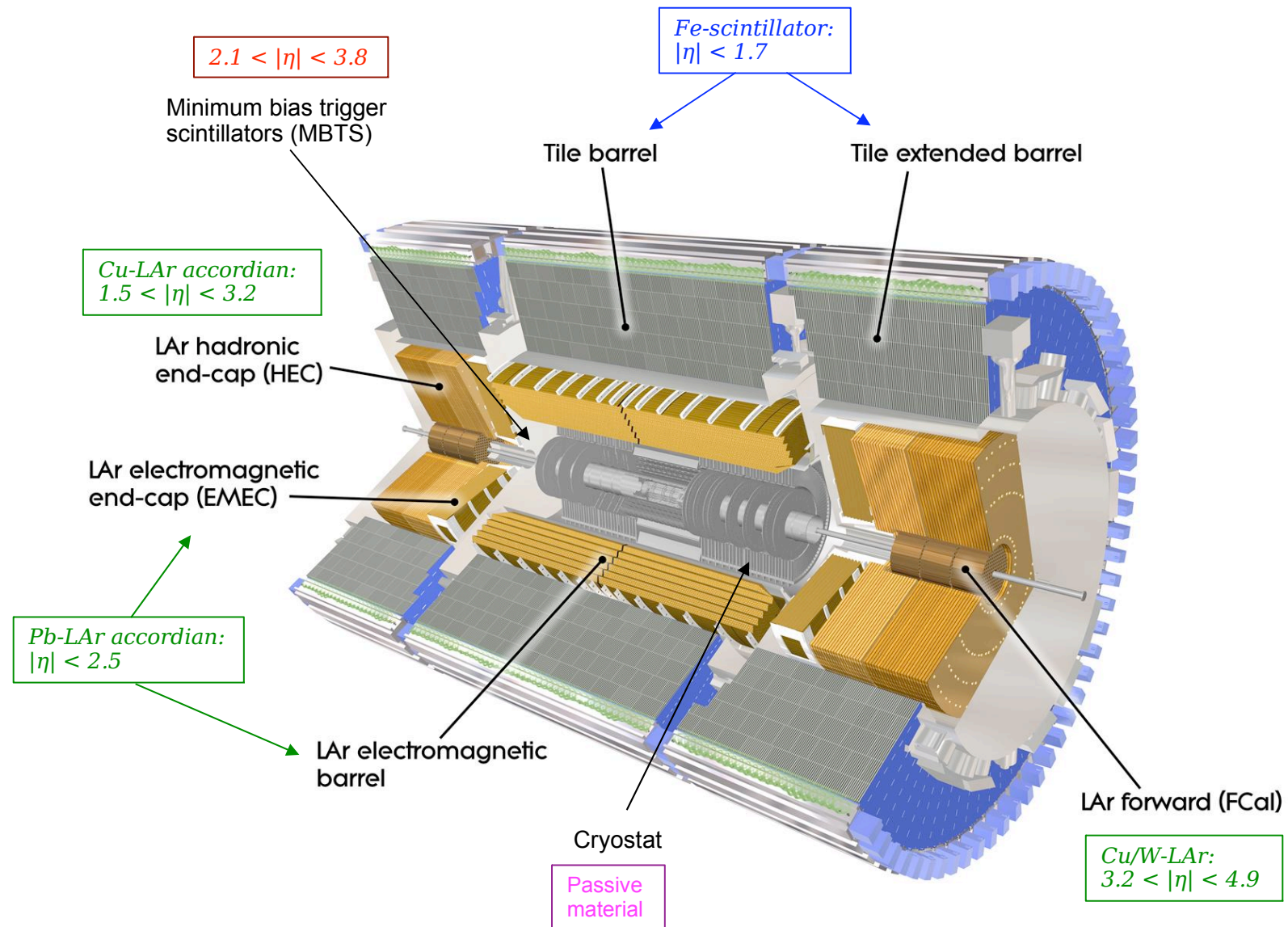
Inner Detector ($|\eta| < 2.5$, $B=2$ T):
Si Pixels, Si strips, Transition Radiation
detector (straws)
Precise tracking and vertexing,
 e/π separation
Momentum resolution:
 $\sigma/p_T \sim 3.8 \times 10^{-4} p_T (\text{GeV}) \oplus 0.015$



EM calorimeter: Pb-LAr Accordion
 e/γ trigger, identification and measurement
E-resolution: $\sigma/E \sim 10\%/\sqrt{E}$

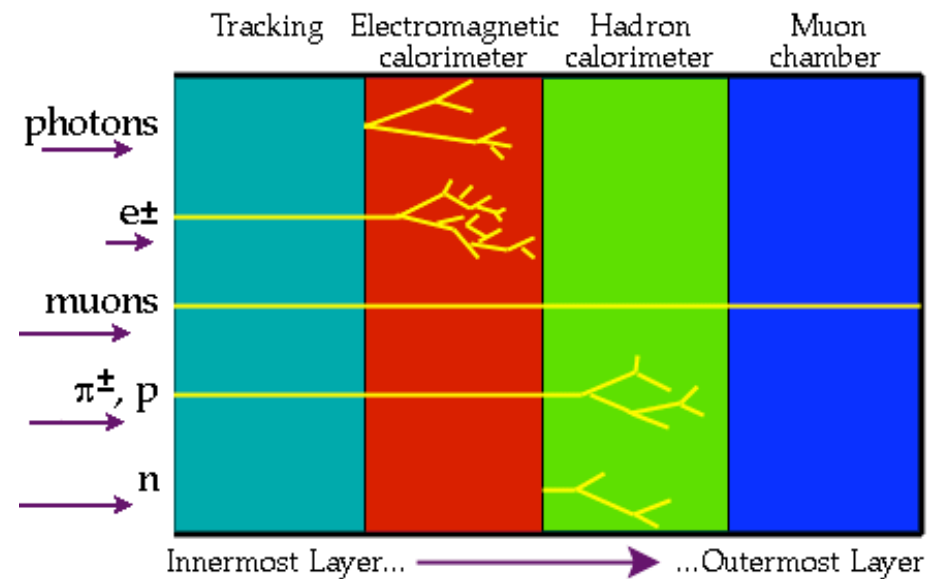
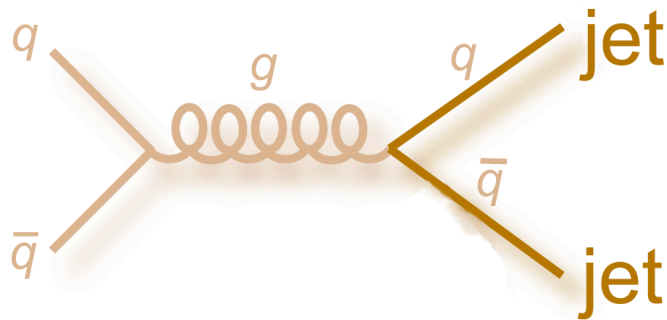
HAD calorimetry ($|\eta| < 5$): segmentation, hermeticity
Fe/scintillator Tiles (central), Cu/W-LAr (fwd)
Trigger and measurement of jets and missing E_T
E-resolution: $\sigma/E \sim 50\%/\sqrt{E} \oplus 0.03$

ATLAS Calorimeter



Inclusive jet production


- Leading order diagram in SM is dijet production
 - Deposits energy primarily in hadronic calorimeter
- Define jets inclusively as: “calorimeter energy deposition”
 - Backgrounds from electrons, photons, etc are negligible because QCD cross-sections are so large



“QCD in Year One”: Then and Now

- At the ATLAS Workshop of the Americas at NYU in 2009, I described in the QCD plenary the various jet measurements we expected to make with the first year of data.
- After ~ 8 months of pp collisions at 7 TeV, where do we stand now?
 - Inclusive jet p_T ☒
 - Dijet mass spectrum ☒
 - Dijet χ angular distribution ☒
 - Dijet $\Delta\phi$ decorrelation ☒
 - Dijets with rapidity gaps ☒
 - Multi-jets ☒
 - W/Z + jets ☒
 - Jet shapes ☒
 - Searches for exotica ☒
 - Plus a bonus (jet quenching) in lead ion collisions! ☒

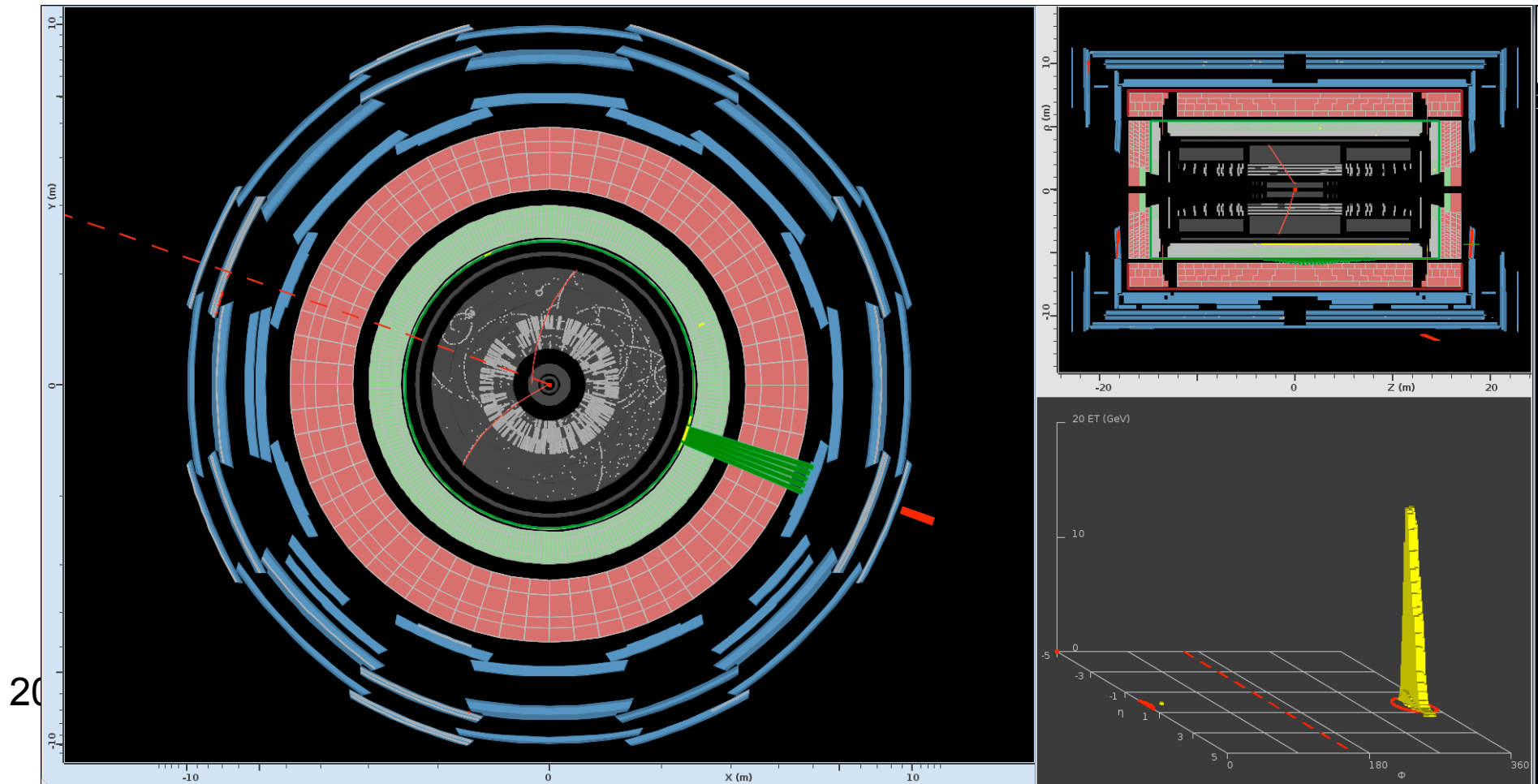
“QCD in Year One”: Then and Now

- At the ATLAS Workshop of the Americas at NYU in 2009, I described in the QCD plenary the various jet measurements we expected to make with the first year of data.
 - After ~ 8 months of pp collisions at 7 TeV, where do we stand now?
 - **Inclusive jet p_T** ☒
 - **Dijet mass spectrum** ☒
 - **Dijet χ angular distribution** ☒
 - Dijet $\Delta\phi$ decorrelation ☒
 - Dijets with rapidity gaps ☒
 - Multi-jets ☒
 - W/Z + jets ☒
 - Jet shapes ☒
 - **Searches for exotica** ☒
 - **Plus a bonus (jet quenching) in lead ion collisions!** ☒
- 
- Will focus on these analyses today

What do jets look like in the ATLAS calorimeter?

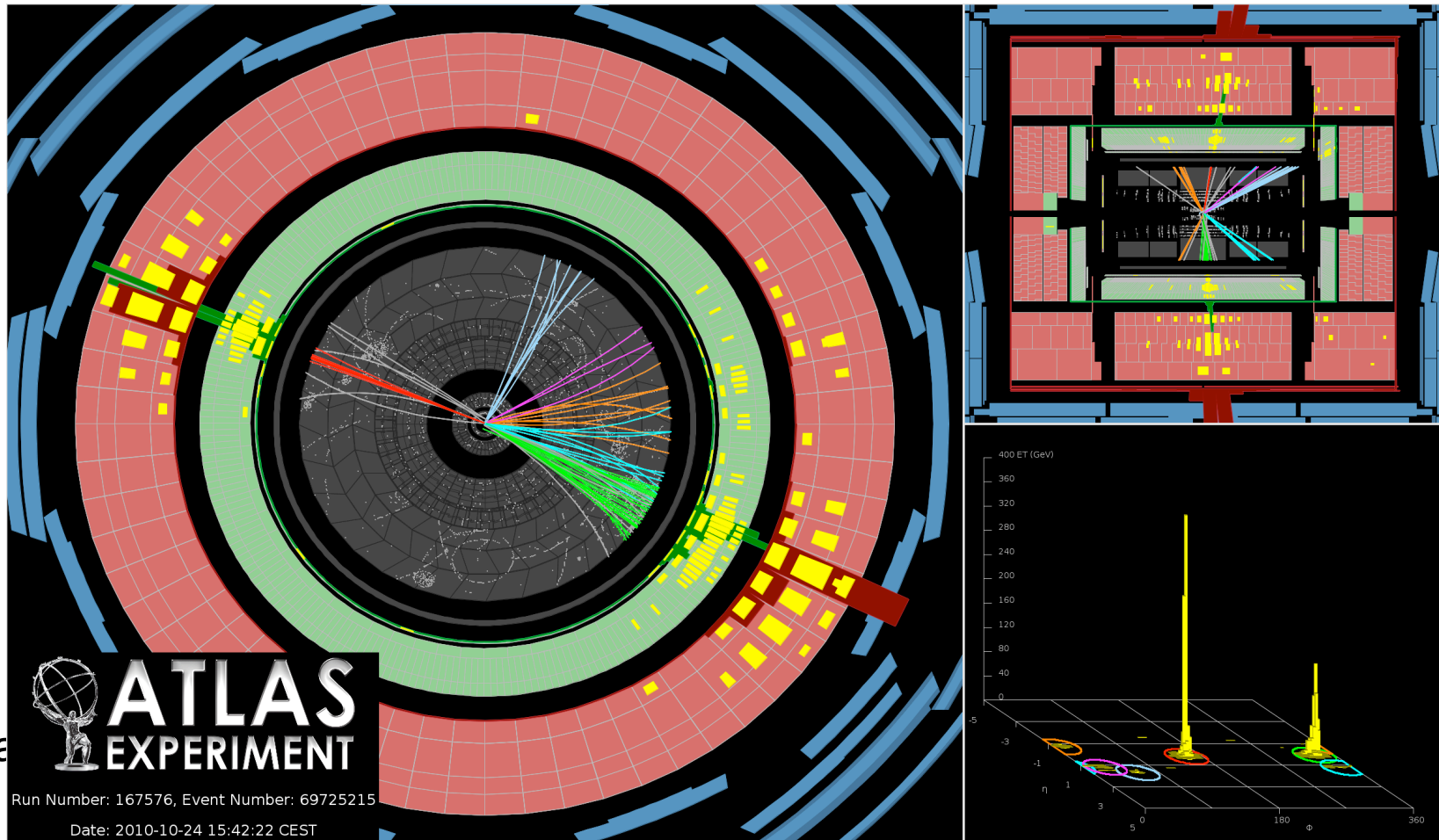
What a high p_T jet does NOT look like

- **Fake** jet with p_T of 1.1 TeV
 - Beam halo particle showers longitudinally in EM presampler so its energy receives large weight
- Missing ET = 1.3 TeV (exactly opposite in ϕ to leading jet)
- Add jet cleaning cuts to reject fake jets like this



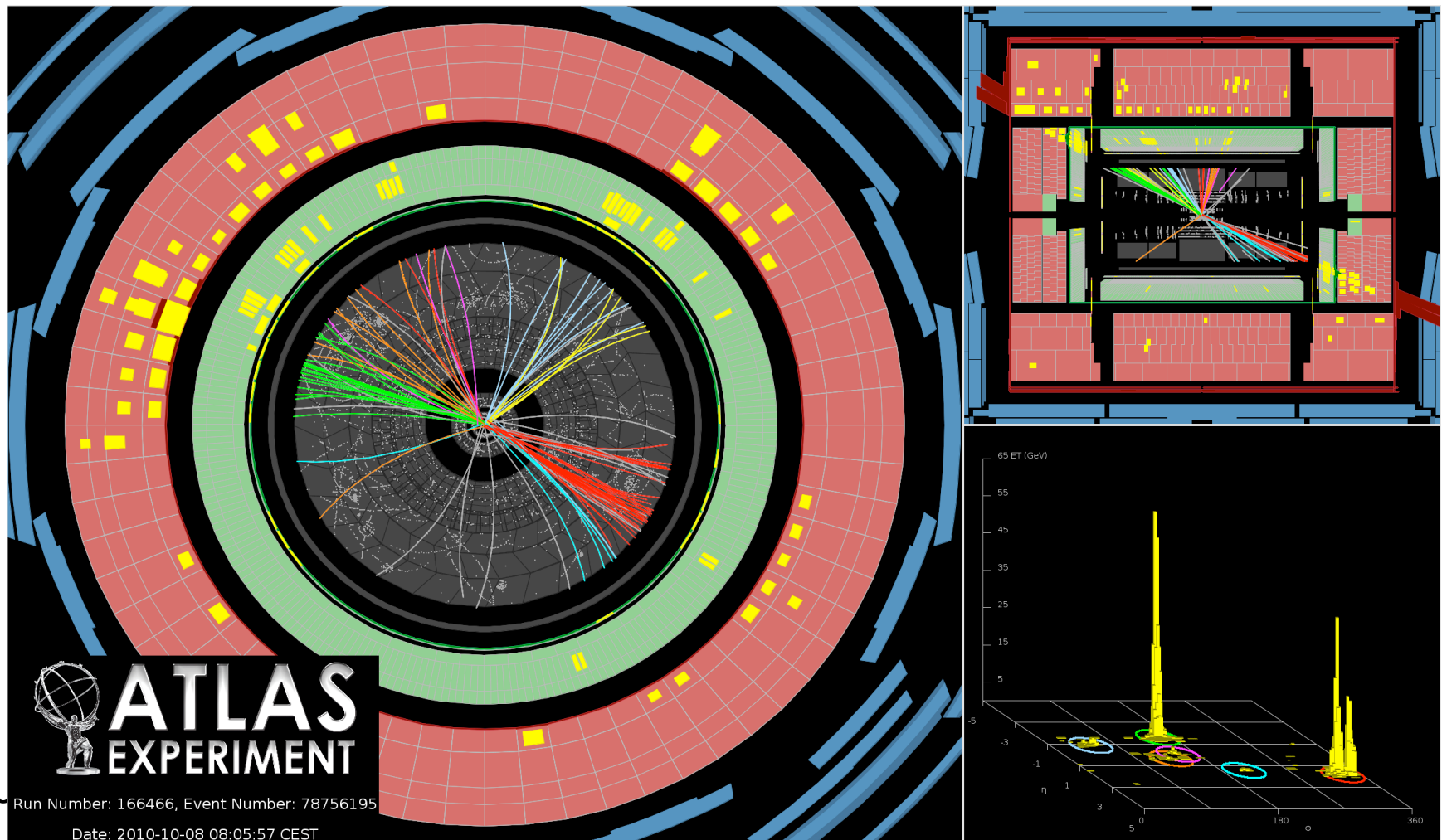
High p_T jet (1.3 TeV) and large central dijet mass (2.6 TeV)

- Two central, well-measured jets in $|y| < 0.8$ with very high- p_T
 - 1st jet: $p_T = 1.3$ TeV, $\eta = 0.2$, $\phi = 2.8$
 - 2nd jet: $p_T = 1.2$ TeV, $\eta = 0.0$, $\phi = -0.5$
- These events are the most interesting because they have large momentum transfer and s-channel is more sensitive to new physics



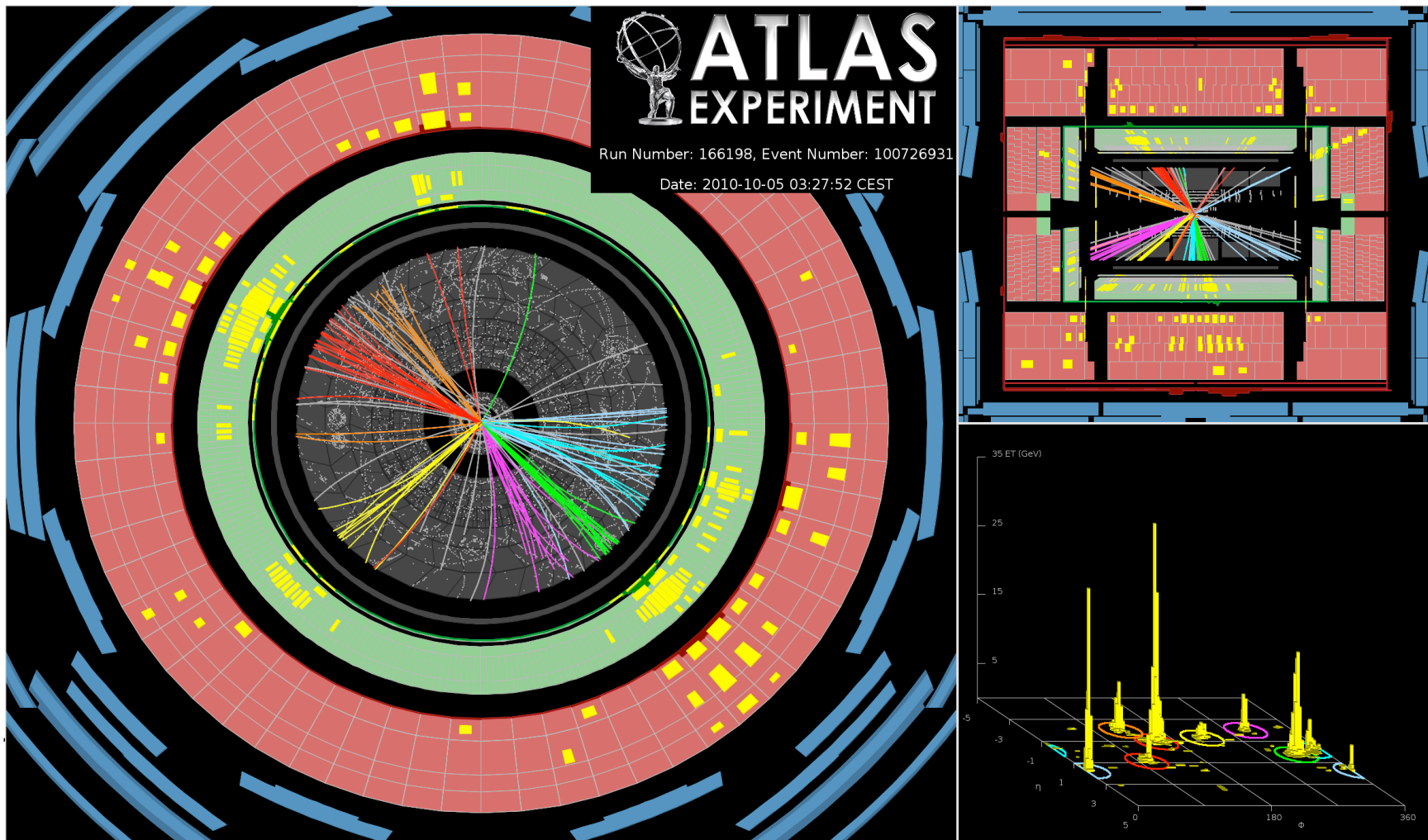
Large dijet mass (3.7 TeV)

- Dijet mass generated by rapidity separation of forward jets
 - 1st jet: $p_T = 670$ GeV, $\eta = 1.9$, $\phi = -0.5$
 - 2nd jet: $p_T = 610$ GeV, $\eta = -1.6$, $\phi = 2.8$
- Characteristic of t-channel and u-channel scattering in QCD



High jet multiplicity event (8 jets above $p_T = 60$ GeV)

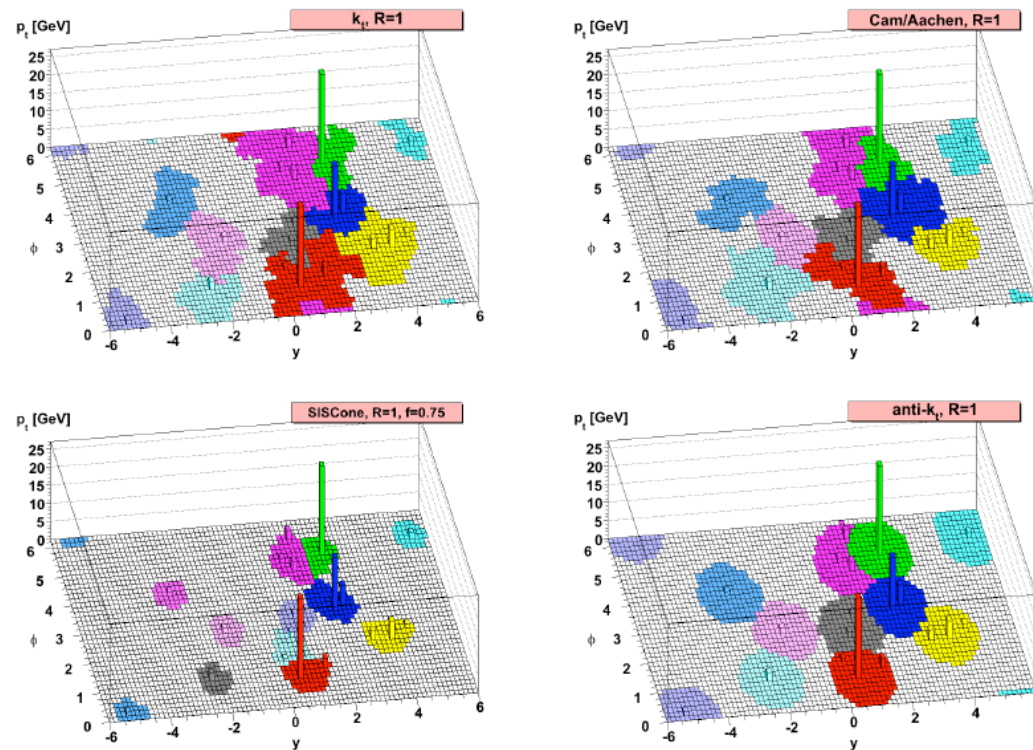
- Eight jets between 60-300 GeV (associated to single primary vertex)
 - 1st jet: $p_T = 290$ GeV, $\eta = -0.9$, $\phi = 2.7$
 - 2nd jet: $p_T = 220$ GeV, $\eta = 0.3$, $\phi = -0.7$
- Exemplifies large amount of gluon radiation



Jet trigger, reconstruction, selection, and calibration

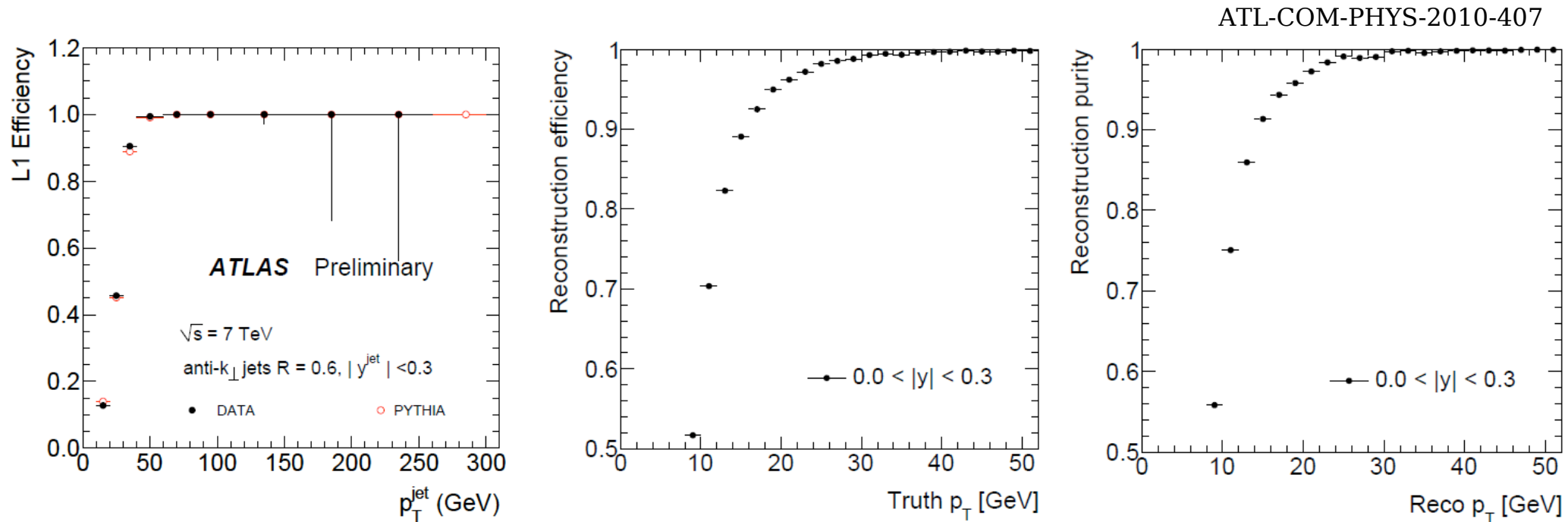
Jet reconstruction

- Jets reconstructed offline from calorimeter energy clusters using anti- k_T jet algorithm with clustering parameter $R=0.6$
 - Topological clusters are formed from seeds of calorimeter cells above noise thresholds to reject noise
 - Iteratively add neighbors farther away
 - Anti- k_T is an infrared and collinear safe jet algorithm
 - Stable against underlying event and pileup
 - Uniform, cone-like jets



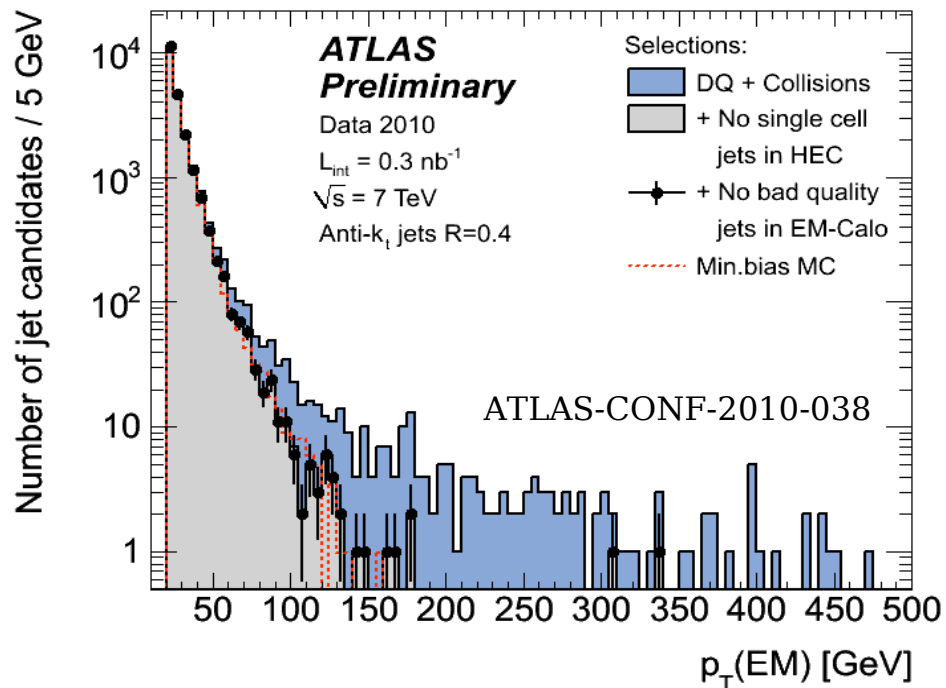
Jet trigger & reconstruction

- Require jet trigger fired
 - Trigger uses simpler and faster algorithms than offline reconstruction
 - Lowest threshold jet trigger efficiency (left) is above 99% for $p_T > 60$ GeV
 - Jet reconstruction efficiency (center) & purity (right) are each above 99% for $p_T > 30$ GeV
- Restrict leading (sub-leading) jet to $p_T > 60$ GeV (30 GeV)



Jet cleaning

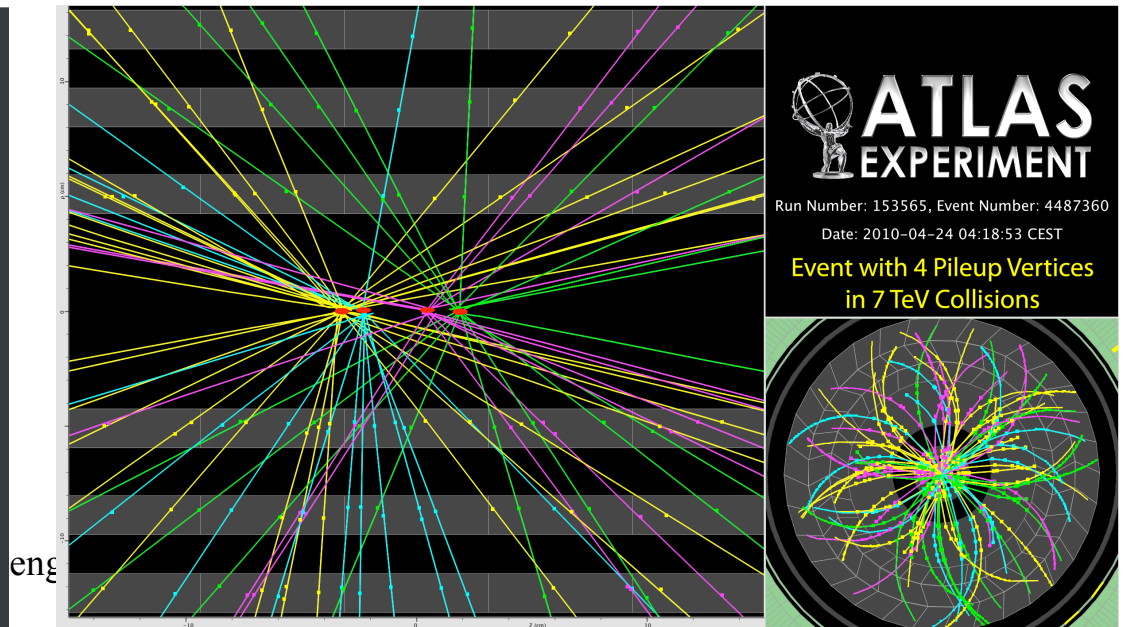
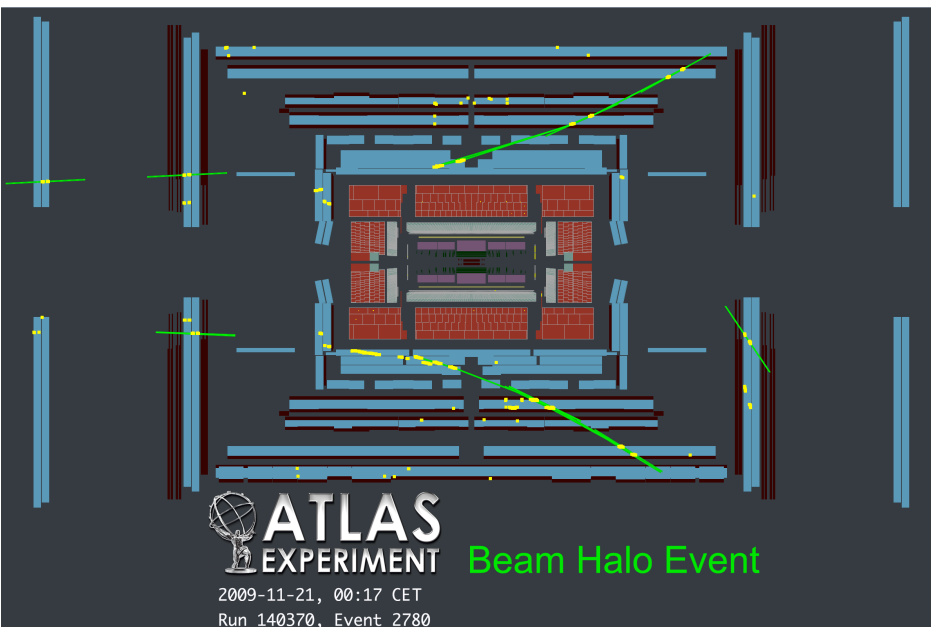
- Events with at least one “bad” jet with $p_T > 10$ GeV at electromagnetic scale anywhere in detector are removed
- “Bad” jet definition is based on cuts designed to remove:



- Noisy cells in the hadronic endcap calorimeter
- Coherent noise in the electromagnetic calorimeter
- Large out-of-time energy depositions, e.g. from cosmic ray muons

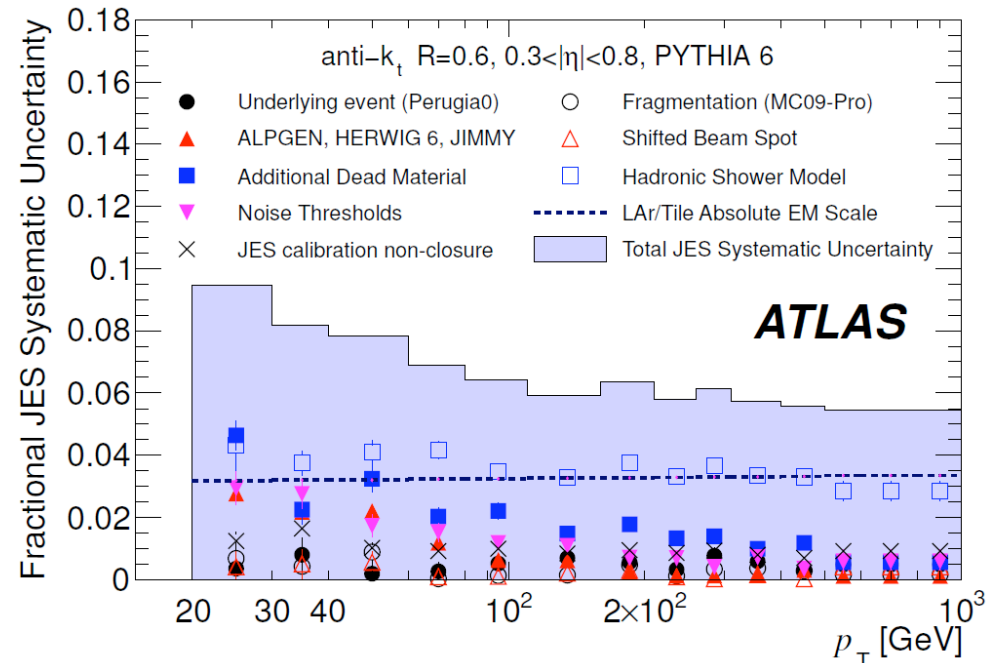
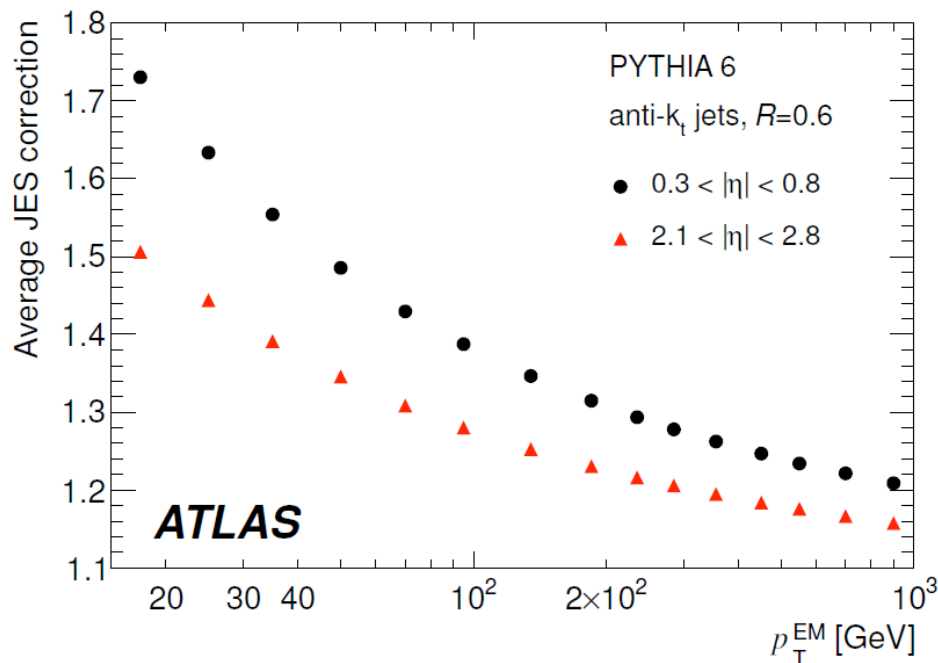
Vertex requirement

- Require at least one vertex reconstructed with at least 5 tracks and $|z| < 10\text{cm}$ (luminous region is $\sim 5\text{cm}$ in early data, somewhat wider later)
 - Suppresses contamination from non-collision backgrounds such as beam halo and beam gas
 - 99% efficient for early data
- Effect of pileup is accounted for in absolute JES uncertainty
- $|z|$ vertex cut also helps to ensure that jets are well-measured because they originate from near the detector center



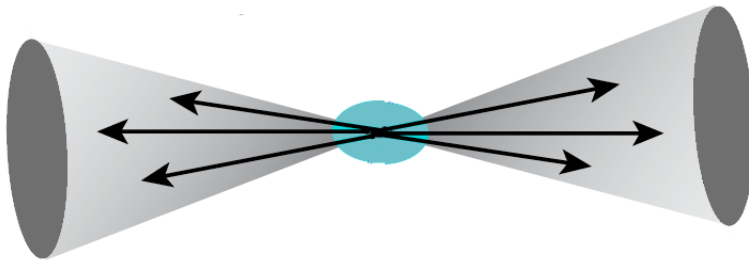
Jet energy scale (JES) calibration

- Jet p_T corrected on average from “EM scale” back to the hadron level using “numerical inversion”
 - MC-based calibration as a function of jet p_T and η
 - Non-linearity for hadrons due to *non-compensation* from nuclear interactions as well as *dead material* upstream
- Absolute JES uncertainty derived via systematic variation of parameters in MC
 - Conservative uncertainty within 7% for central jets with $p_T > 60$ GeV (dominant systematic uncertainty for most jet measurements)
 - Includes pileup uncertainty estimated using tower energy density



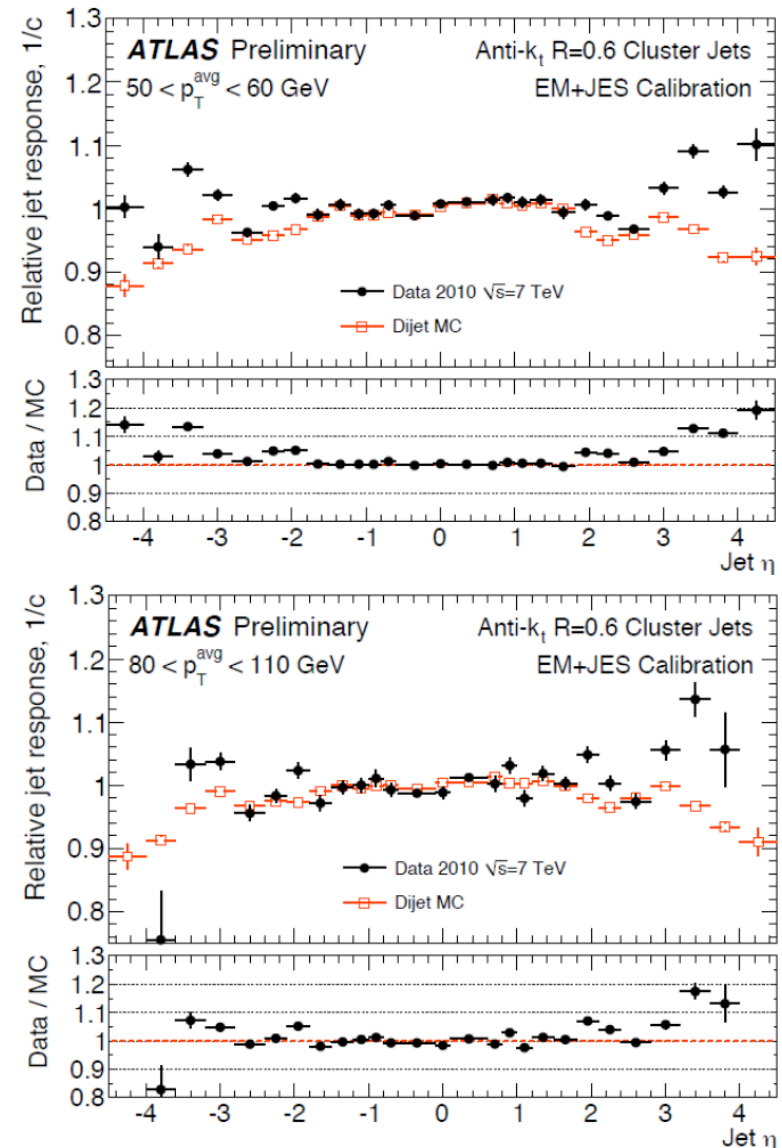
Relative jet energy scale

- Absolute JES assumed fully correlated in pseudorapidity
- Unlike single jets, dijets can span a large pseudorapidity
→ dependence also on the relative JES



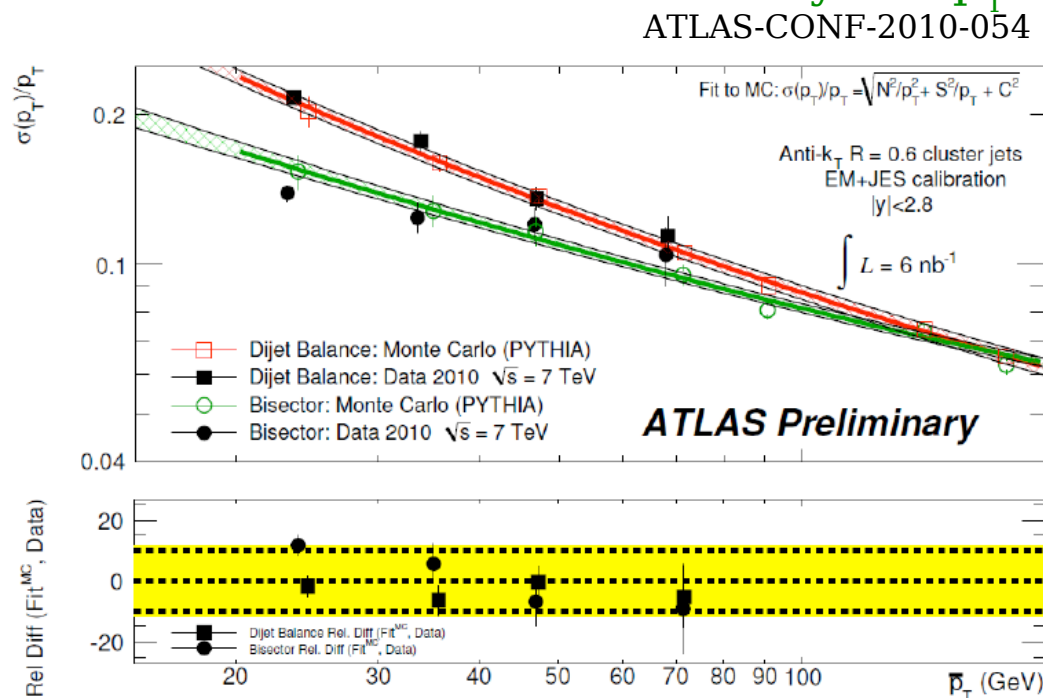
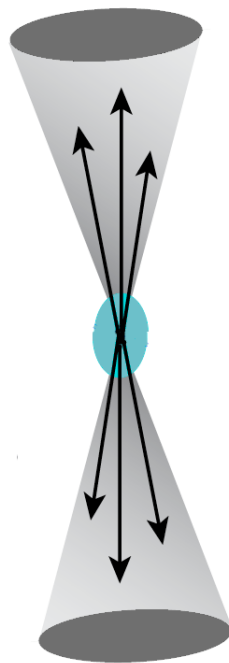
- Dijet balance indicates relative JES of 5% within $|y| < 2.8$
- Diverges to 15% in $2.8 < |y| < 4.5$
- Thus restrict to $|y| < 2.8$ when possible

ATLAS-CONF-2010-055



Jet energy resolution

- Jet energy resolution in MC validated to $\sim 14\%$ via dijet balance and bisector methods (in-situ)
 - Control for systematic uncertainties from underlying event, initial state radiation, etc
 - Initial studies with more data show agreement within 10%
- Jet angular resolution also verified at the level of 20% at very low p_T using track jets as a proxy



What the internal structure of jets looks like

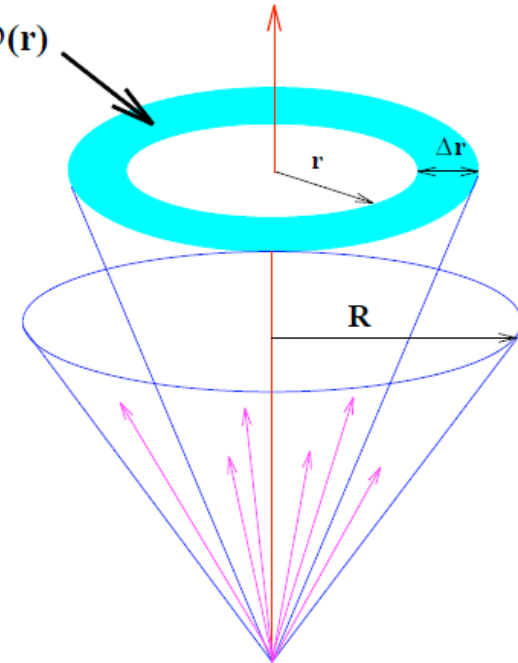
Differential jet shape: Method

- Differential jet shape in inclusive jet production:

$$\rho(r) = \frac{1}{\Delta r} \frac{1}{N^{jet}} \sum_{jets} \frac{p_T(r - \Delta r/2, r + \Delta r/2)}{p_T(0, R)}, \quad 0 \leq r \leq R$$

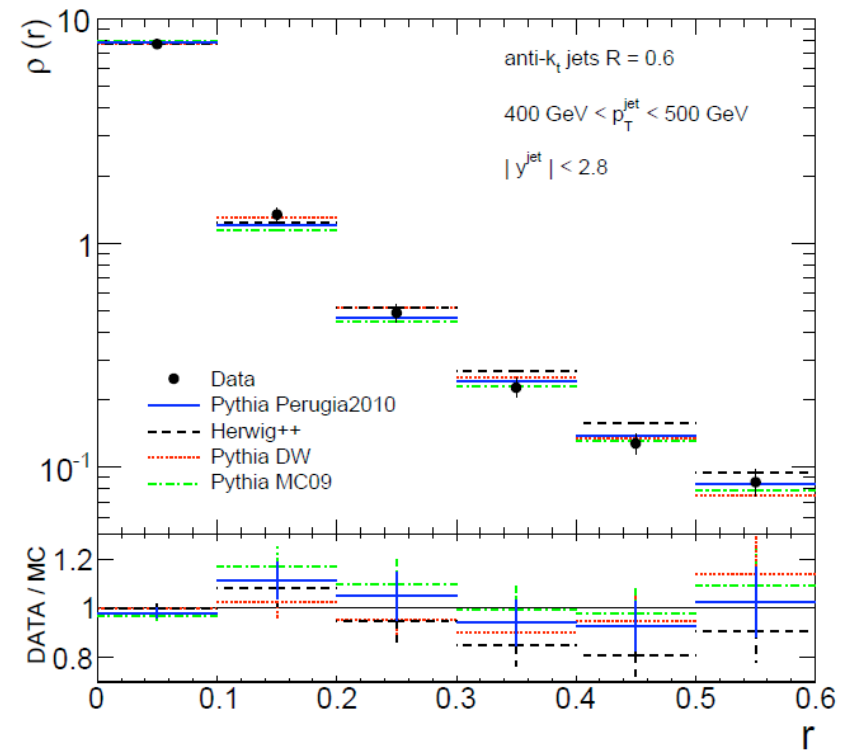
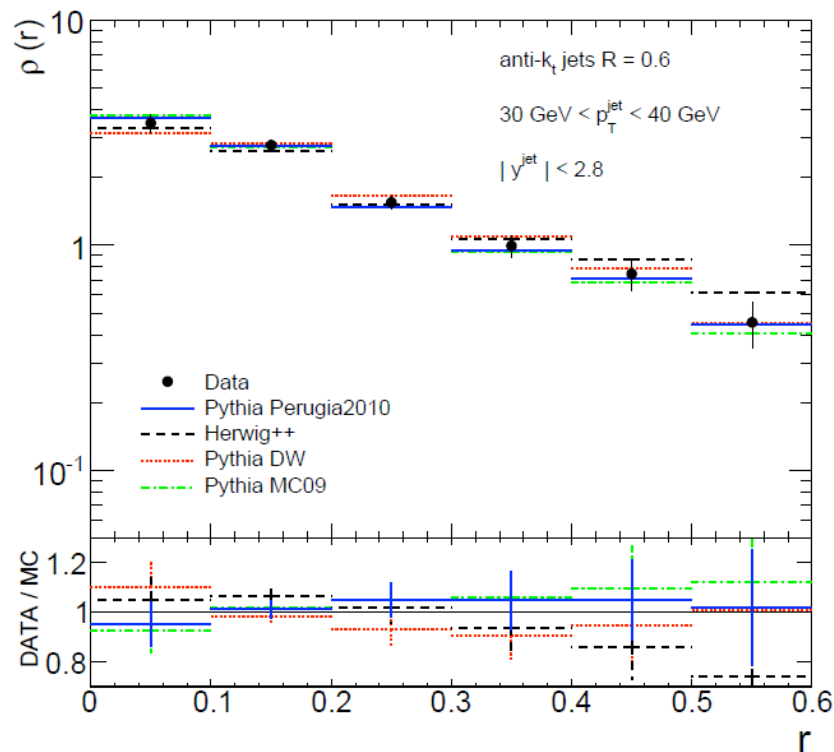
is the *average fraction* of jet transverse momentum within annulus of inner radius $(r - \Delta r/2)$ and outer radius $(r + \Delta r/2)$

- Proportional to transverse momentum density inside the jet
 - Relatively insensitive to the jet energy scale because jet p_T normalized away
- Here p_T is computed as the scalar sum of transverse momenta of calorimeter energy clusters that lie within the annulus



Differential jet shapes: Results

- Jet shapes from calorimeter clusters used as basic validation
- Density of transverse momentum peaks at low r with most of jet p_T within $r < 0.3$, indicating collimated flows of particles around jet axis
- Shifts to lower r for higher p_T jets, indicating they are more collimated



How often are jets produced, and does
this agree with NLO pQCD?

Unfolding

- Bin-by-bin unfolding back to hadron level, where all particles with lifetime > 10 ps (including muons and neutrinos) are included
- Correct for all detector effects: efficiencies, scales, and resolutions
 - Jet trigger efficiency
 - Vertex reconstruction efficiency
 - Jet reconstruction efficiency
 - Absolute and relative jet energy scale
 - Jet energy resolution
 - Jet angular resolution
- Strategy: Restrict kinematic region and bin the observable sufficiently coarsely so that corrections are both small and stable
- Do not correct for acceptance from p_T and rapidity cuts
 - These are part of definition of the observable and no measurement is made outside this range

Unfolding systematics

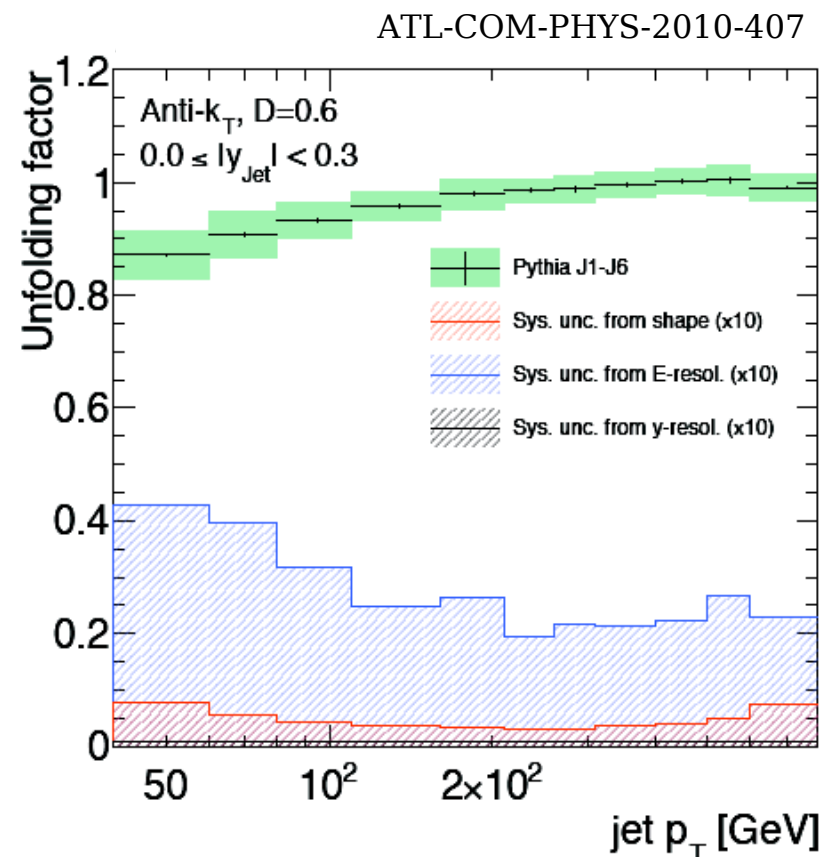
- Use Pythia MC09 to derive correction factors:

$$C = \sigma_{\text{truth}} / \sigma_{\text{reco}}$$

- Systematic uncertainty on this correction factor studied by:

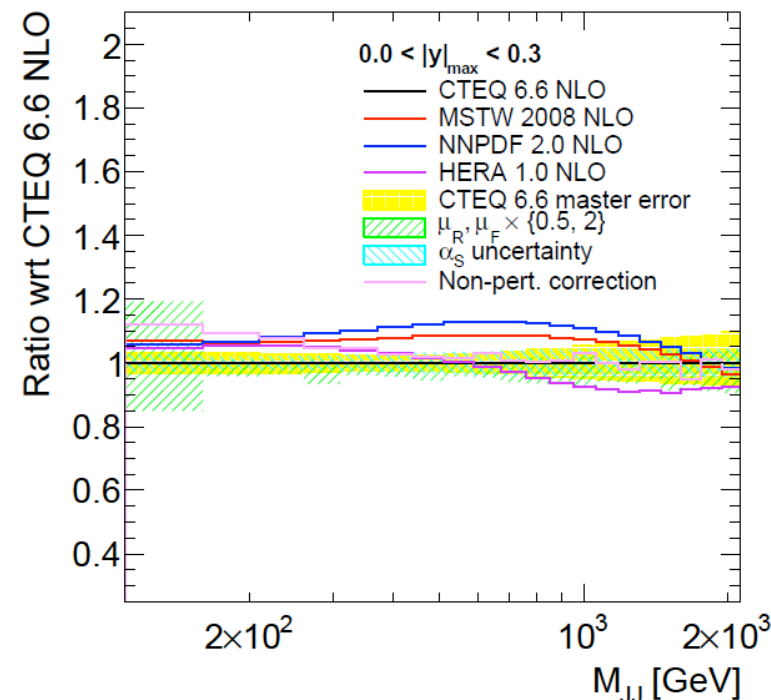
- Scaling up/down by JES uncertainty (dominant effect, not shown)
- Worsening jet energy resolution by 15%
- Smear angular resolution by 5%
- Reweight cross-section to alter shape of distribution

- Also perform closure tests against Pythia 8, Herwig++, and Alpgen



Theory prediction & uncertainties

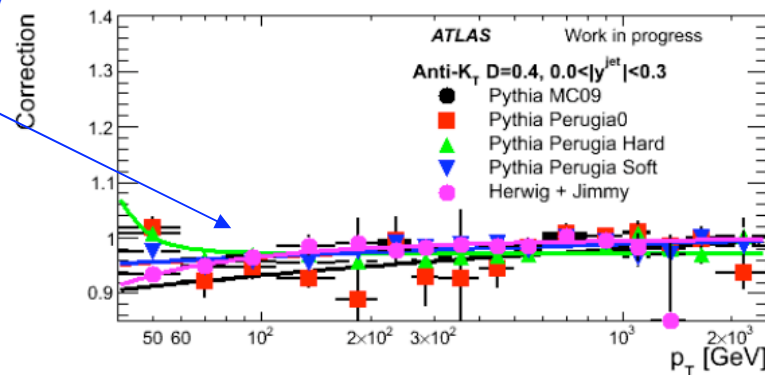
- Monte Carlo used for observables with high jet multiplicity
 - **LO 2->2:** Pythia, Herwig
 - **LO 2->N:** Alpgen (matrix element generator)
- NLOJet++ used to calculate NLO pQCD prediction for low jet multiplicity
 - **APPLgrid** program used for efficient evaluation of uncertainties
 - **CTEQ 6.6 NLO PDF** is baseline, but also compared to **MSTW 2008 NLO**, **NNPDF 2.0 NLO**, **HERA 1.0 NLO** ATL-COM-PHYS-2010-407
- **Renormalization scale μ_R** varied by factor of 2 to account for neglected higher order terms
- **Factorization scale μ_F** varied by factor of 2 to account for scale separating matrix element from PDF evolution
- **Strong coupling constant $\alpha_s(M_Z)=0.118$** varied by 0.002 from world's best estimate



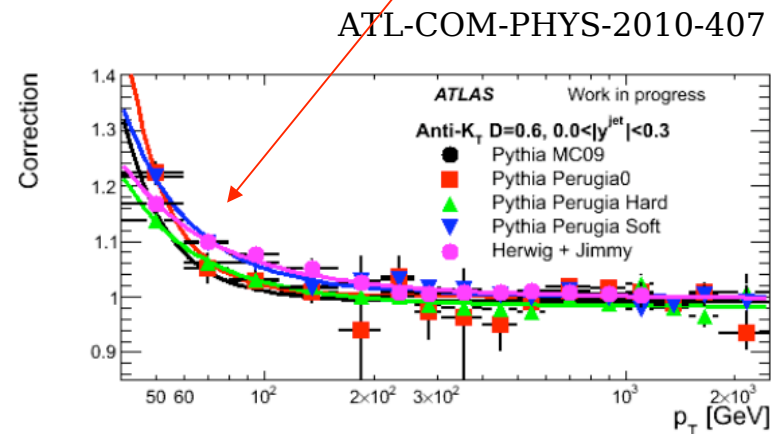
Non-perturbative correction

- **Parton-level NLO calculation** corrected for non-perturbative effects calculated using Rivet framework:
 - *Hadronization* and *underlying event*
 - Different dependence for $R=0.4$ (left) and 0.6 (right) \rightarrow tune MC!
- Systematic variations assessed using:
 - Perugia0, Perugia hard, Perugia soft, Herwig

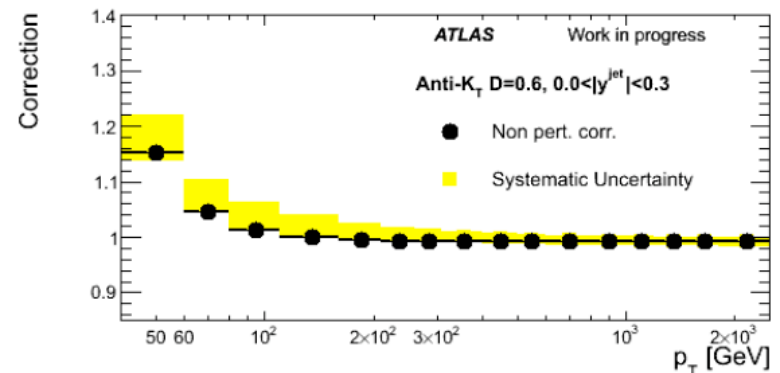
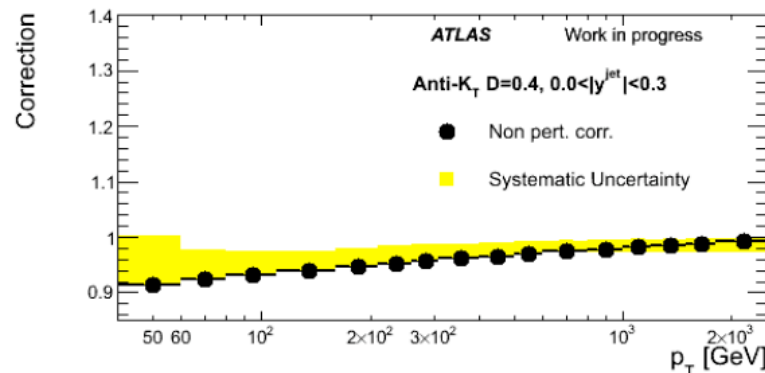
Dominated by hadronization



Dominated by UE

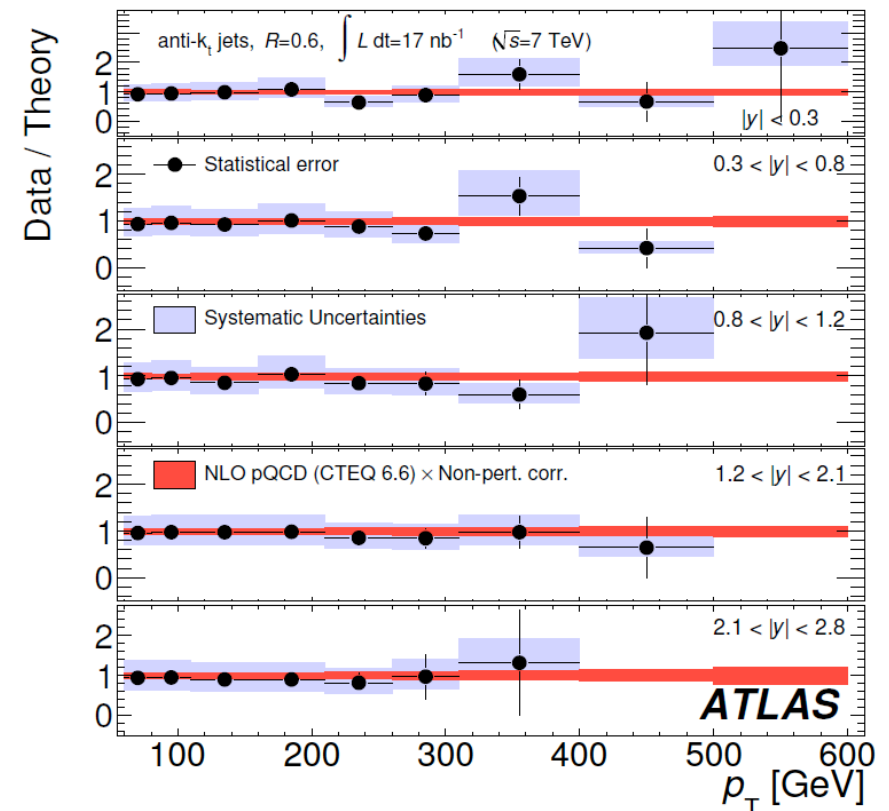
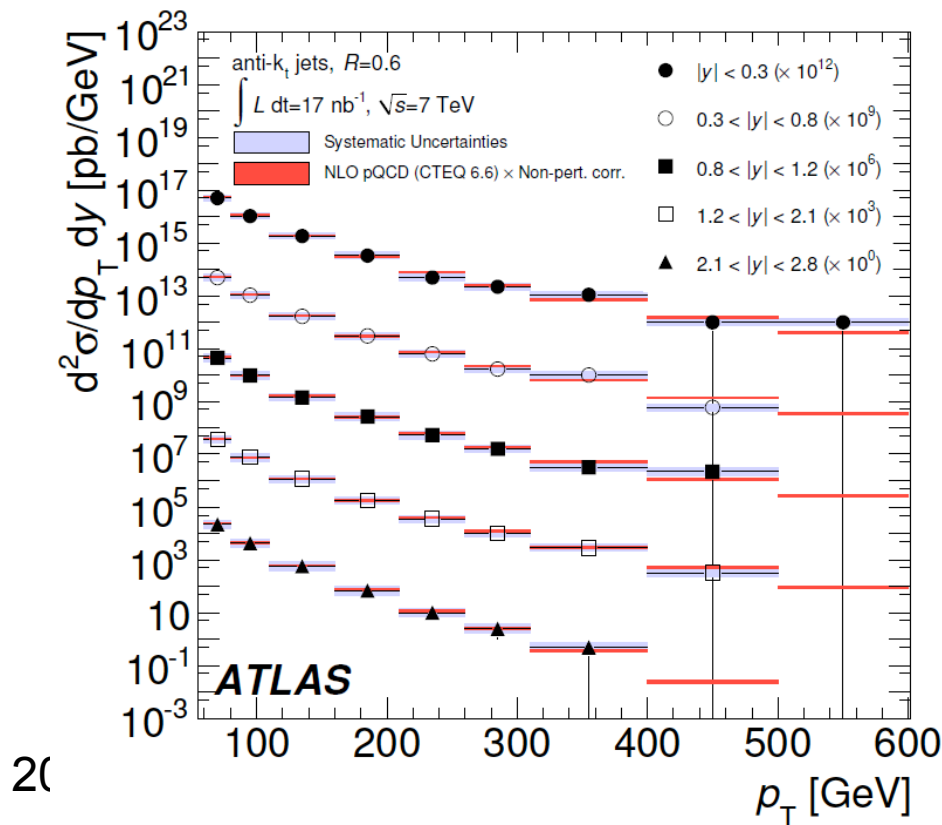


ATL-COM-PHYS-2010-407



Inclusive jet p_T cross-section

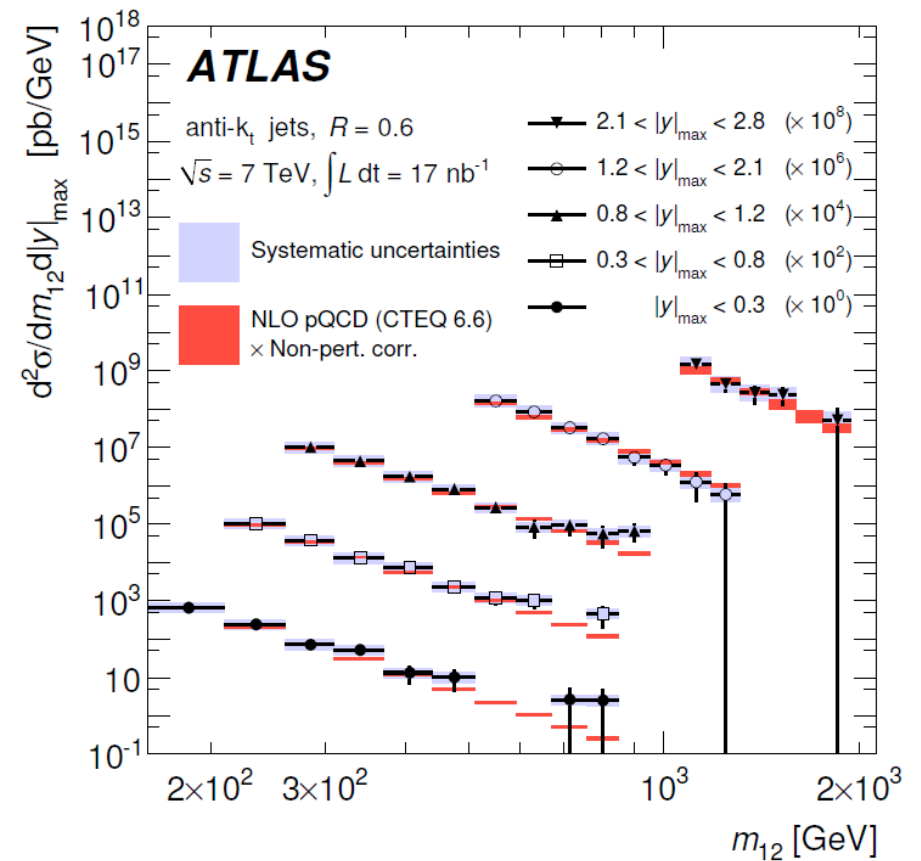
- ATLAS Collaboration. "Measurement of inclusive jet and dijet cross sections in proton-proton collisions at 7 TeV centre-of-mass energy with the ATLAS detector."
arXiv:1009.5908 [hep-ex]. Accepted by Eur. Phys. J. C.
- First cross-section measurements at a center-of-mass energy of 7 TeV of inclusive jet and dijet production, using 17 nb^{-1} integrated luminosity
- Inclusive jet cross-section = Probability to observe a jet in a pp collision as a function of the jet p_T and rapidity (canonical single-jet observable)



Dijet mass spectrum

Dijet mass = invariant mass of two leading jets measured in bins of maximum rapidity of two leading jets: $|y_{\max}| = \max(|y_1|, |y_2|)$

- Exotic resonances would tend to decay to high p_T central jets
- QCD produces more low p_T forward jets separated by large opening angle
- No discrepancy observed between data and NLO pQCD prediction

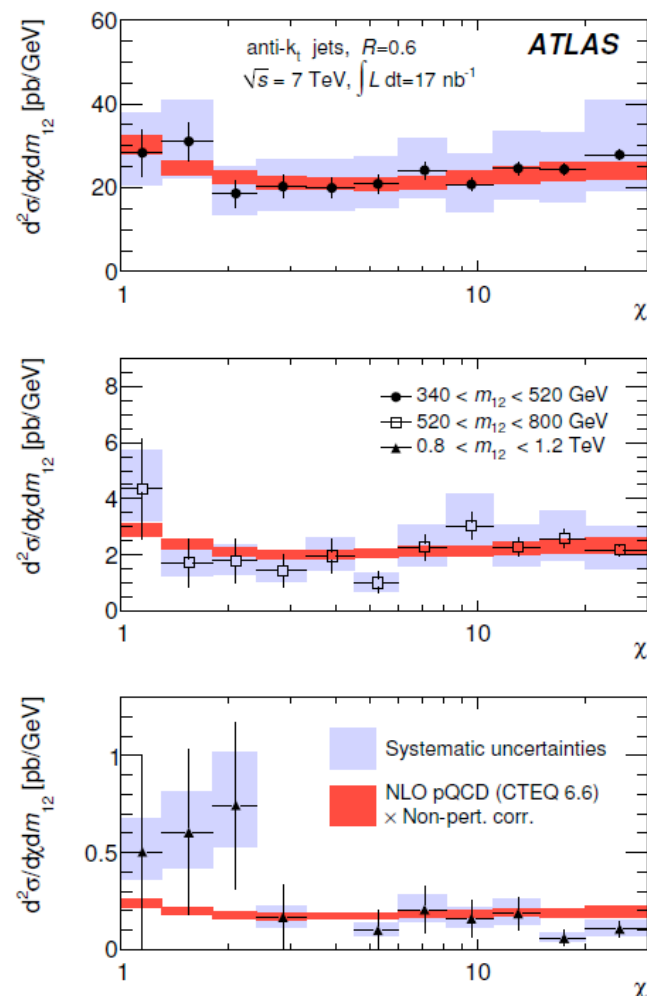


Dijet χ angular distribution

Dijet angular distribution: $\chi = \exp(|y_1 - y_2|) = (1 + \cos(\theta^*)) / (1 - \cos(\theta^*))$

measured in bins of dijet mass m_{12}

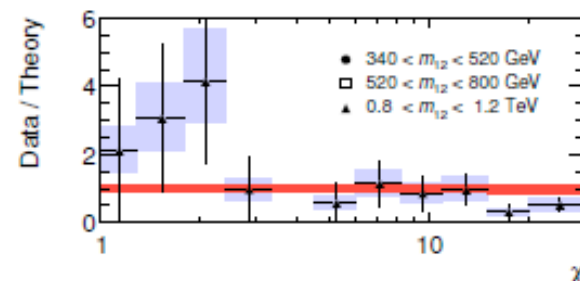
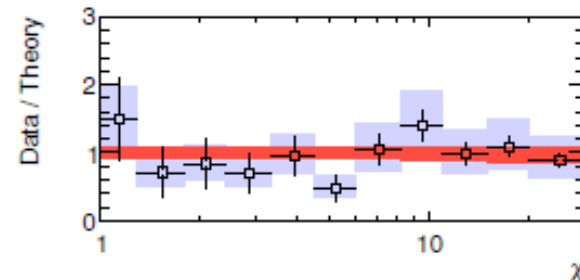
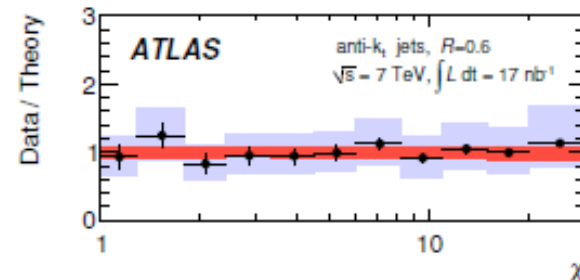
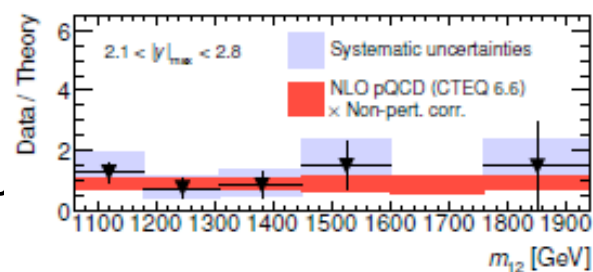
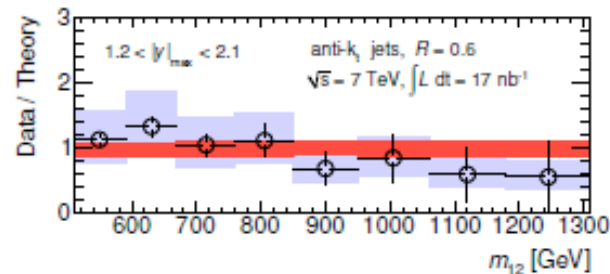
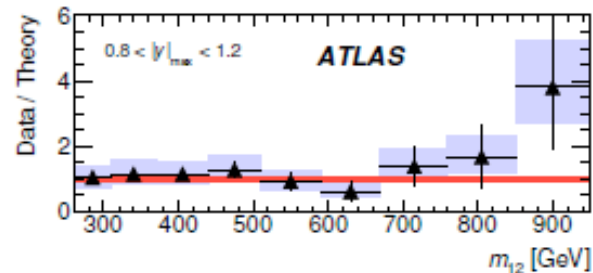
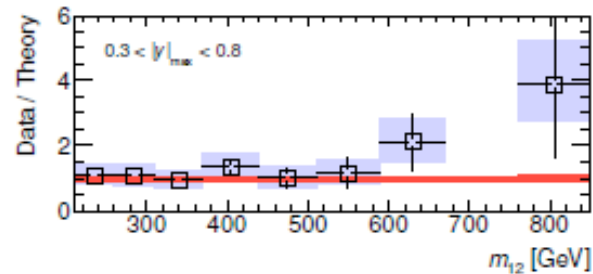
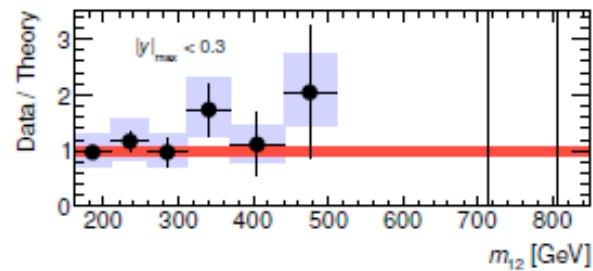
- Measures scattering angle θ^* in dijet center-of-mass frame
- Contact interactions such as compositeness would produce peak at low χ (small scattering angle), whereas QCD is \sim flat as we see
- Relatively insensitive to parton distribution functions because predictions for gg , qg , and qq subprocesses are similar
- No statistically significant deviations seen wrt pQCD prediction



Dijet mass and χ : Data/theory ratio

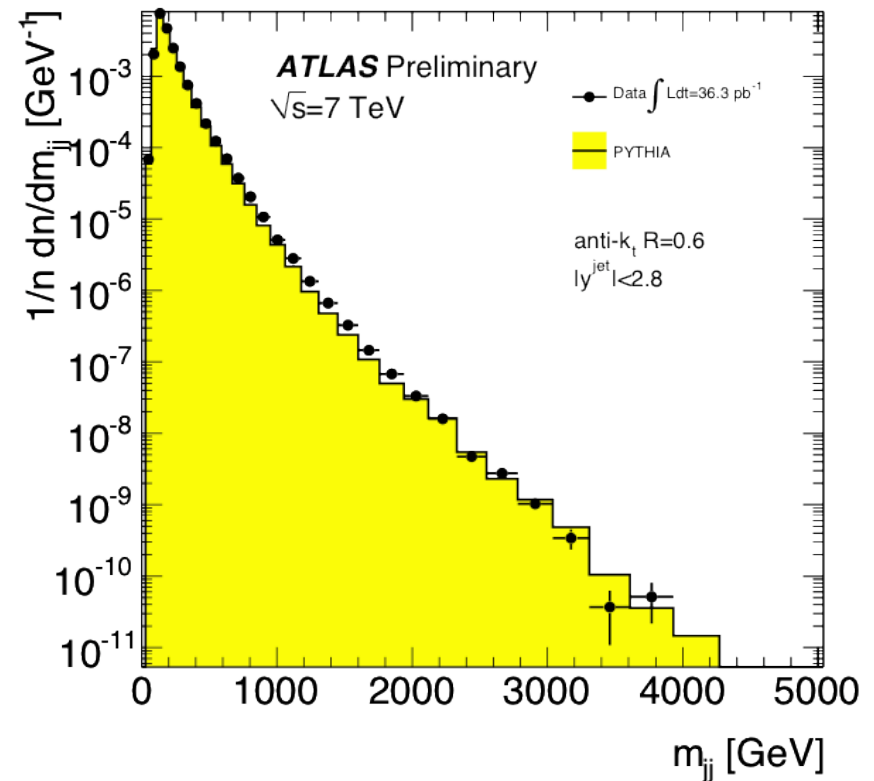
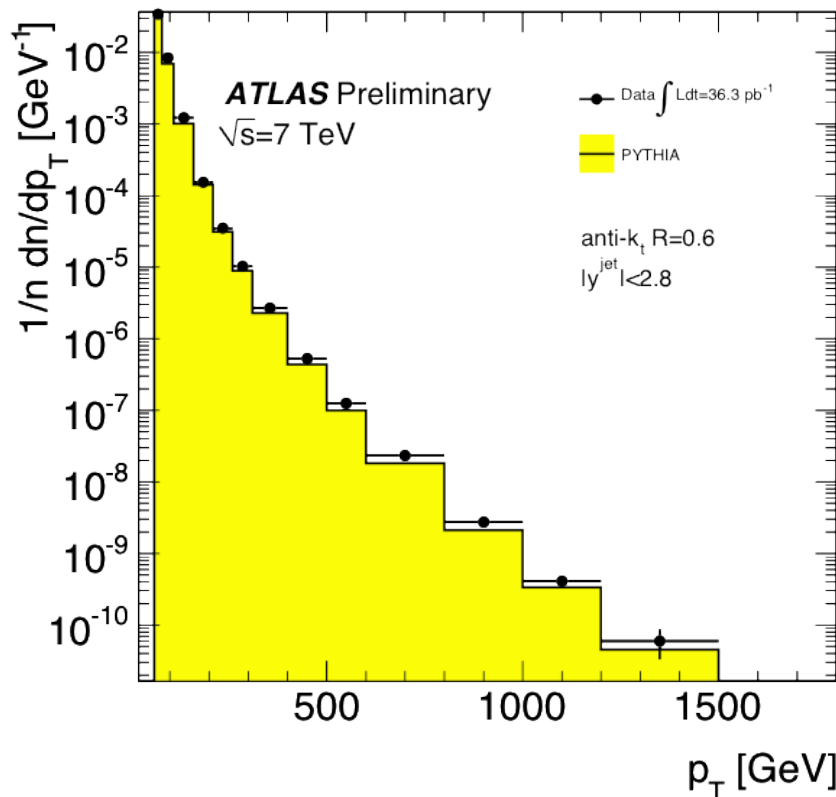
NLO pQCD describes data well in all regions of phase space

- Both central and forward dijet mass follow the data (left)
- Angular distribution is as expected from pQCD at large dijet mass (right)



Updated analysis with full 2010 dataset

- Full cross-section measurement with $\sim 45 \text{ pb}^{-1}$ integrated lumi taken in 2010 is in progress
- Jets with transverse momentum up to 1.3 TeV are observed
- Invariant mass of two leading jets is observed up to 3.7 TeV
 - LO parton shower Monte Carlo provided to guide the eye
- For Winter 2011 conferences, also extending analysis down to jet p_T of 20 GeV and higher in rapidity to $|y| < 4.4$

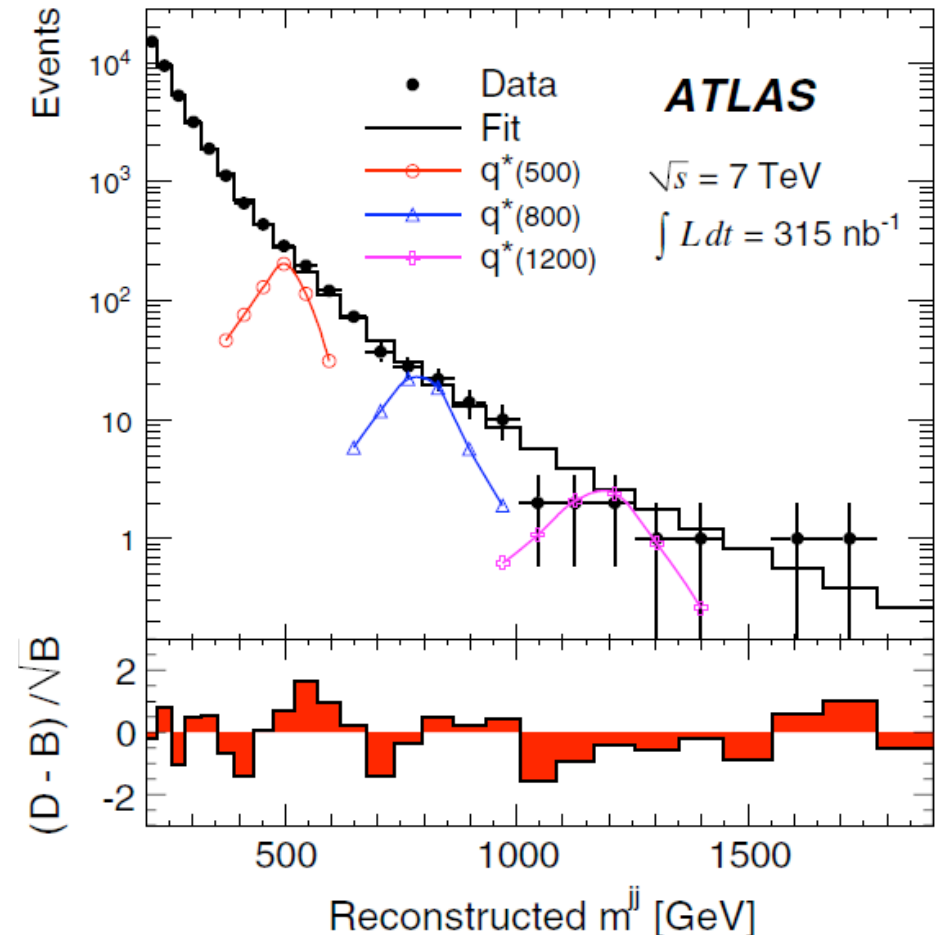
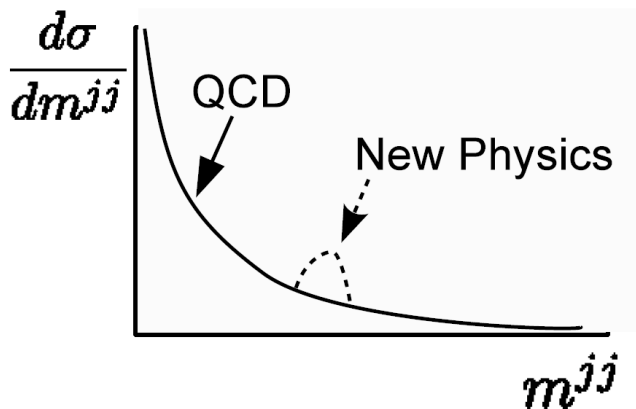


Are there any signs of new exotic physics at these short length scales?

Search for dijet resonance using the dijet mass spectrum

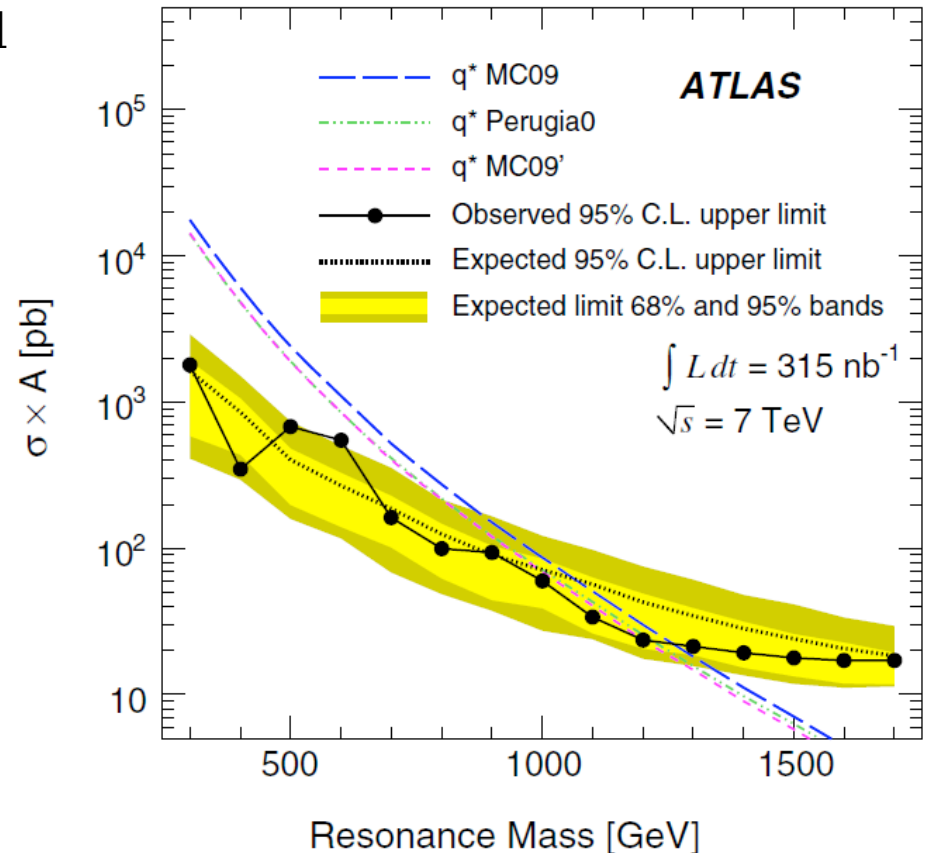
- There are direct extensions to searches for resonances decaying to two jets in final state (excited quarks, technirho, KK graviton, W'/Z' , etc)
- Performed a search for bumps in the dijet mass spectrum by comparing it against a smooth continuum as predicted by QCD:

$$f(x) = p_0 \frac{(1-x)^{p_1}}{x^{p_2+p_3 \ln x}}, \quad x \equiv \frac{m^{jj}}{\sqrt{s}}$$



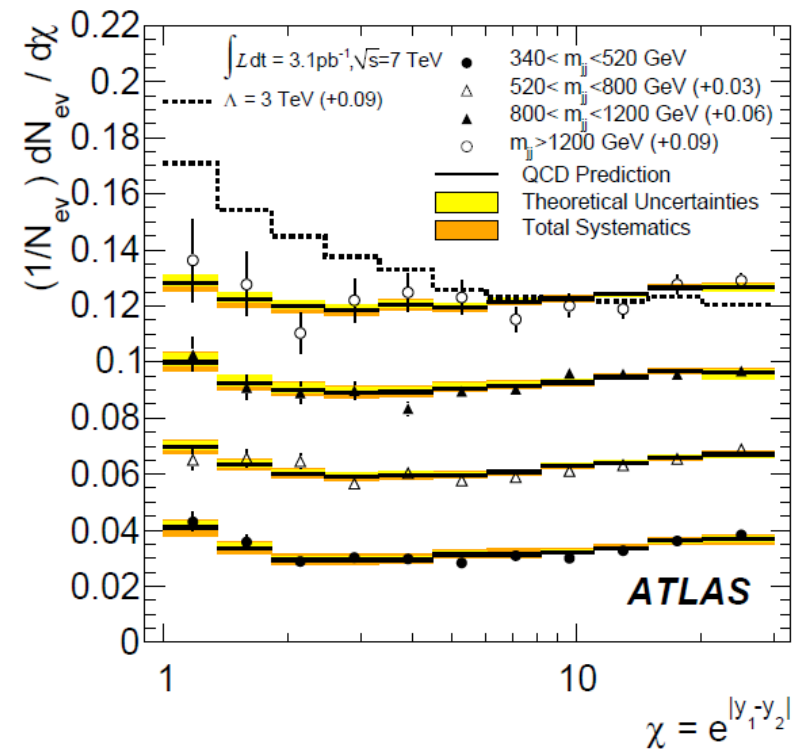
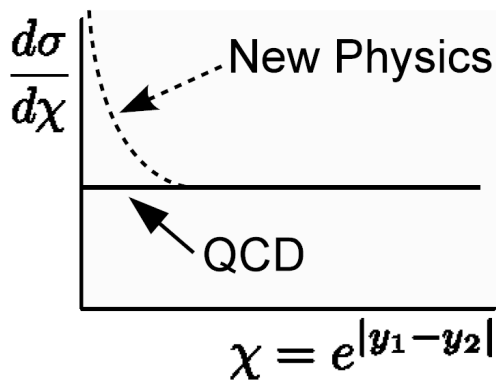
Limit on excited quarks

- No evidence of a resonance observed
→ set new limit on dijet resonances arising from excited quarks
 - Bayesian approach used to set limit, cross-checked with frequentist method
- Excited quarks with mass up to 1.26 TeV excluded at 95% CL
 - Tevatron limit = 870 GeV
 - Systematics including JES (dominant), luminosity, background fit, etc also accounted for
- ATLAS Collaboration. "Search for New Particles in Two-Jet Final States in 7 TeV Proton-Proton Collisions with the ATLAS Detector at the LHC." Phys Rev. Lett. 105, 161801 (2010)



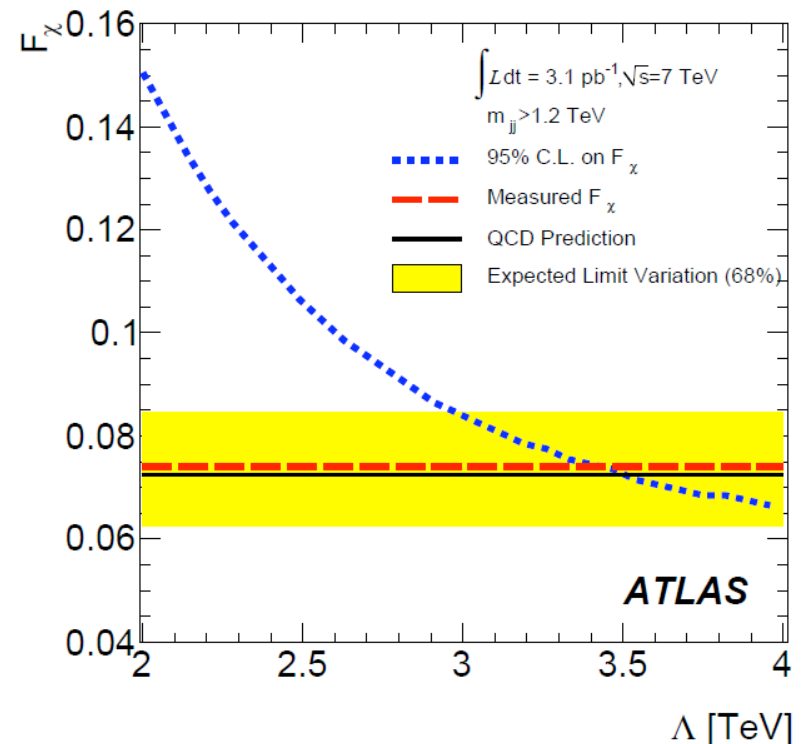
Search for contact interactions with the dijet χ angular distribution

- Examined dijet $\chi = \exp(|y_1 - y_2|)$ angular distribution for excess of low-angle scattering compared to NLO QCD prediction:
 - Normalized distribution mostly cancels out absolute JES uncertainty, leaving relative JES
- Any tail could be indication of contact interaction that might arise from quark compositeness, gravitational scattering, etc.



Limits on contact interactions

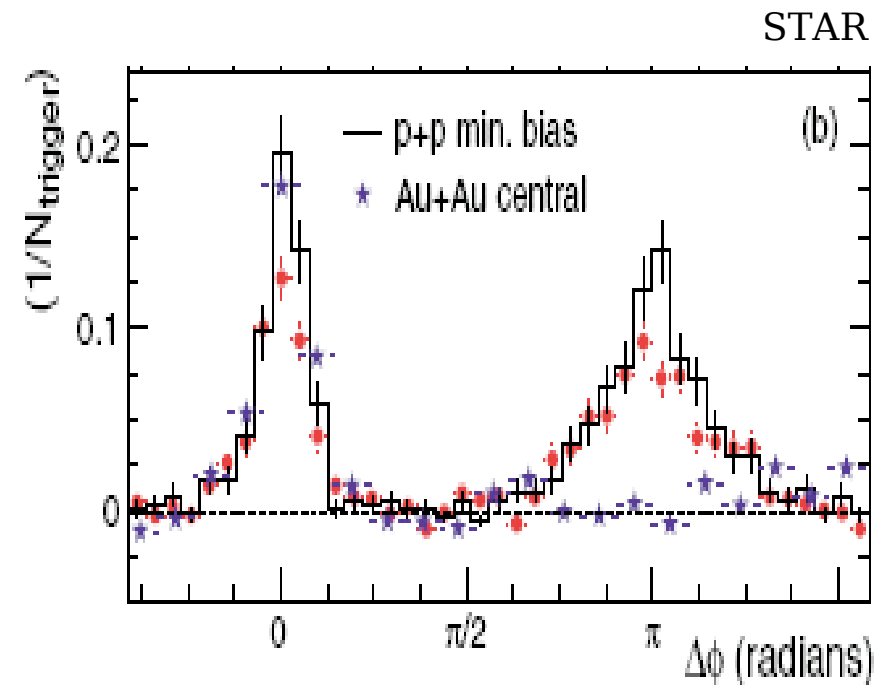
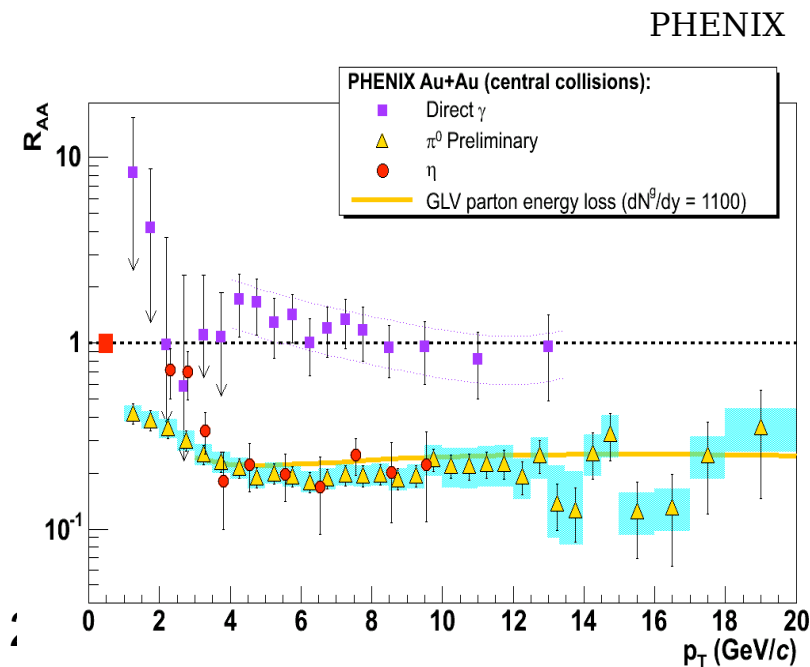
- No significant excess observed
- Set new limit on contact interactions that may arise from quark compositeness
 - Define F as fraction of events at low χ
 - Limit set using frequentistic method, cross-checked by Bayesian approach
- Using integrated luminosity of 3.1 pb^{-1} , compositeness scale $\Lambda < 3.4 \text{ TeV}$ excluded at 95% CL
 - Tevatron limit = 3.1 TeV
- ATLAS Collaboration. "Search for Quark Contact Interactions in Dijet Angular Distributions in pp Collisions at $\sqrt{s} = 7 \text{ TeV}$ Measured with the ATLAS Detector." arXiv:1009.5069 [hep-ex]. Accepted by Phys. Lett. B.



Surprises from jets in lead ion collisions

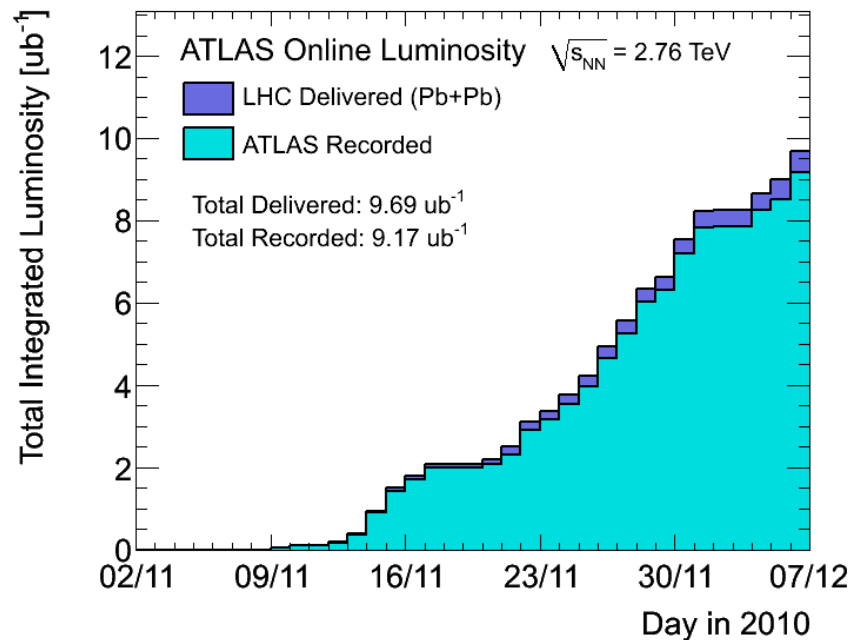
Jet quenching at RHIC

- Jet quenching was first observed in gold ion collisions at $\sqrt{s_{NN}} = 100$ GeV at the Relativistic Heavy Ion Collider
 - Single hadron suppression, no photon suppression (PHENIX)
 - Dijet “disappearance” in di-hadron correlations (STAR)
 - LBL theorists & experimentalists in nuclear physics played key roles in theory, hardware, and analysis



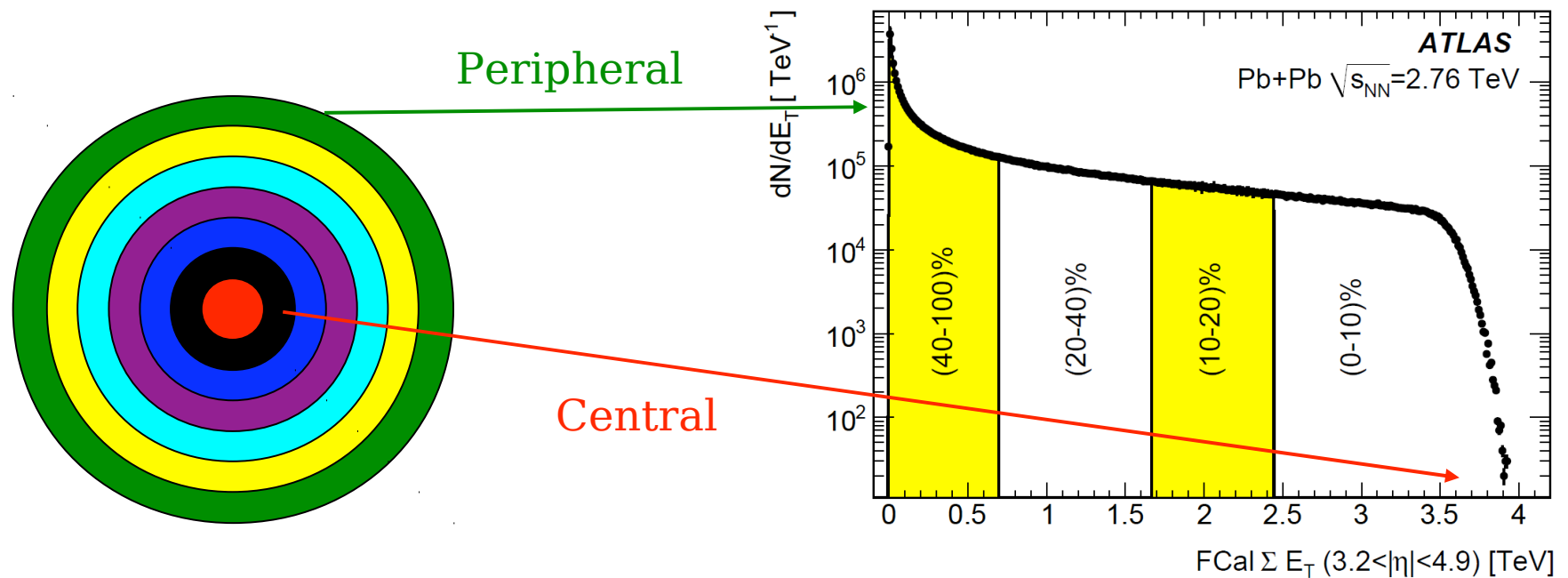
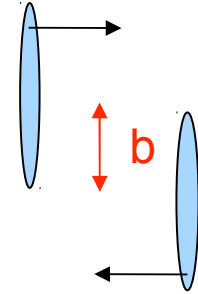
Lead ion collisions at the LHC

- LHC collided lead ions at $\sqrt{s_{NN}} = 2.76$ TeV in November
- Approximately 9 ub^{-1} recorded
 - Results shown here use 1.7 ub^{-1} , with analysis of rest of data on-going



Centrality definition

- Particle multiplicity increases as classical impact parameter b decreases
- Characterize centrality by percentiles of total cross-section using ΣE_T in Forward Calorimeter (FCal) spanning $3.2 < |\eta| < 4.9$
 - Recover pp behavior in peripheral collisions where nuclear "overlap" is small



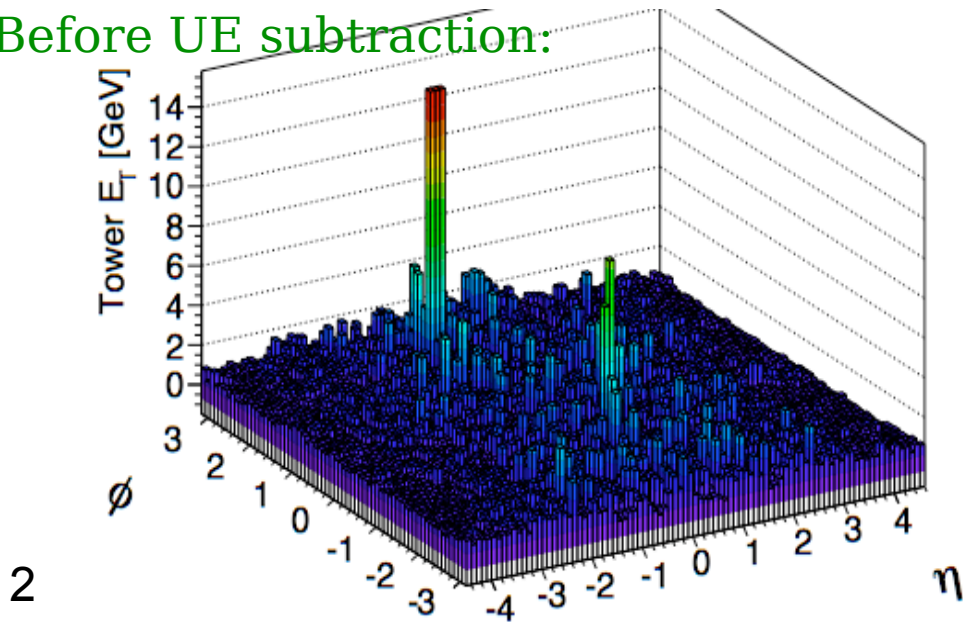
Event selection

- Events triggered using minimum bias trigger
- Jets reconstructed from calorimeter towers using anti- k_T algorithm with $R=0.4$
 - Calibrated with energy density cell weighting
 - UE subtraction performed afterwards (next slide)
- Two leading jets are required to be within $|\eta_{1,2}| < 2.8$ where relative JES uncertainty is within 5% from pp data
- Jet $E_{T,1} > 100$ GeV so jet reconstruction in lead ion collisions is fully efficient
- Jet $E_{T,2} > 25$ GeV to be above UE background
 - Opposite hemisphere ($\Delta\phi > \pi/2$) to select fairly “back-to-back” dijet events

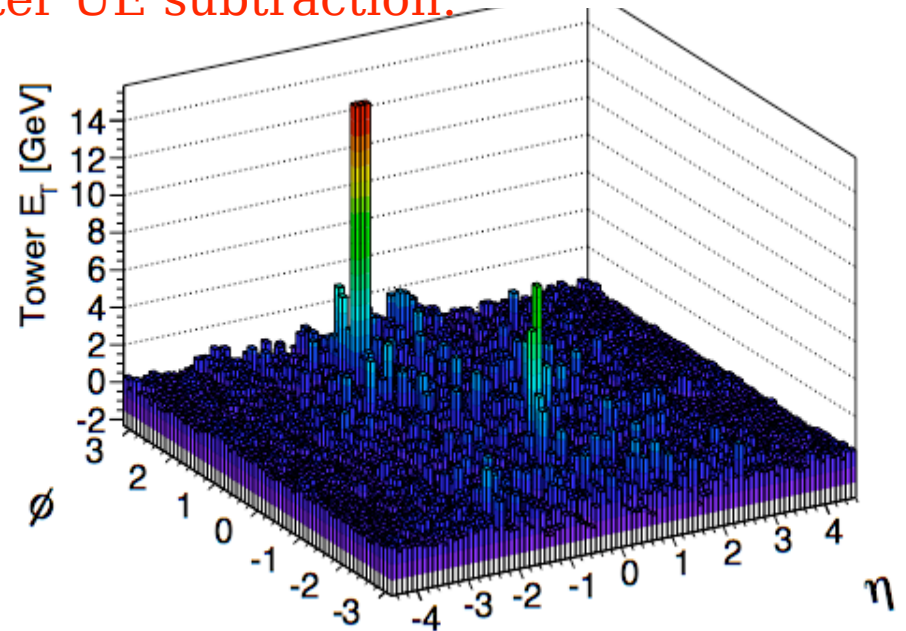
UE subtraction from jet

- Underlying event in heavy ion collisions is huge → critical to correct jet E_T
- UE density is computed for each longitudinal layer, in slices of $\Delta\eta = 0.1$
 - Average over ϕ (elliptical flow)
 - Exclude towers from calculation of UE density if discriminant $D = E_t^{\text{tower, max}} / E_t^{\text{tower, mean}} > 5$ (no jets are removed from analysis)
- Jet correction is the UE density integrated against jet area
 - $R=0.2$ and $R=0.4$ used for cross-checks because UE pedestal for each jet scales with area i.e. R^2 → results are consistent

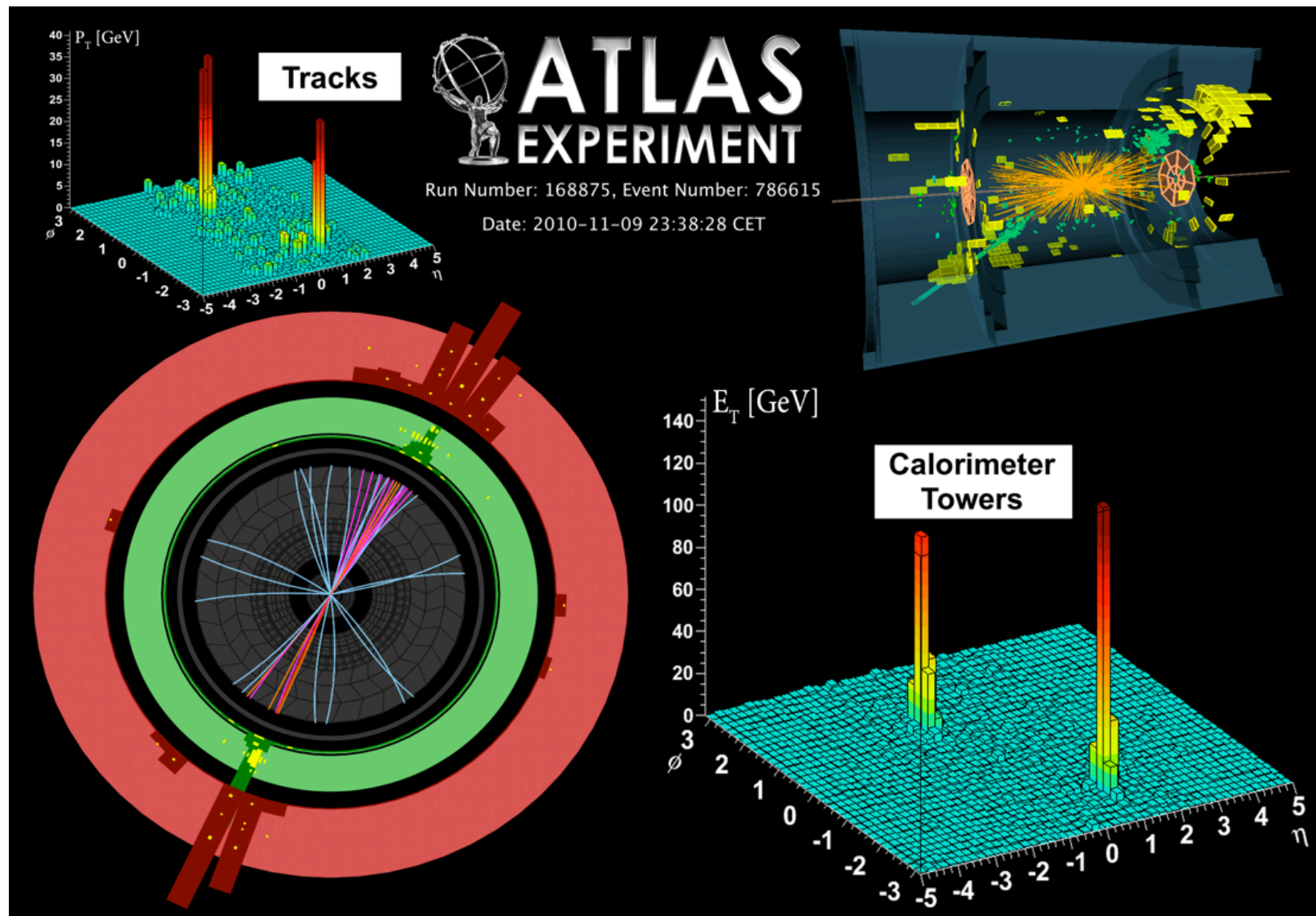
Before UE subtraction:



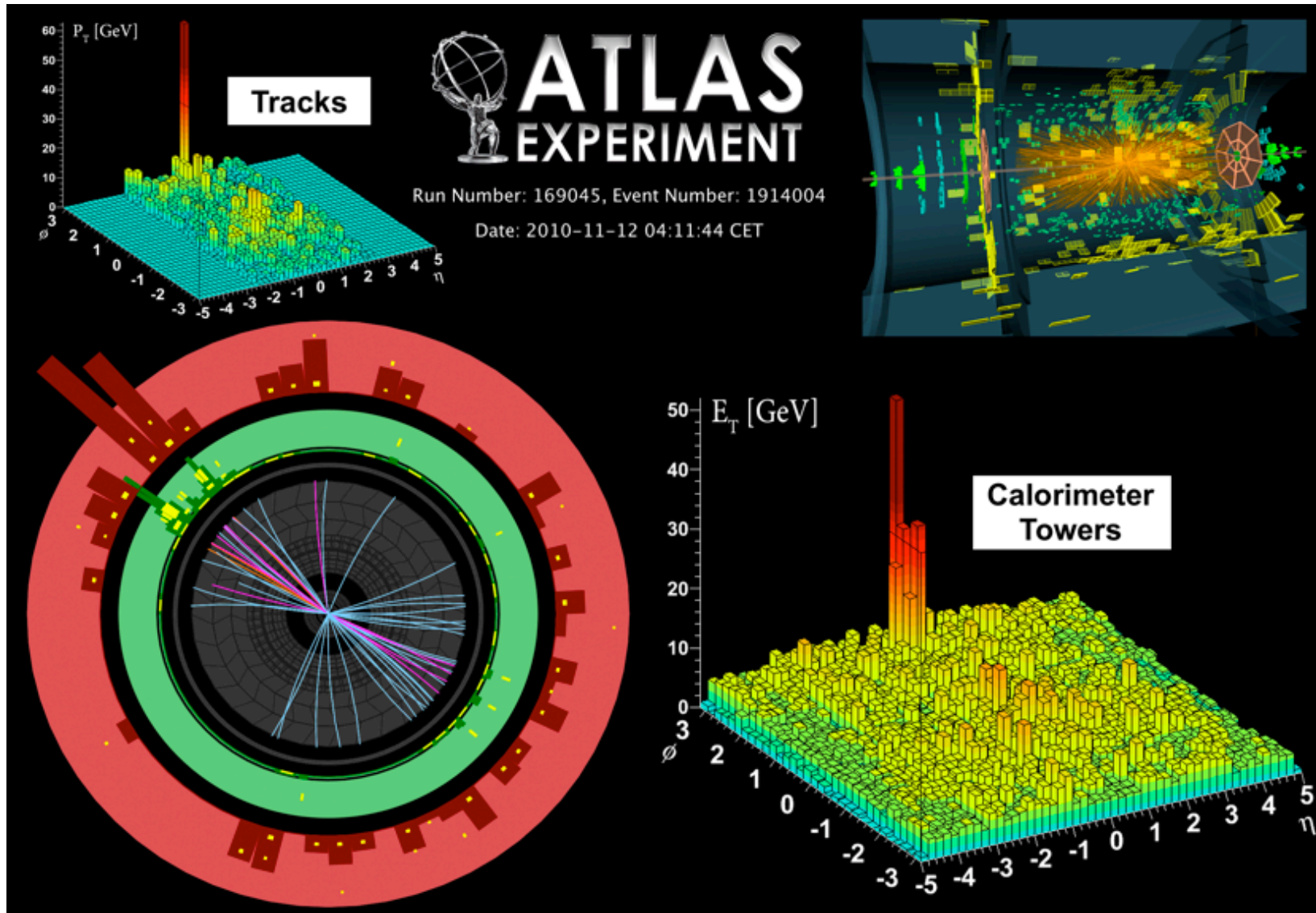
After UE subtraction:



Peripheral, symmetric dijet event

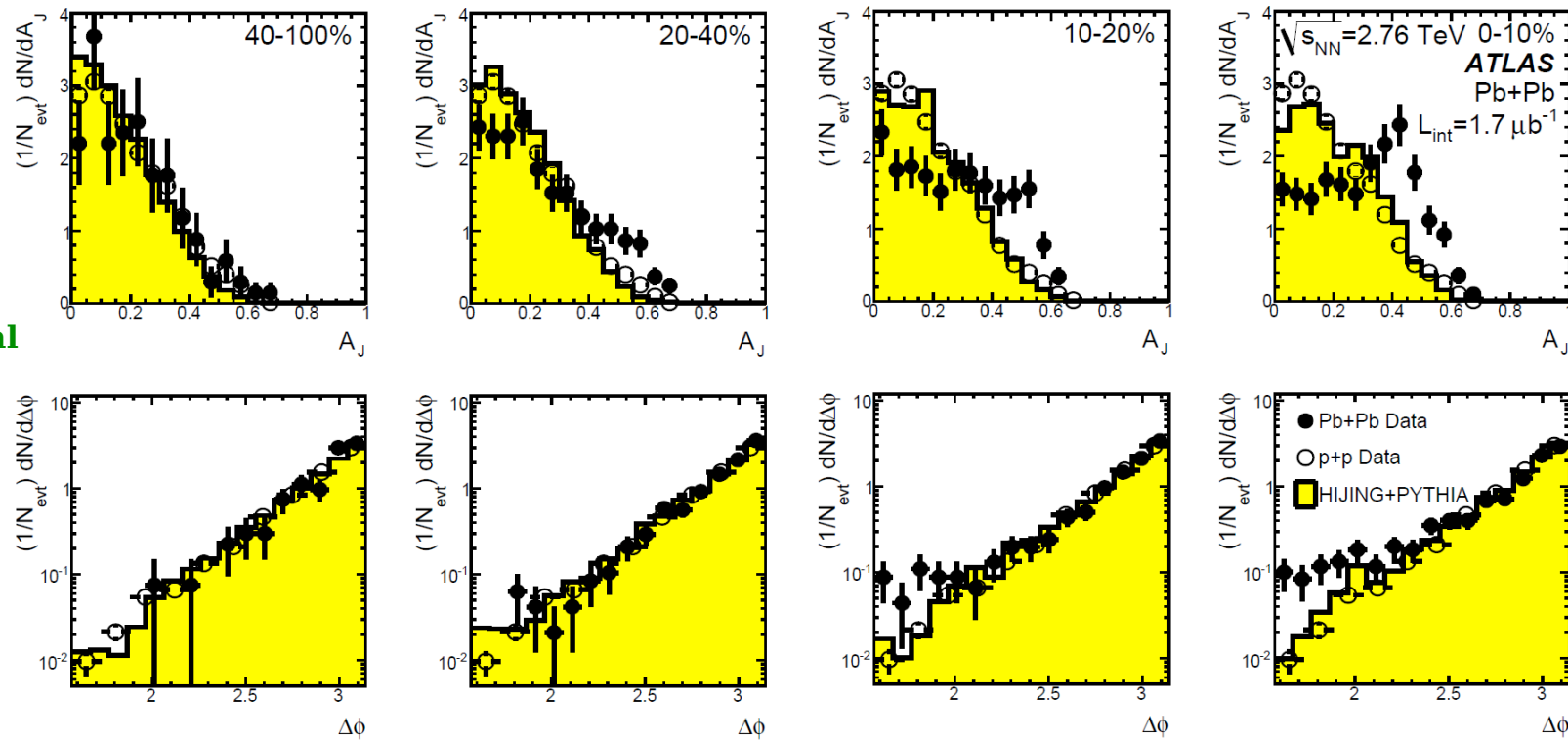


Central, *asymmetric* dijet event



Jet quenching at the LHC

- Asymmetry $A_J = (E_{T,1} - E_{T,2}) / (E_{T,1} + E_{T,2})$
 - Compare Pb+Pb data to pp data and HIJING Monte Carlo (with PYTHIA dijets overlaid)
- **Dijet asymmetry observed that increases with centrality**
 - Most symmetric in peripheral collisions, where pp behavior is recovered (left)
 - But very *asymmetric* in central collisions with largest nuclear overlap (right)



Conclusions

- With $\sim 45 \text{ pb}^{-1}$ of data, jet $p_T \sim 1.3 \text{ TeV}$ and dijet mass $\sim 3.7 \text{ TeV}$ have already been observed and surpass the Tevatron reach
- First cross-section measurements of inclusive jet and dijet production at $\sqrt{s} = 7 \text{ TeV}$ using 17 nb^{-1} (accepted by Eur. Phys. J. C)
 - First measurements at hadron collider using anti- k_T algorithm
 - Monte Carlo based calibration scheme was developed to calibrate jets as a function of p_T and y
 - JES uncertainty of 7% for central jets above 60 GeV
- New limit on dijet resonance mass: $0.87 \text{ TeV} \rightarrow 1.26 \text{ TeV}$ (published in PRL)
- New limit on contact interaction scale: $3.1 \text{ TeV} \rightarrow 3.4 \text{ TeV}$ (accepted by Phys. Lett. B)
 - QCD probed in new kinematic regime of high jet p_T and large dijet mass
- First observation of jet quenching at $\sqrt{s_{NN}} = 2.76 \text{ TeV}$ (published in PRL)

Outlook

- ATLAS jet measurements and searches will have exciting new results for the Winter 2011 conferences
 - The full 2010 dataset of 45 pb^{-1} is being analyzed and will further extend the kinematic reach in both jet p_T and rapidity, and in dijet mass
 - Significantly reduced JES uncertainty using in-situ calibration methods is expected to be finished soon
 - Luminosity uncertainty will also be reduced
 - Other QCD analyses on dijets, multi-jets, jet shapes, etc have produced conference notes and are advancing towards publication
- Next year promises to be even more exciting with 1 fb^{-1} or more of data
 - Steve Myers has optimistically suggested that $2\text{-}5 \text{ fb}^{-1}$ may be possible, so the future for jet measurements at the LHC is very bright!

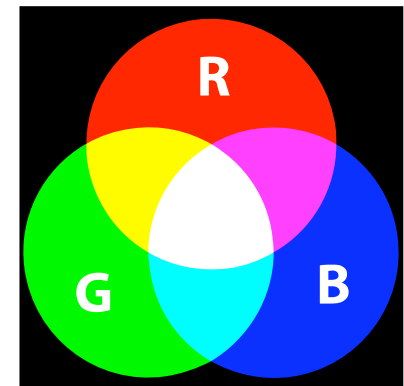
Acknowledgments



ADDITIONAL MATERIAL

Quantum *chromodynamics* (QCD)

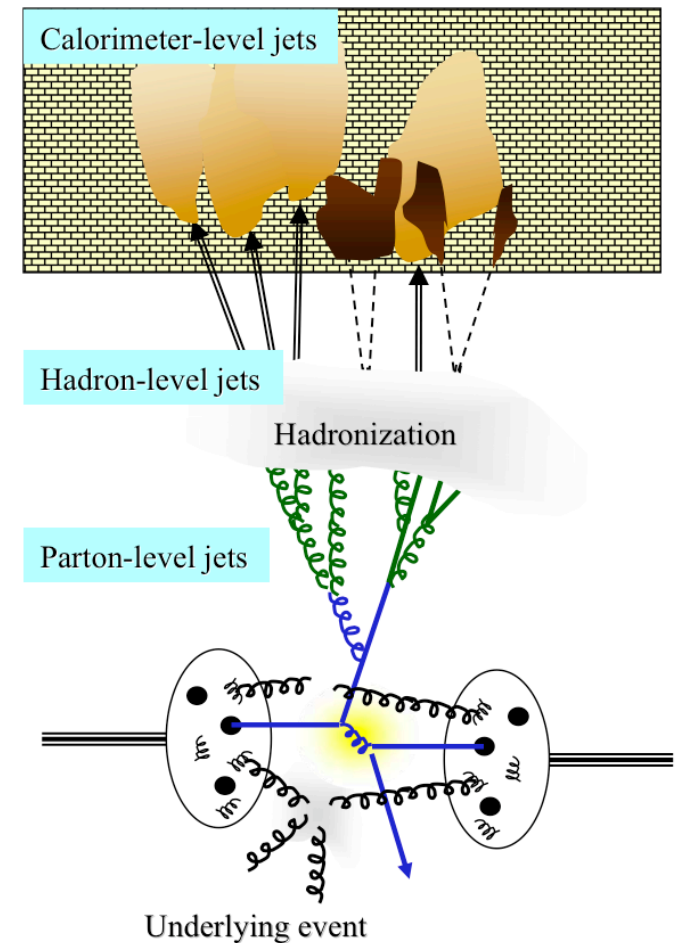
- Non-abelian gauge theory where:
 - Quarks have “color”,
anti-quarks have “anti-color”
 - Gluons have both color and anti-color
 - Hadrons (bound states of quarks)
are color neutral



Complications with QCD

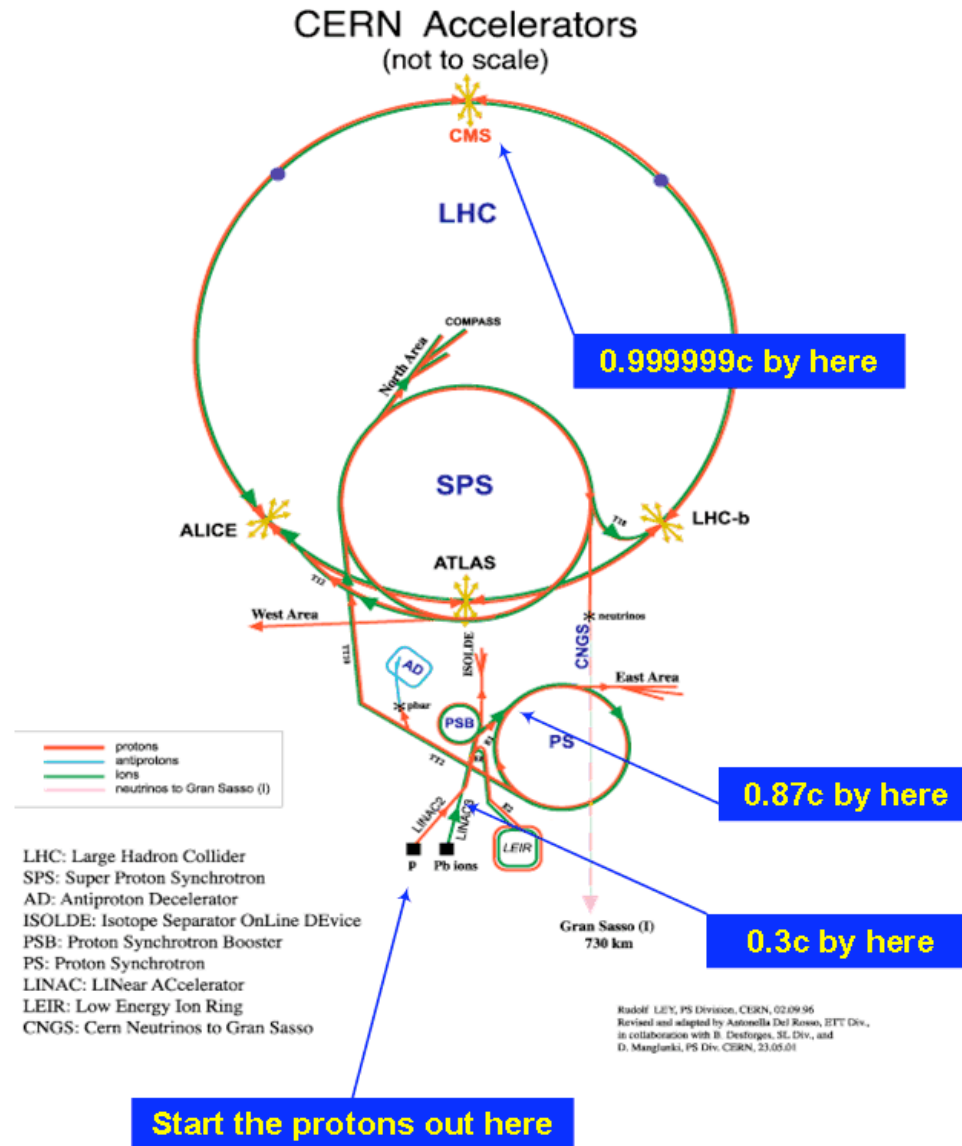
- So what's the difficulty?
- Asymptotic freedom \rightarrow Partons behave as if free at large Q^2 i.e. very short distances
- But QCD becomes non-perturbative at low Q^2 (long distances)

- Quark confinement
- We measure jets (collimated flows of hadrons), not partons



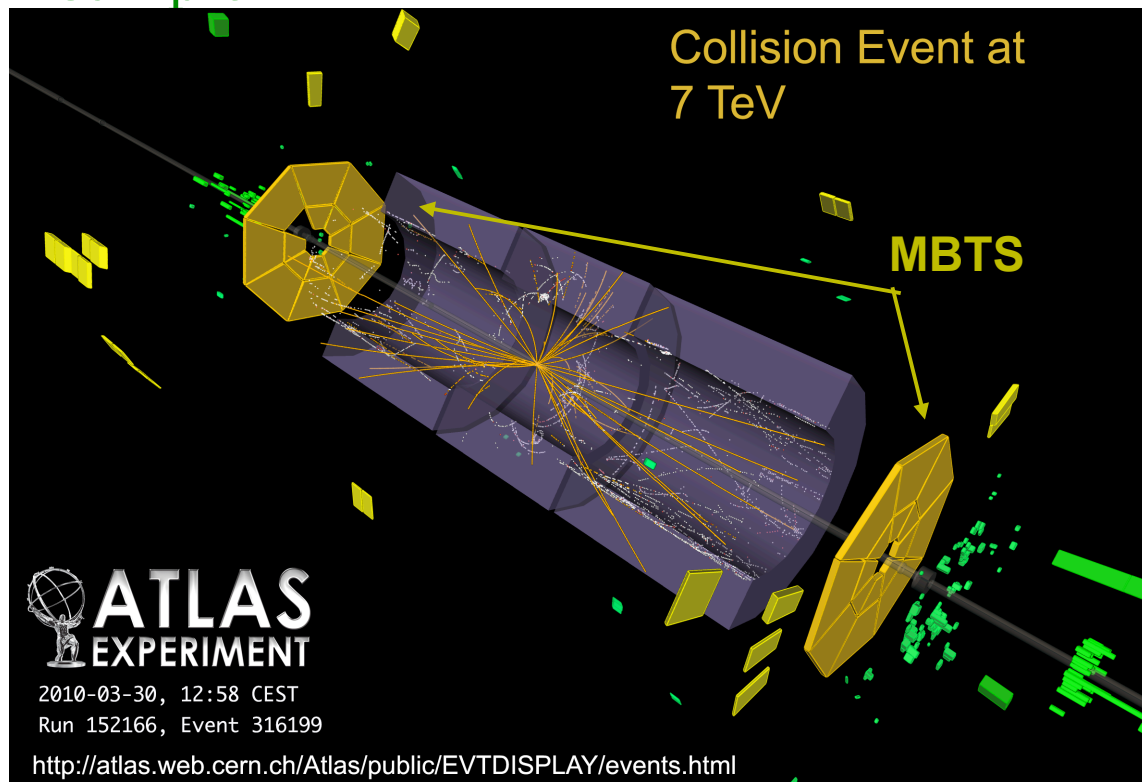
- This talk discusses how we have performed jet measurements in the ATLAS experiment and used these to probe *partonic* predictions of NLO pQCD, as well as to search for **new physics**

LHC accelerator complex



MBTS Trigger

- MBTS (Minimum Bias Trigger Scintillator) inclusive trigger
 - Require at least one scintillator fired from either η hemisphere: $2.09 < |\eta| < 3.84$
 - No significant bias introduced to the inclusive jet sample



Online and offline selection

- *Only summarize briefly below due to time constraints - MUCH more detail in backup slides!*
- Data sample studied is between 17 – 300 nb⁻¹ of data at 7 TeV collected through Period D before ICHEP
- Official Jet/EtMiss Good Run Lists and require “green” flag for luminosity
- Events with at least one “bad” (noisy) jet with $p_T > 10$ GeV at EM scale are removed
- Require at least one vertex reconstructed within $|z| < 10$ cm of detector center to suppress beam halo and beam gas
- Require L1_J5 trigger fired from L1Calo stream
 - Restrict leading (sub-leading) jet to $p_T > 60$ GeV (30 GeV) so that jet trigger and reconstruction are both fully efficient

What is the anti- k_T jet algorithm?

- Cone jet algorithms (sum all energy in some region)
 - ATLAS Cone (seeded \rightarrow not infrared nor collinear safe)
 - SIS-Cone (Seedless Infrared Safe)
- Clustering AKA “sequential recombination” jet algorithms (invert the radiation and fragmentation)

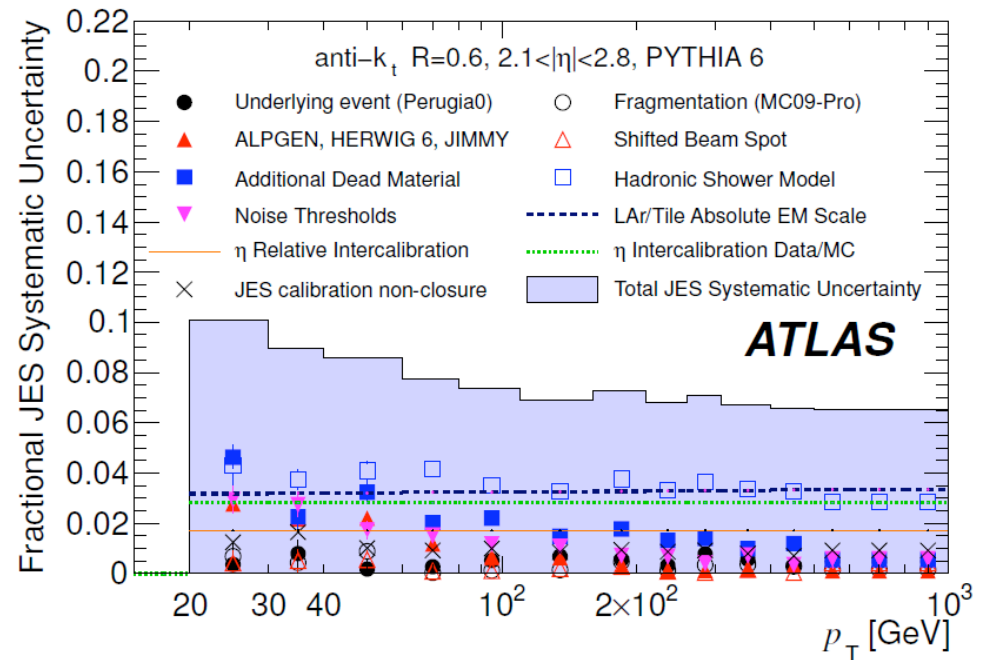
$$d_{ij} = \min(k_{ti}^{2p}, k_{tj}^{2p}) \frac{\Delta_{ij}^2}{R^2} \quad \Delta_{ij}^2 = (y_i - y_j)^2 + (\phi_i - \phi_j)^2$$

- K_T (p= 1): Clusters softest constituents first
- Cambridge (p= 0): Clusters closest constituents first
- **Anti- k_T (p=-1): Clusters hardest constituents first**

\rightarrow Reconstructs the same jets no matter whether there's soft radiation near the initial constituents

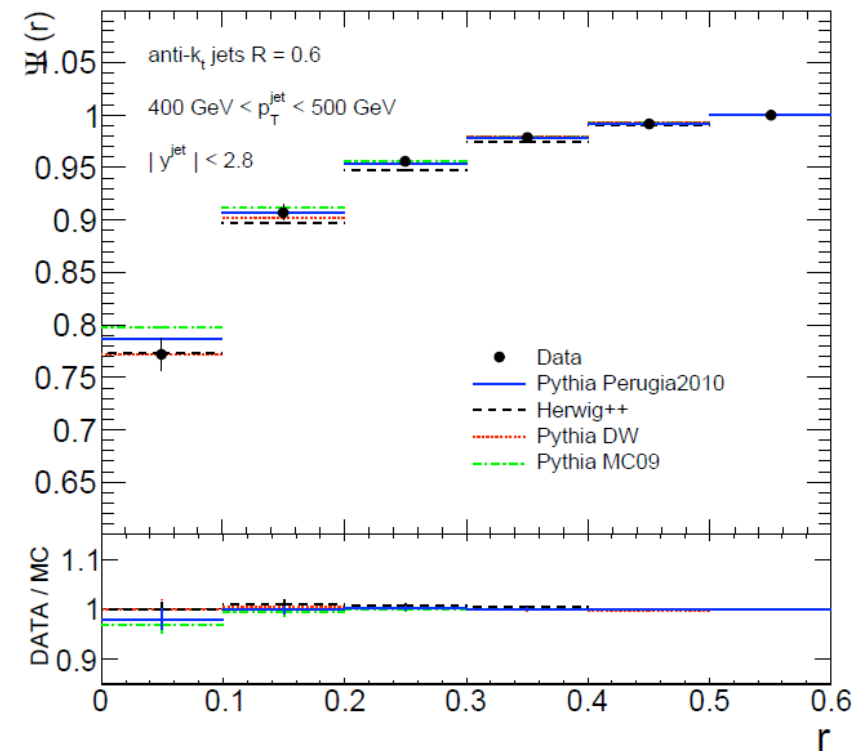
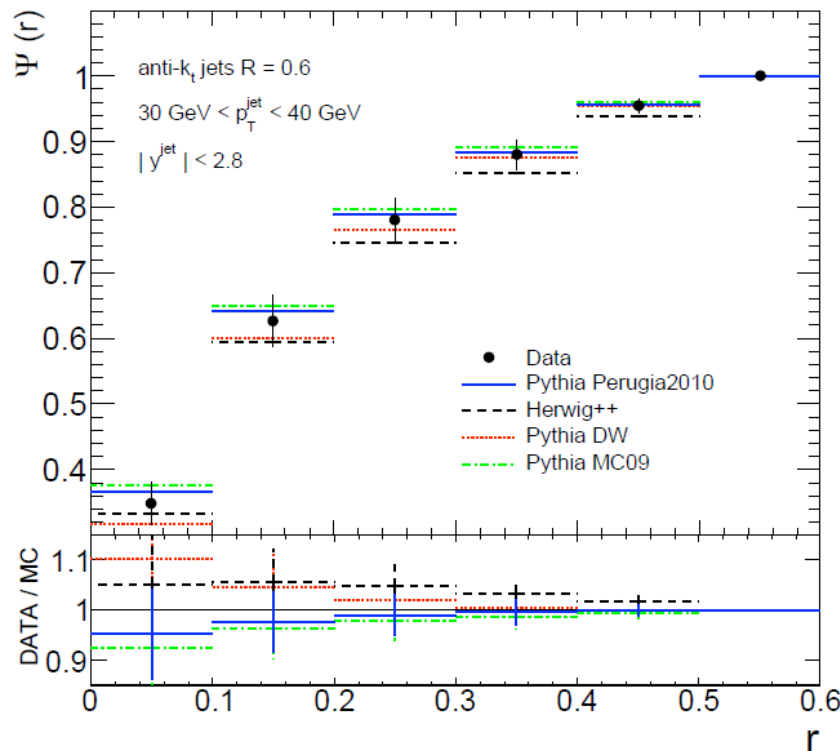
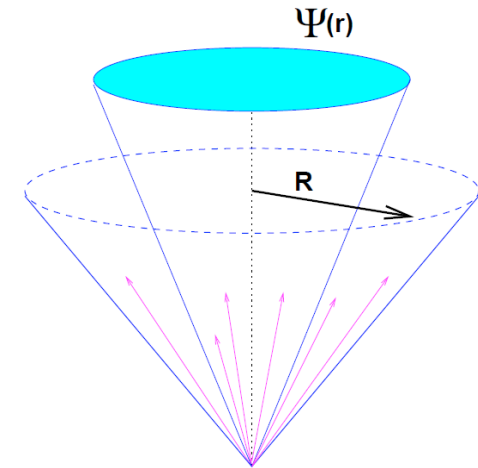
Absolute JES uncertainty

- Absolute JES uncertainty is slightly larger for forward jets and significantly bigger at lower jet p_T
 - Up to 10% at $p_T = 20$ GeV
- Dominant sources:
 - LAr/Tile EM scale: 3%
 - Hadronic shower: ~2-4%
 - Cluster noise thresholds
 - Material description
 - η intercalibration
 - Physics: Alpgen vs. Pythia
- ATLAS Collaboration. "Measurement of inclusive jet and dijet cross sections in proton-proton collisions at 7 TeV centre-of-mass energy with the ATLAS detector." arXiv:1009.5908 [hep-ex]. Accepted by Eur. Phys. J. C.



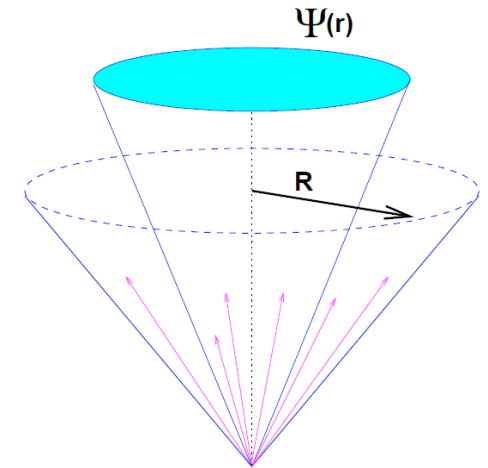
Integral jet shape method

- Integral jet shapes can be computed as integral of the differential jet shape from the jet axis out to some radius R
 - Dominated by transverse momentum near jet axis

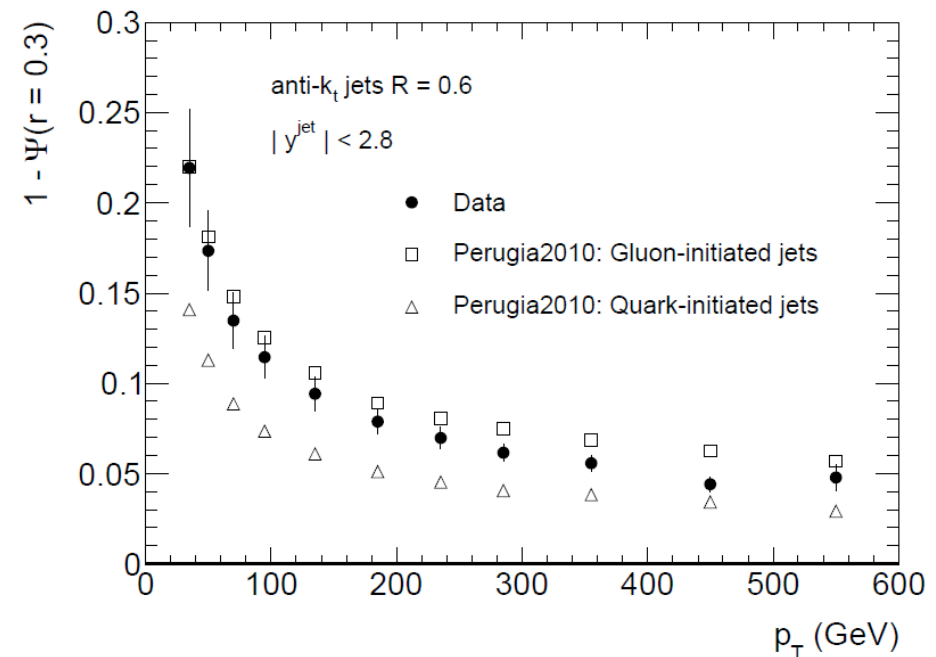
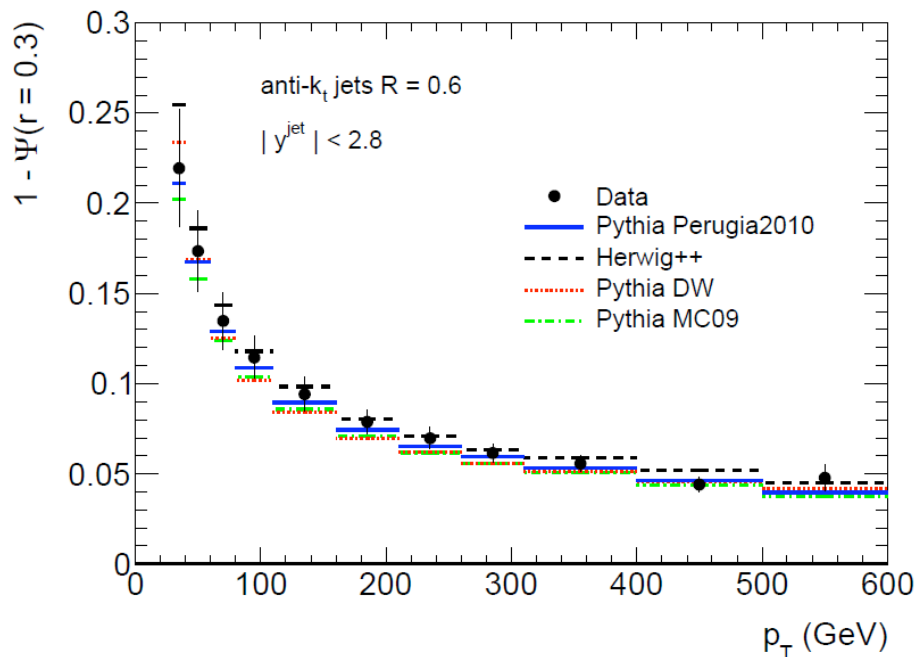


Integral jet shape

- Integral jet shapes $\Psi(r)$ can be computed as integral of the differential jet shape from the jet axis out to some radius R
 - Dominated by measurement nearest to jet axis
- Thus $1 - \Psi(r=0.3)$ is the fraction of transverse momentum outside of $r=0.3$
- May eventually be useful to separate gluon and quark jets



ATL-COM-PHYS-2010-828



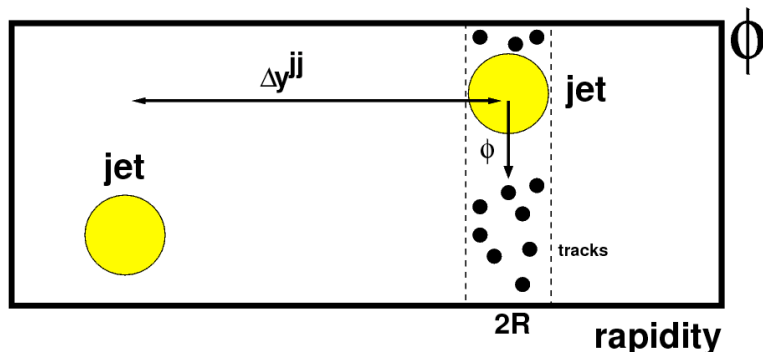
Charged particle flow: Method

- Charged particle flow in inclusive dijet events:

$$\langle \frac{d^2 p_T}{|d\phi| dy} \rangle_{jets} = \frac{1}{2R|\Delta\phi|} \frac{1}{N_{jet}} \sum_{jets} p_T(|\phi - \Delta\phi/2|, |\phi + \Delta\phi/2|), \text{ with } 0 \leq |\phi| \leq \pi$$

is the average transverse momentum as a function of the azimuthal distance from the jet axis and rapidity separation between the two leading jets

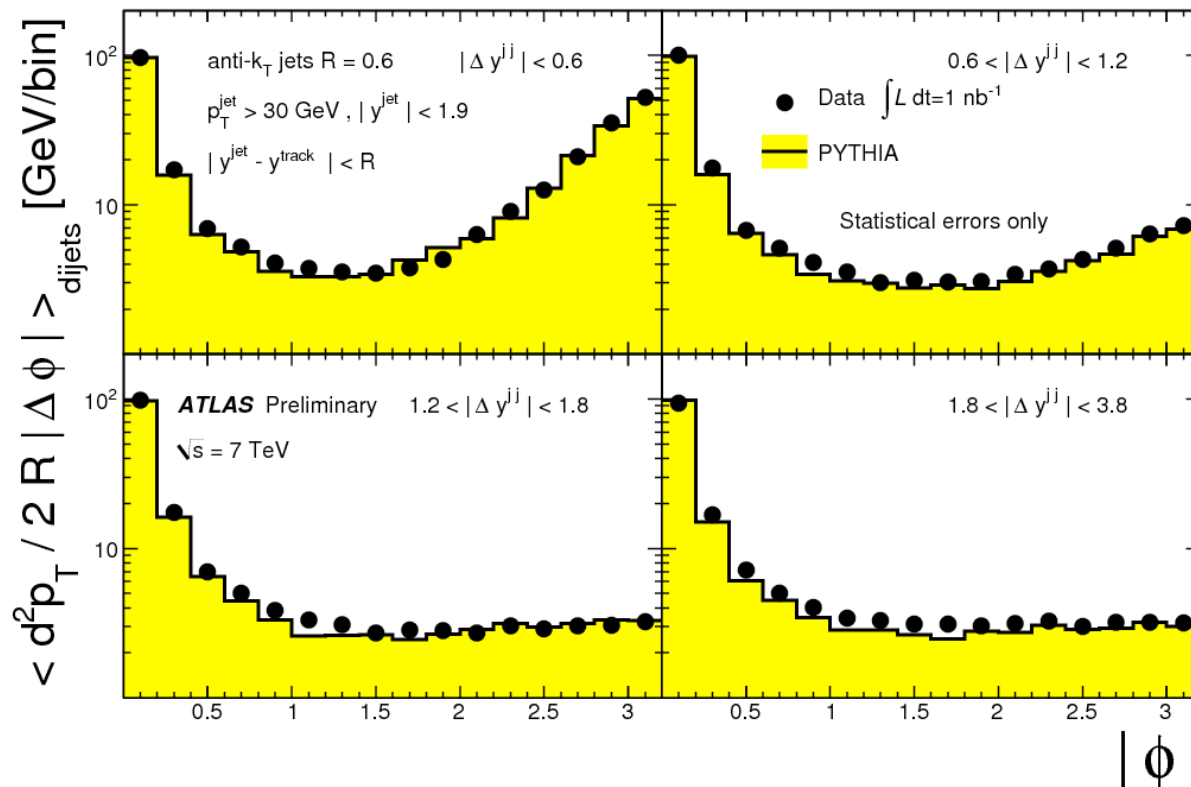
- Here p_T is computed as the scalar sum of the transverse momenta of tracks at a given angle ϕ with respect to jet axis



- Only tracks within rapidity range occupied by jet are used
- Jet required to be within $|y| < 1.9$ to ensure that jet is fully within tracker acceptance $|y| < 2.5$
- Track-based method is useful to confirm results from calorimeter-based jet shapes

Charged particle flow: Data distributions

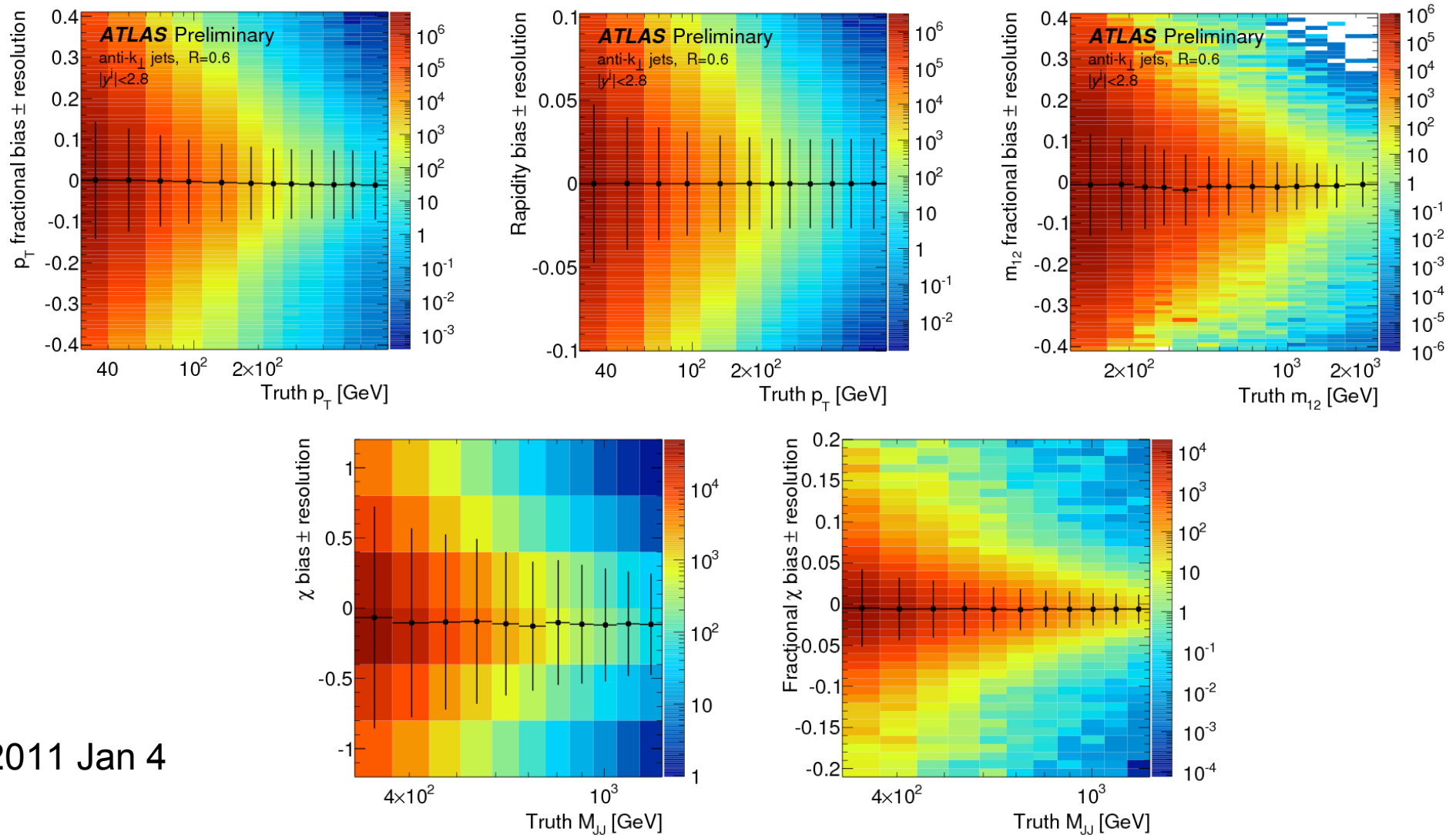
- For $|\Delta y^{ij}| < 0.6$, two collimated flows of charged particles (dijets) observed at $|\phi|=0$ and $|\phi|=\pi$
- For $|\Delta y^{ij}| > 1.2$, jet structure observed at low $|\phi|$ followed by plateau of remaining hadronic activity as $|\phi|$ increases
- Monte Carlo provides reasonable description of data, but slightly underestimates hadronic activity away from the jet direction (see backup)



Resolutions of jet observables

- Jet energy and angular resolutions studied in Monte Carlo in order to assign appropriate bin widths

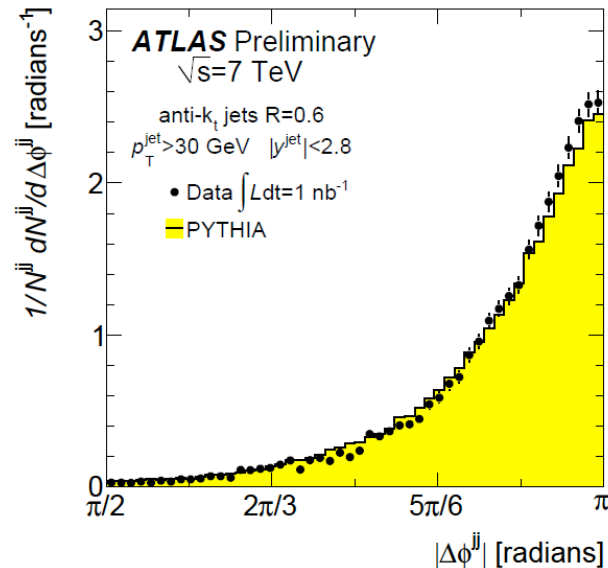
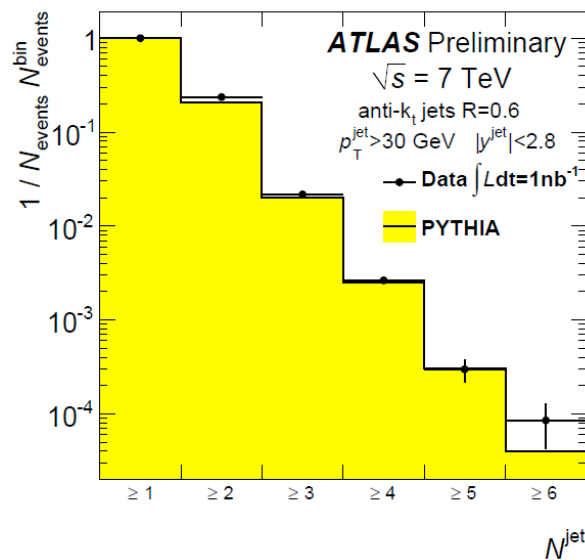
ATLAS-CONF-2010-050



2011 Jan 4

Jet observation at $\sqrt{s} = 7$ TeV

- With 1 nb^{-1} , reported observation of jets at center-of-mass energy of 7 TeV on behalf of Jet/EtMiss and Standard Model groups
- Measured inclusive jet p_T spectrum, dijet mass spectrum, and dijet azimuthal decorrelation

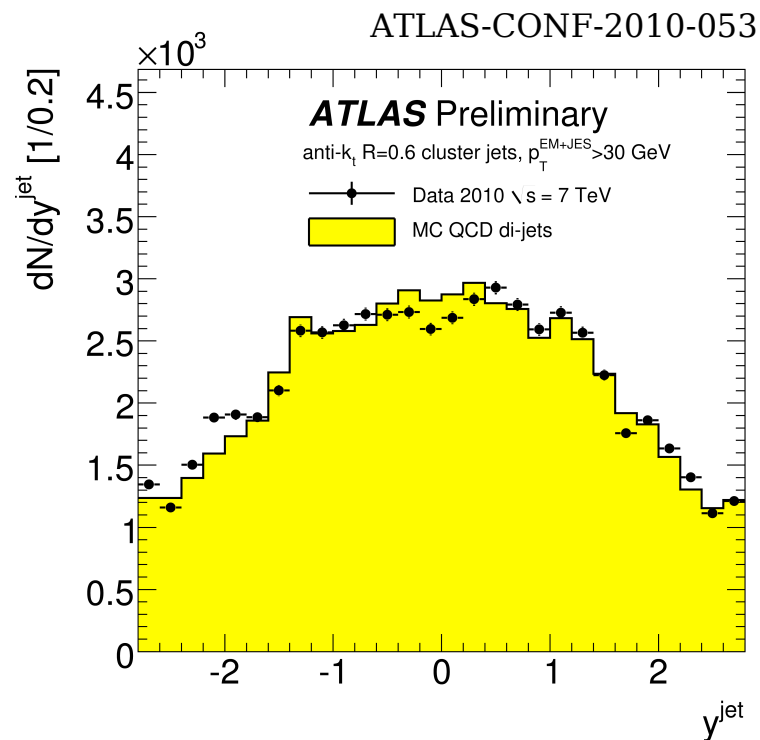
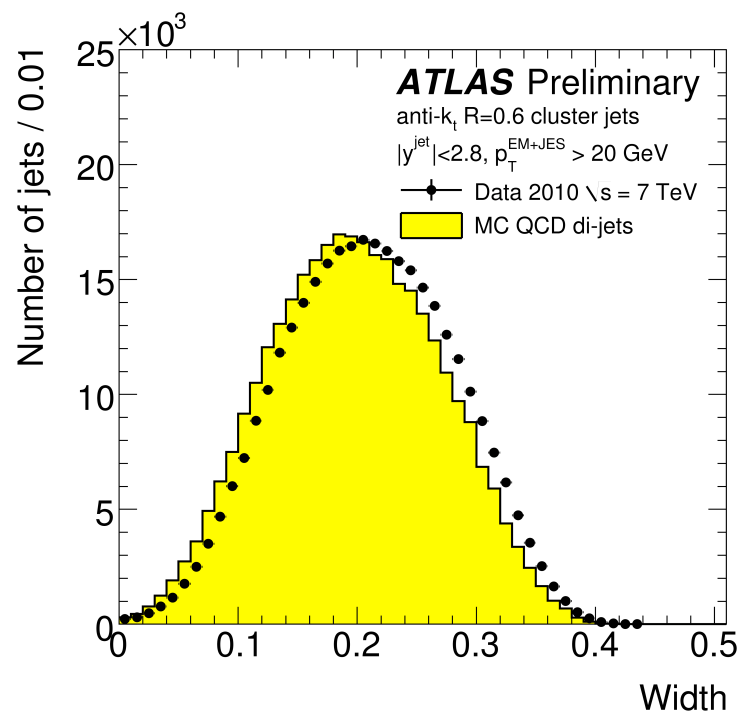


- E. Feng (for the ATLAS Collaboration). "Observation of Energetic Jet Production in pp Collisions at $\sqrt{s} = 7$ TeV using the ATLAS Experiment at the LHC." arXiv:1010.1974 [hep-ex]. To appear in *Proceedings of PLHC 2010*, Hamburg, Germany, June 2010.

Jet properties

Jet width and rapidity

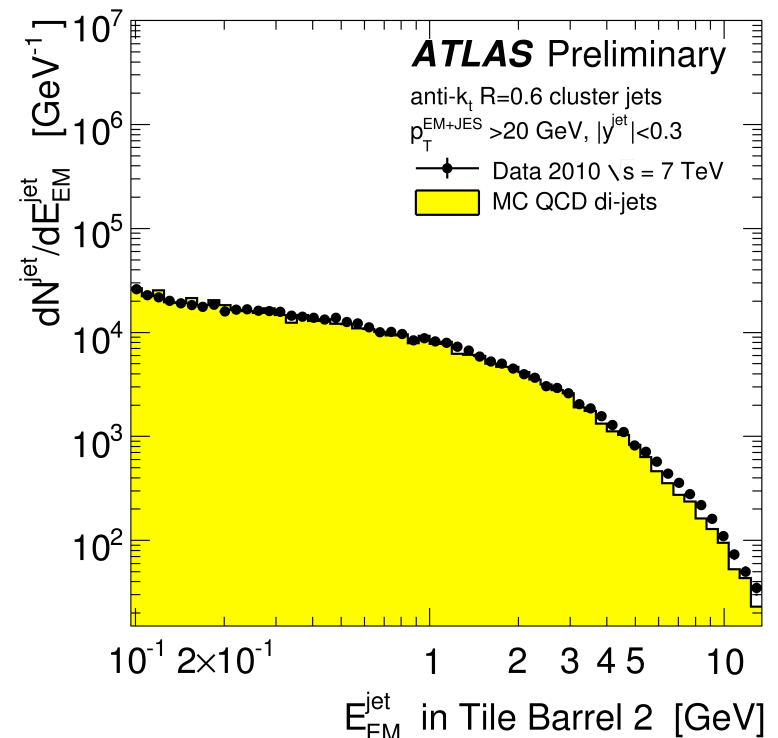
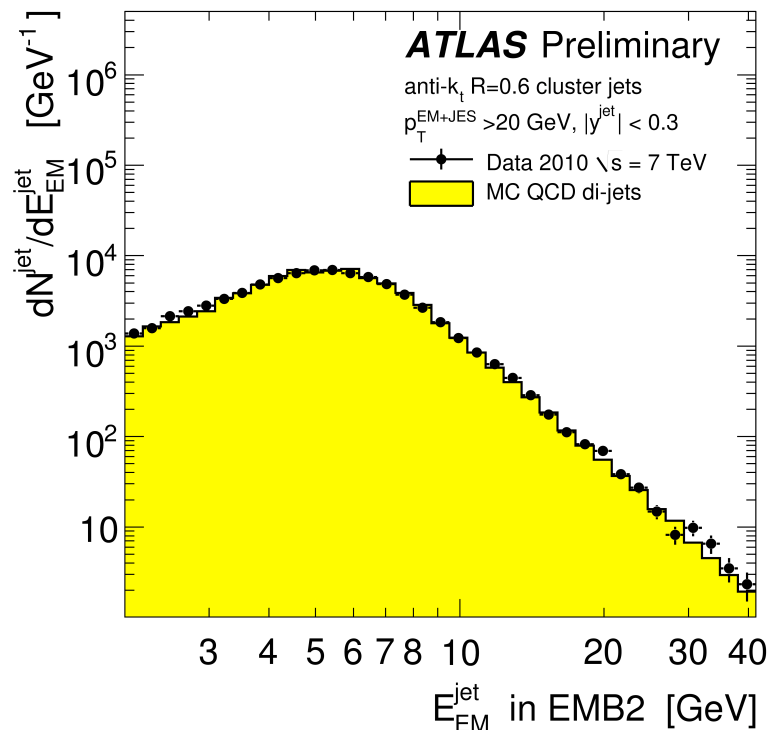
- Studied inclusive jet, dijet, and multi-jet observables to test description of calorimeters, jets, and missing E_T in Monte Carlo
- Jet radial width shown to be wider in data than predicted by MC09
 - Consistent with jet shapes!
- Monte Carlo description was shown to be satisfactory for jets in $|y| < 2.8$



Jet energy in different calorimeter layers

- Detailed studies of jet energy deposited in each layer of calorimeter
- Second layer of EM and hadronic calorimeters shown below
 - Good agreement between data and MC

ATLAS-CONF-2010-053

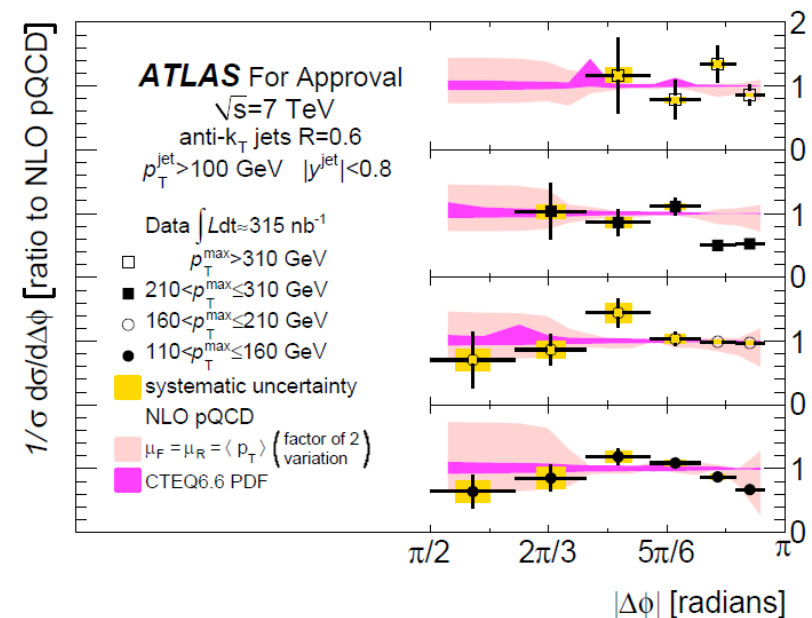
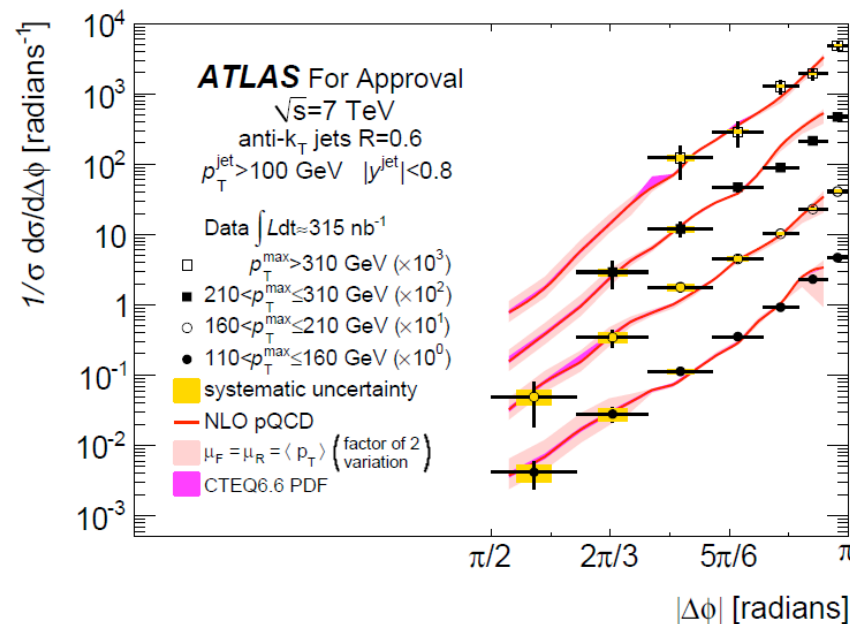


More tests of perturbative QCD

Dijet Azimuthal Decorrelation ($\Delta\phi$)

- Dijet angular distribution: $\Delta\phi = |\phi_1 - \phi_2|$
measured in bins of leading jet p_T
- Peak at $\Delta\phi = \pi \rightarrow$ dominant final state is back-to-back dijets
 - Deviation from $\Delta\phi = \pi$ due to radiation of one or more gluons
 - 3-jet final state calculated using NLO pQCD

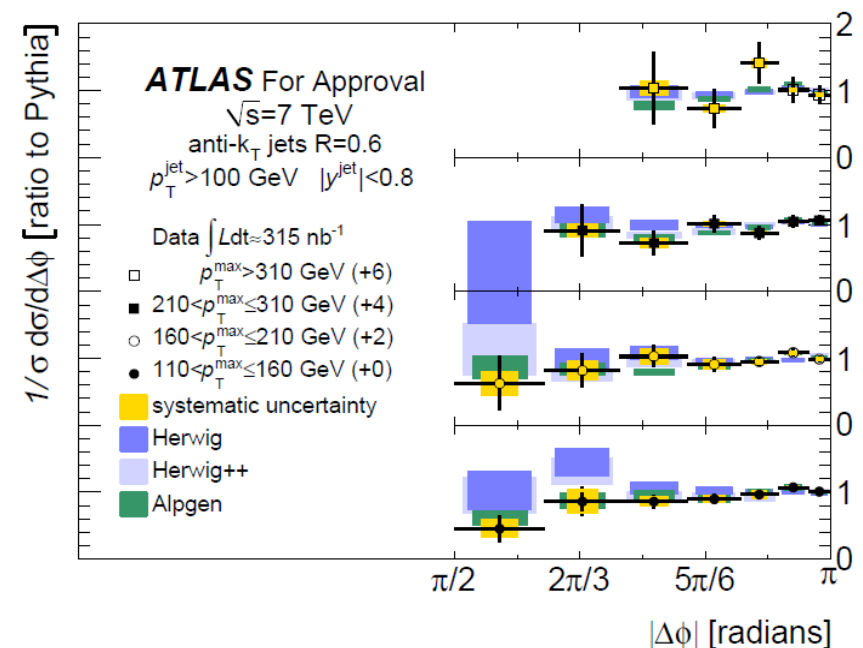
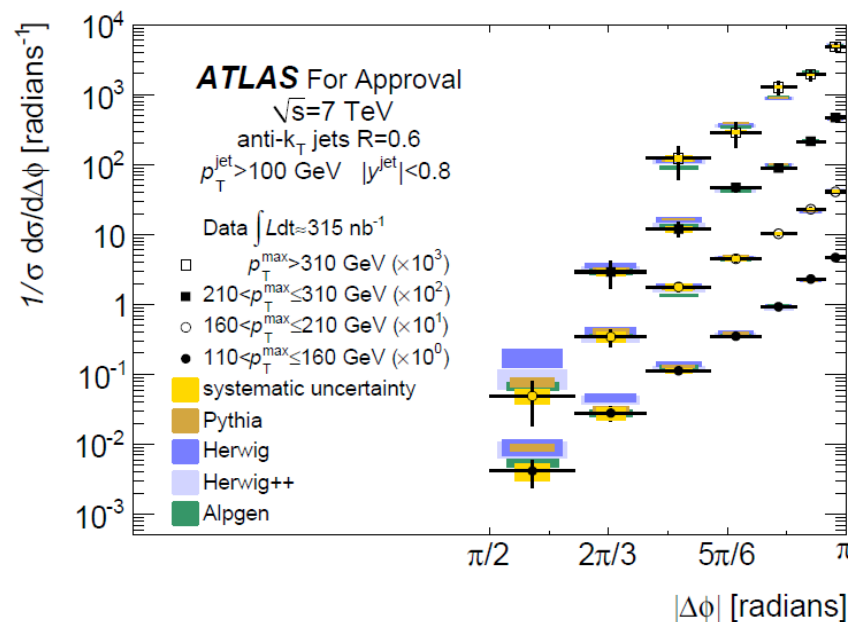
ATLAS-COM-CONF-2010-080



Dijet Azimuthal Decorrelation ($\Delta\phi$)

- Four or more real emissions is best modeled using a leading-order ME generator with 2->N matrix elements
 - Sensitive to different angular distributions produced by 2->2 vs. 2->N parton shower Monte Carlos
- Useful to tune amount of ISR/FSR and underlying event in parton shower Monte Carlo

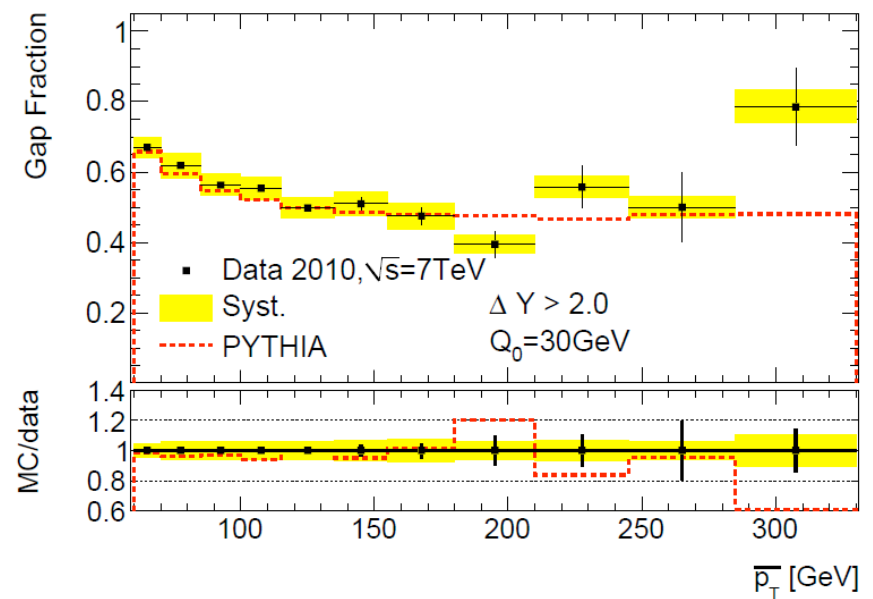
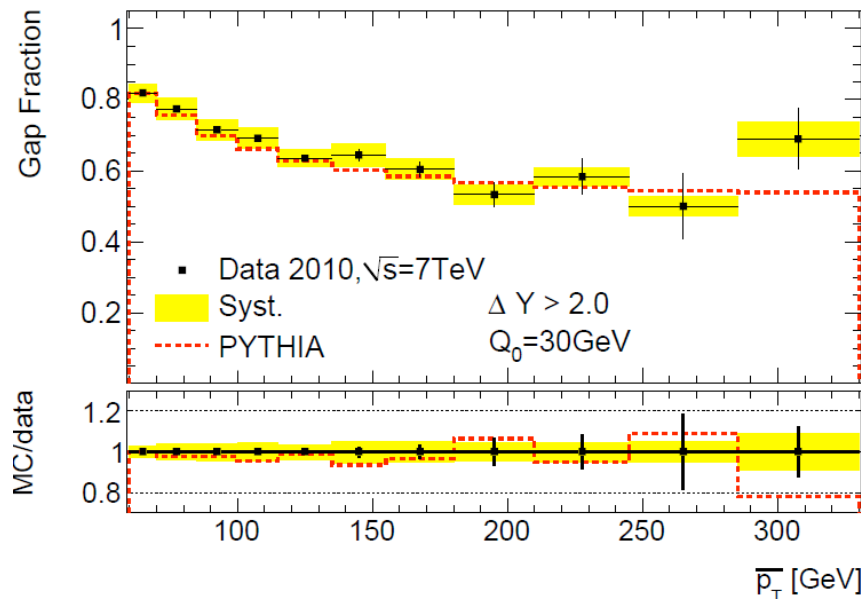
ATLAS-COM-CONF-2010-080



Dijets with Rapidity Gaps

- Measure fraction of events with gap between two boundary jets:
 - Two highest p_T jets (left), OR
 - Most forward and most backward jet (right)
- Sensitive to BFKL dynamics vs. DGLAP evolution
- Also can study wide-angle soft-gluon radiation
- Uses Monte-Carlo based JES uncertainty up to $|y| < 4.5$

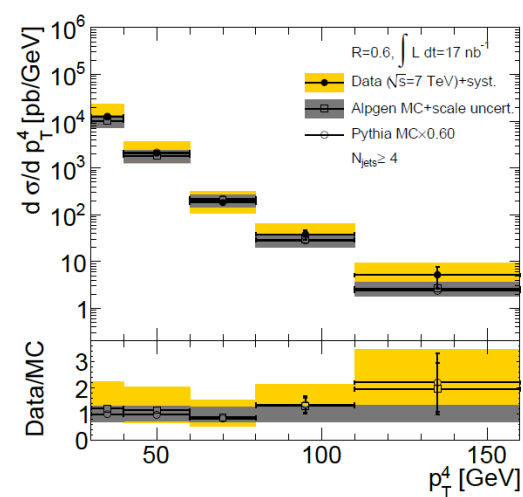
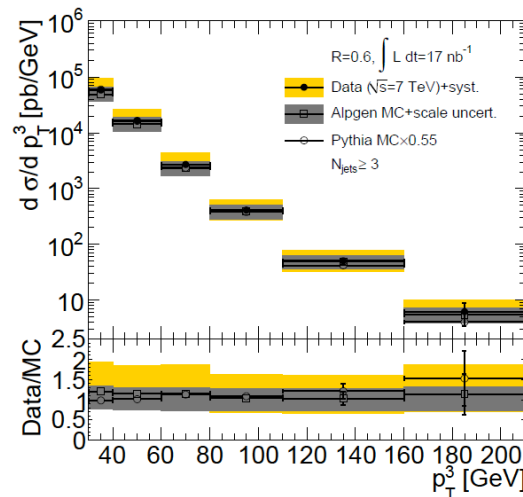
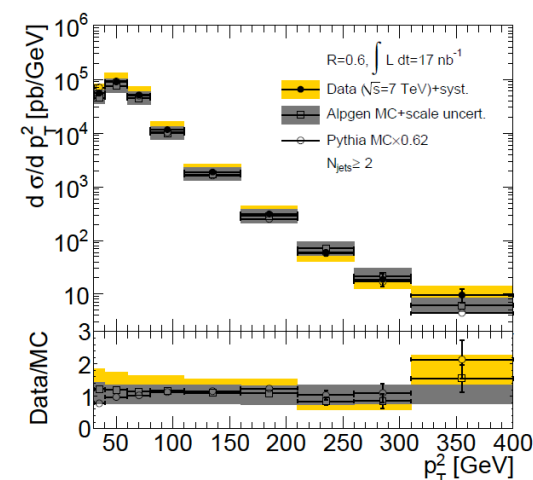
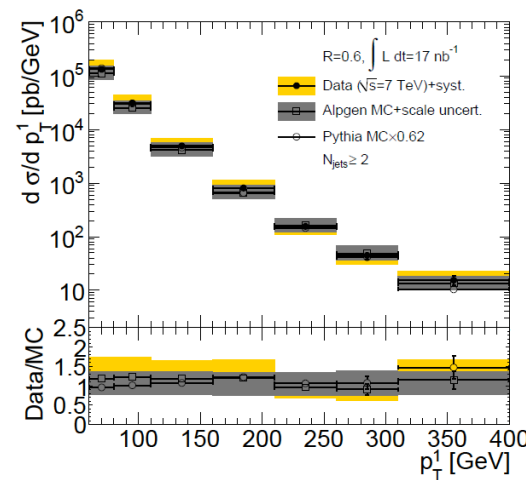
ATL-COM-PHYS-2010-597



Multi-Jets: p_T -ordered cross-sections

- Subdivision of the inclusion jet cross-section into separate cross-sections for each of the p_T -ordered jets
- Sensitive to matrix element and final state radiation

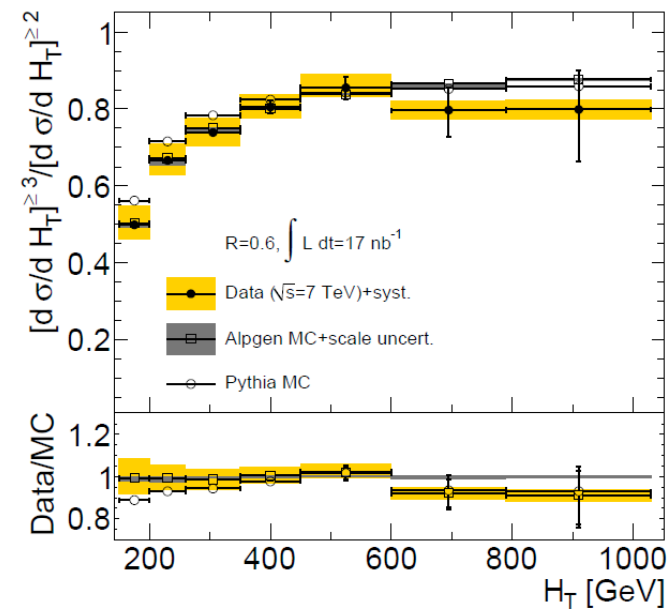
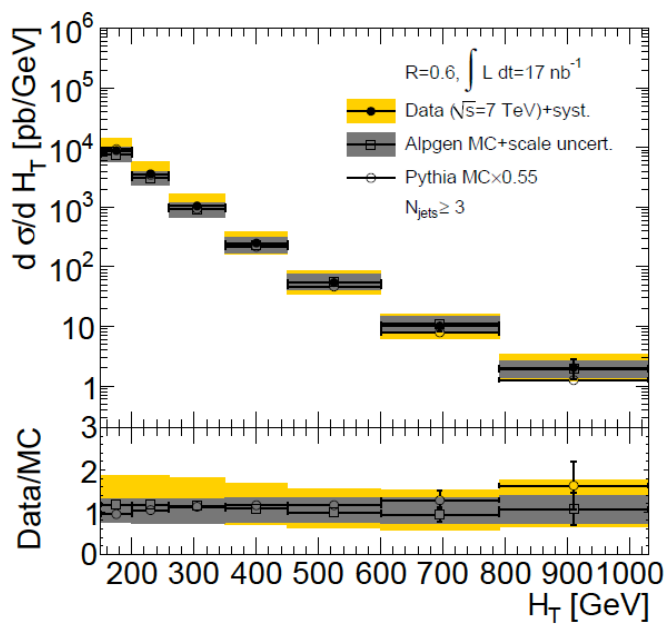
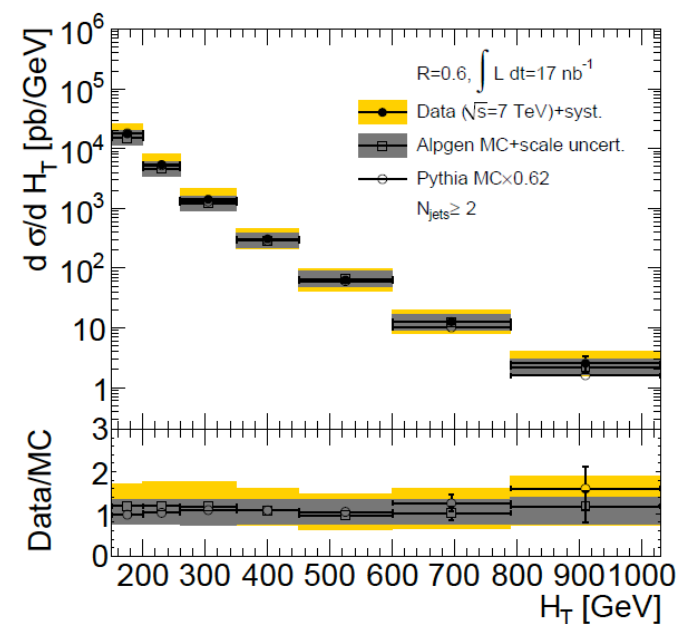
ATL-COM-PHYS-2010-571



Multi-Jets - H_T

- H_T = scalar sum of jet p_T
- Ratio of 3-jet and 2-jet cross-sections in H_T is a direct probe of α_s
- Additional uncertainty in absolute JES due to flavor (quark vs. gluon) as well as close-by jets has been studied

ATL-COM-PHYS-2010-571



Even more QCD analyses

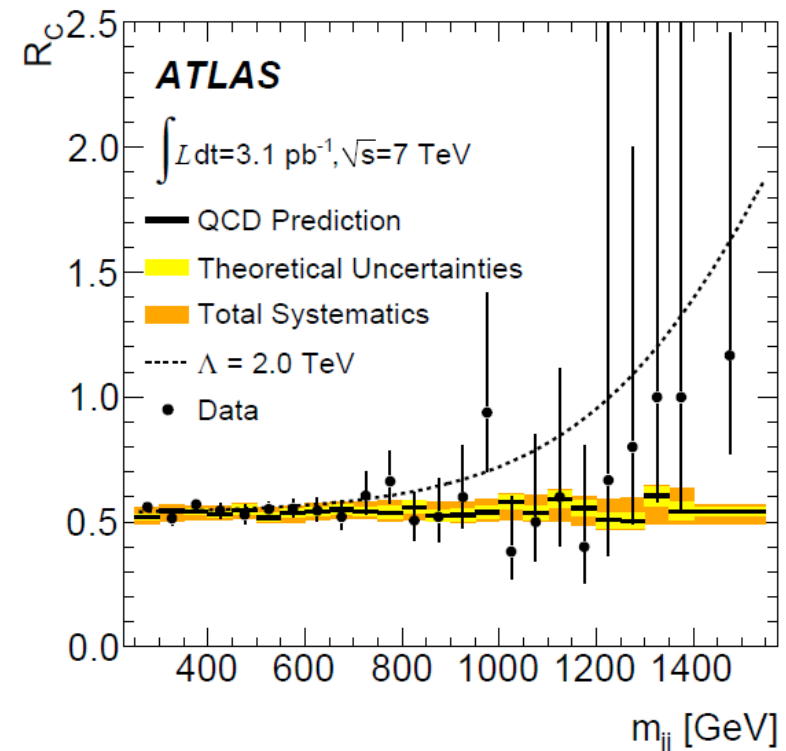
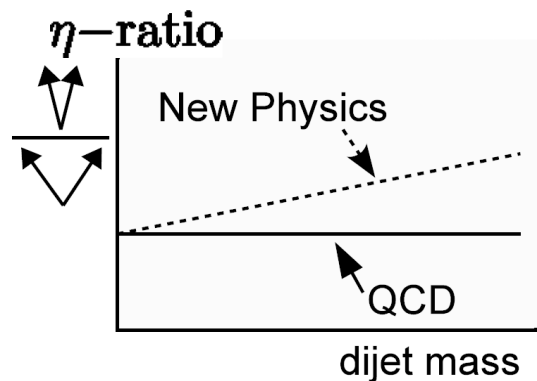
- Many more jet and QCD-related analyses finished or in progress
 - Inclusive jet cross-section measured using track-jets
 - Jet fragmentation measured using tracks
 - Vector boson production in association with jets (W/Z + jets)
 - Diffractive dijets
 - Etc...
- All of these analyses are very interesting, but unfortunately do not have time to describe them here...

Search for contact interactions using the η ratio

- Checked ratio of large-opening to small-opening jets for tail as a function of dijet mass:

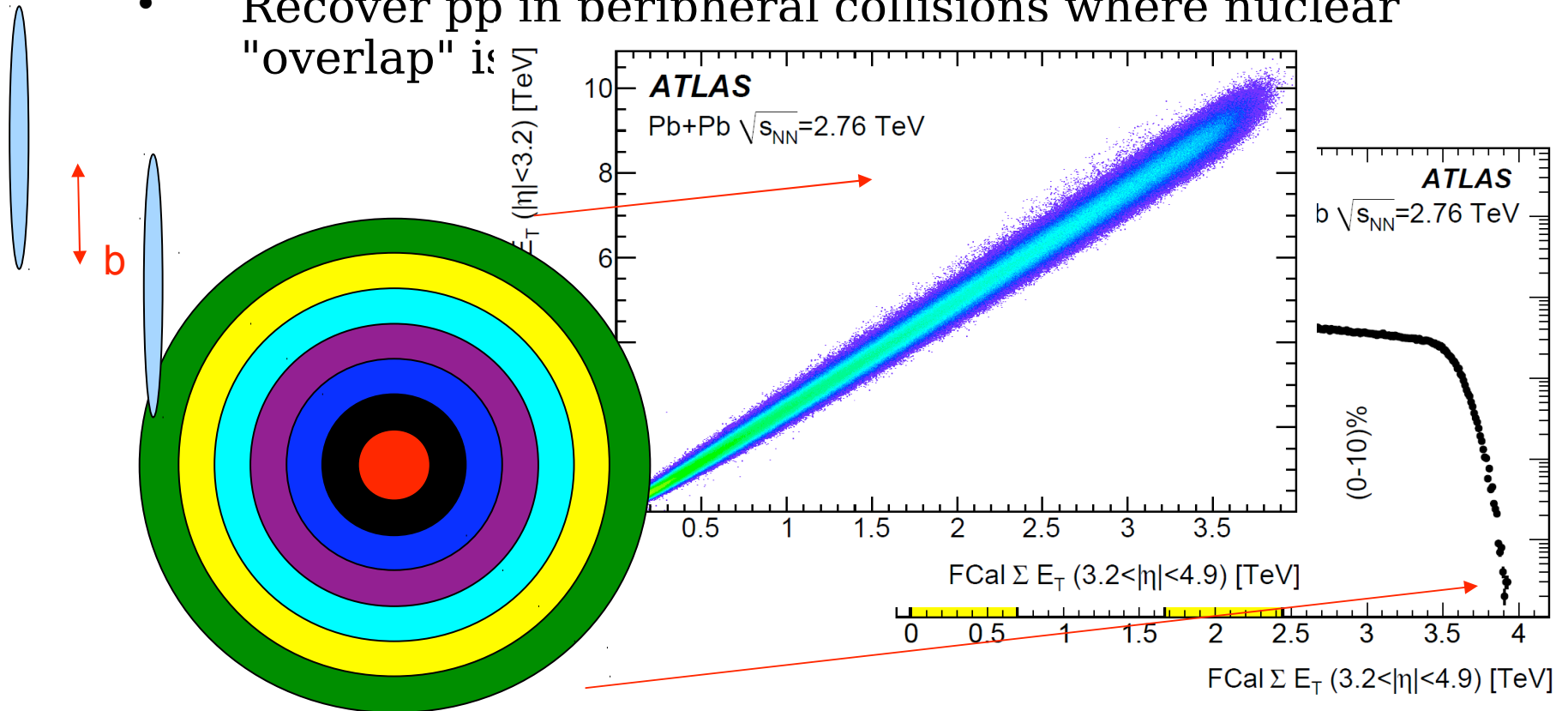
$$\eta\text{-ratio} = \frac{N(|\eta_{1,2}| < 0.5)}{N(0.5 < |\eta_{1,2}| < 1)}$$

- Like χ , largely cancels out JES uncertainty and leaves relative JES
- Also sensitive to contact interactions from small-angle scattering

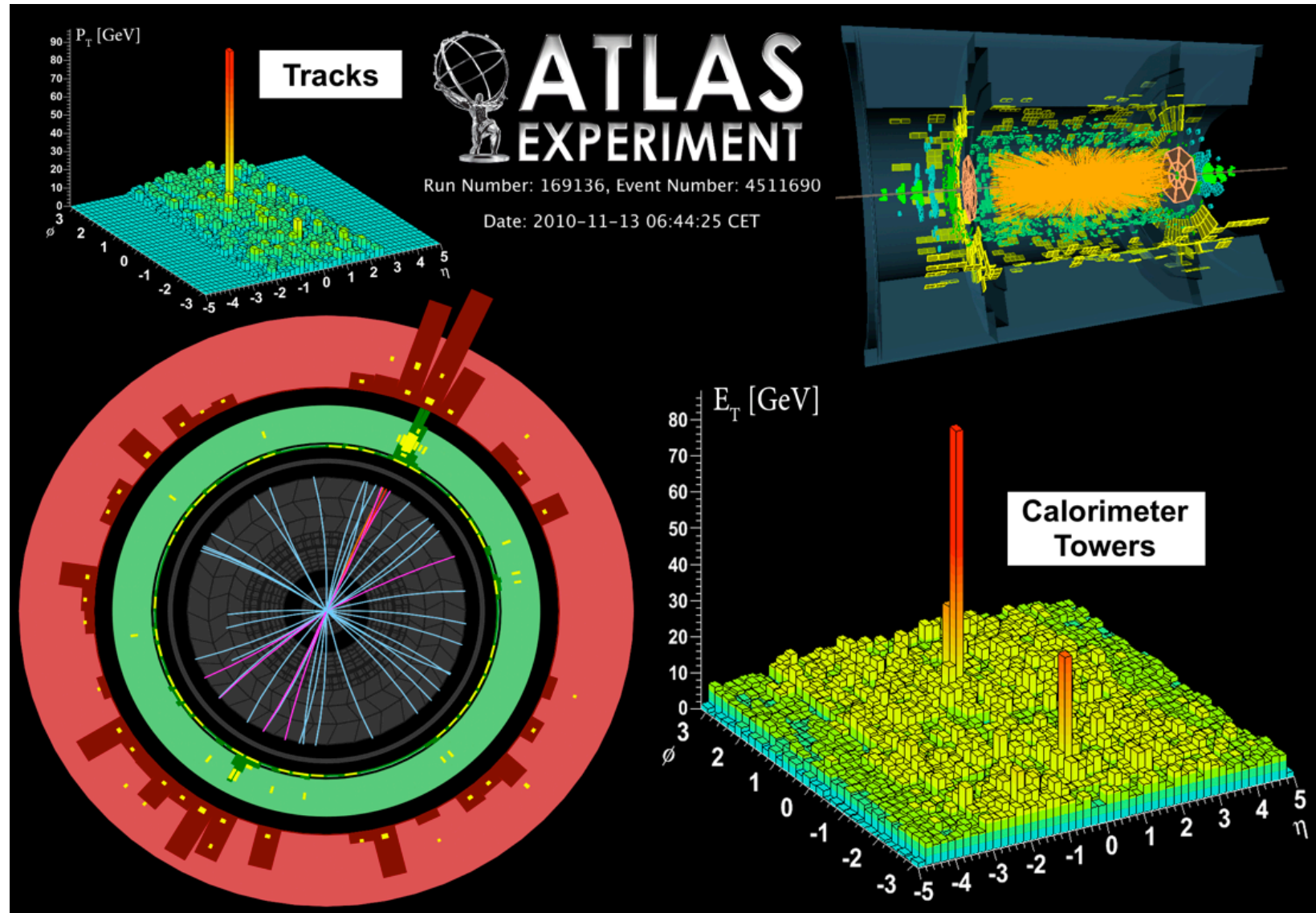


Centrality definition

- Particle multiplicity increases as classical impact parameter b decreases
- Characterize centrality by percentiles of total cross-section using ΣE_T in Forward Calorimeter (Fcal) spanning $3.2 < |\eta| < 4.9$
- Recover pp in peripheral collisions where nuclear "overlap" is



More central, asymmetric dijet event



Central event, with split dijet and additional activity

